1994

Dynamics and controls for robot manipulators with open and closed kinematic chain mechanisms

Sam-Sang You
Iowa State University

Order Number 9518459

Dynamics and controls for robot manipulators with open and closed kinematic chain mechanisms

You, Sam-Sang, Ph.D.

Iowa State University, 1994

U·M·I
300 N. Zeeb Rd.
Ann Arbor, MI 48106

Dynamics and controls for robot manipulators

with open and closed kinematic chain mechanisms

by

Sam-Sang You

A Dissertation Submitted to the

Graduate Faculty in Partial Fulfillment of the

Requirements for the Degree of

DOCTOR OF PHILOSOPHY

Department: Mechanical Engineering
Major: Mechanical Engineering

Approved:

Signature was redacted for privacy.

In Charge of Major Work

Signature was redacted for privacy.

For the Major Department

Signature was redacted for privacy.

For the Graduate College

Iowa State University
Ames, Iowa

1994

TABLE OF CONTENTS

GENERAL INTRODUCTION

Robot manipulators have attracted considerable interest from many researchers during recent years because they have a very wide range of potential applications. Presently different aspects of robotics research are carried out by experts in various fields. This interest covers a broad spectrum like kinematics and dynamics, task planning, robot language, sensing and control, and robot vision. This dissertation, which consists of three parts, focuses on the areas of dynamics and controls of the robotic manipulators (or the mechanical manipulators).

In general, the control methods for robot manipulators fall into two main categories: motion (or position) control and force control. The purpose of this dissertation is to fully address these two broad modes. In the first category (Part I), the position control methods can be used for the robot manipulator to move in the free space with open kinematic-chain mechanism. In the secondary category (Part II and III), the hybrid position/force controllers deal with the constrained motion of robot manipulators when the end effectors come into contact with the environment (or external object) with closed kinematic-chain mechanisms.

Considerable effort has been focused on the problem of position control of robot manipulators containing open chain mechanism in which the manipulator does not come in contact with the external environment. There are many tasks of this nature, such as pick and place type operations, paint spraying, and arc welding. In Part I, we discuss the robust motion control of an unconstrained single robot under significant system uncertainties.

In contrast to open-chain manipulators, the closed chain manipulators have received little attention in robotics literature. The increasing demand for contact tasks, coordinated multi-manipulator systems, and more precise manipulators motivates research in rigid body dynamics and control of closed-chain robotic manipulators. As mentioned before, the

control schemes in Part I are mainly concerned with motion control of the robotic system in which its end-effector does not significantly interact with the environment. However, many practical tasks (higher level tasks) require extensive physical contact of the robot end-effector with the external environment in the workspace in applications such as machining tasks (grinding, deburring, polishing, etc.), writing, turning a crank, inserting a peg into a hole, various material handling tasks, and others. Part II of the dissertation deals with the hybrid position/force control of a single robot system subject to geometric constraints.

So far a single robot arm has been extensively used in modern industries for performing relatively simple tasks. Unfortunately, real applications of such a system to a higher level of intelligent tasks are still limited due to its capability and performance. To overcome the above limitations as well as greatly enhance system performance, there has been growing interest in investigating the problem of coordinated control of multiple robot systems. In the execution of the advanced tasks, such as grasping big and heavy objects, various material handling, and sophisticated assembly operations, cooperation among two or more robots is required to accomplish such tasks in a desired manner. Additionally, like human arms, the multi-manipulator systems provide higher flexibility and dexterity in performing complex tasks. The last topic of this dissertation (Part III) considers the dynamic modeling and coordinated controls of constrained multiple robot system. In this part, we provide a unified formulation for the dynamics of multiple robots manipulating a common object on the constraint surface. And the hybrid controllers presented enable us to control both the position and the contact forces (internal grasping forces and constraint forces) simultaneously.

This dissertation is organized as follows. First, the robust motion tracking controllers for uncertain single robot manipulator will be presented in Part I. Next, a class of hybrid position and force controllers for a single robot manipulator with constrained motion tasks are introduced in Part II. After that, dynamics and controls of multiple robot system with

constrained motion tasks are presented in Part III. Finally, general conclusions and acknowledgments are given. Each of the three parts of this dissertation begins with an overview. And equations, references, and figures are numbered independently in each part with references and appendices given at the end of each part.

PART I

ROBUST MOTION TRACKING CONTROLLERS FOR UNCERTAIN SINGLE ROBOT MANIPULATOR

OVERVIEW

This part of the dissertation considers the problem of designing a class of robust algorithms for the trajectory tracking control of a single robot manipulator whose nonlinear dynamics contains various uncertain elements. To ensure high-performance system, the general control structure consists of two parts: The nominal control laws, utilizing a model-based feedforward scheme plus proportional-derivative (PD) compensation, are first introduced to stabilize the system in the absence of uncertainties. Then a class of robust nonlinear control laws are adopted to compensate for both the resulting errors (or the structured uncertainties) and the unstructured uncertainties by using a deterministic approach. The uncertainties assumed in this study are bounded by polynomials in the Euclidean norms of system states with known (or unknown) bounding coefficients. The possible bounds of uncertainties are assumed to be known for the nonadaptive version of robust nonlinear controls with less computational burden. If no information on these bounds is available, then the adaptive bound of the robust controller is presented to overcome possible time-varying uncertainties (i.e., decentralized adaptive control scheme). The control schemes presented are relatively simple as well as computationally efficient (i.e., decentralized control approach). With a feasible class of desired trajectories (that is, all desired motions are continuous and bounded), the proposed control laws guarantee that all possible responses of the corresponding closed-loop systems are at least uniformly ultimately bounded by Lyapunov stability theory. The effectiveness of the proposed control algorithms are verified through extensive numerical simulations. Finally, it is shown that all presented controllers are evaluated to be robust with respect to a given class of uncertainties.

1. INTRODUCTION

Industrial robots can be used by many modern industries to meet various demands for fast motion and high-accuracy operations in flexible manufacturing systems. In flexible manufacturing, robot manipulators are expected to accomplish a variety of tasks within a wide range of operating conditions, undertaking tasks such as pick and place from a conveyor belt, spray painting, arc welding, and assembly operations. Furthermore, the future practical applications of robots are likely to be extensive. Therefore, the design of high-performance and reliable control algorithm is one of the key issues in the current robotics research.

The performance of the control system depends largely upon the accuracy of the dynamic model. Unfortunately, a class of nonlinear dynamical systems (including robot manipulators) very often contain uncertainties in system modeling and control processes. These uncertainties can arise in different forms and are typically time-varying. The uncertainties under consideration include structured uncertainties (whose functional structures are known but their parametric values are incorrect due to model parameter variations, unknown payload, and imperfect modeling) and unstructured uncertainties (whose structures are poorly known or unknown due to complexity of their behaviors, such as disturbances, friction, and other unmodelled dynamic effects). However, a wide range of the current control schemes ignore these uncertainties associated with robot systems. Thus those algorithms sometimes cannot provide general solutions. To achieve satisfactory system performance and to extend the usage of control laws, the control strategies should account for the possible uncertainties which deteriorate system performance.

Several model-based control schemes have been presented for motion (positioning and tracking) control of robot manipulators, such as inverse dynamics (also called computed

torque method) and passivity-based controllers. Early outstanding results in this approach are found in Ref. [1]. Although these control schemes have a certain degree of robustness against uncertainties, they are originally based on exact knowledge of the manipulator system (i.e., a perfect dynamic model as well as exact a priori knowledge of the system parameters). Increasing demands on high-performance systems have led to the development of various advanced control strategies. During the last ten years, numerous papers dealing with the control of uncertain dynamical systems (including robot manipulators) have been published [1-19]. In general, the uncertainties are hard to identify, thus they are usually unknown or poorly known. Since the control strategy of uncertain systems is based on the deterministic approach [2-14, 19] in this study, no statistical information (by using stochastic approach) about the uncertainties will be assumed and utilized. In the deterministic approach, only possible upper bounds on uncertainties are required for the control synthesis. One useful design method for controlling uncertain systems is variable structure (VS)-type robust control schemes [2-14, 19] which are usually fixed-structures for a given uncertainty set, such as discontinuous (min-max or sign) functions, saturation functions, and continuous functions in the control laws. Unfortunately, to implement a controller, most of the control approaches generally require *a priori* knowledge of uncertainty bounds. Abdallah *et al.* [7] gives a recent survey of robust control of robot manipulators. An alternative approach to solving the control problem of such systems is an adaptive control method which has the capability of adjusting and tuning time-varying uncertain parameters of the system. So far a considerable amount of research has been accomplished in the field of adaptive control (see, e.g., Refs [1, 7, 15-18]). However, most of current research has emphasized on the estimating the system model-parameters (i.e., centralized adaptive control method). Ortega and Spong [17] presents an overall review of the adaptive robot control. As a matter of fact, the robust controllers are simpler to implement in practice. Contrary to most existing methods, a

decentralized control technique will be introduced in this research. At present, a class of papers discuss either the stability problem under the effects of higher-order uncertainties [11, 13] or the adaptive bounds on uncertainties (or decentralized adaptive control) [3, 5, 9] or both [10, 19]. To summarize, many advanced control strategies with imprecise dynamic models, such as robust controls and adaptive controls, suffer from one or more of the following drawbacks: (i) use discontinuous control laws, (ii) synthesize computationally inefficient algorithms, (iii) require *a priori* knowledge of the uncertainty bounds, and (iv) compensate for relatively small system uncertainties.

The main purpose of this research is to develop robust motion controller for an uncertain robotic system in which the uncertainties are time-varying and characterized deterministically rather than statistically. In addition, the corresponding control laws will overcome some or all the defects found in earlier design methods. The control algorithms presented in this study consist of two components: the nominal control, utilizing model-based feedforward approach (which incorporates full-order robot dynamics) plus proportional-derivative (PD) compensation, is first introduced to stabilize the system without uncertainties; then the robust nonlinear control laws are synthesized to cope with both the structured and the unstructured uncertainties in the system. To show that the proposed control schemes are robust enough to overcome significant uncertainties, the uncertainties assumed are bounded by higher-order polynomials in the norms of system states with known (or unknown) bounding coefficients. This is in contrast to other approaches which have made simple assumptions on the strength of uncertainties. That is, the uncertainties are bounded by either constants or known first-order polynomials in the system states. If the possible bounds of uncertainties are assumed to be known, then three nonadaptive versions of robust nonlinear controllers are designed. These are the polynomial-type controller, the saturation-type controller, and the continuous VS-type controller. If no information on these bounds is available, the adaptive version of the robust

controller is presented to directly estimate the unknown bounds. That is, based only on knowledge of functional properties relating to time-varying uncertainties. In this study, instead of updating model-parameters of robot manipulators, the nominal (or known) values of robot parameters can be used in the nominal control laws. Then the resulting errors can be handled by adaptive or nonadaptive version of robust control laws. With a feasible class of desired trajectories, the proposed control laws guarantee that all possible responses of the corresponding closed-loop system are at least uniformly ultimately bounded under a given class of uncertainties.

The organization of this work is outlined as follows: Preliminaries and problem formulations are presented in Section 2. The main results are stated in Sections 3 and 4. In Section 3, nonadaptive bounds of robust controllers have been proposed for uncertain system dynamics with known bounds on uncertainties. In Section 4, without possible knowledge of the bounding functions, adaptive bound of the robust nonlinear controller is formulated. In Section 5, the effectiveness of the proposed control laws are verified through numerical simulation examples, while the contributions and conclusions of this work are summarized in Section 6.

2. PRELIMINARIES AND PROBLEM FORMULATIONS

2.1 Preliminaries

Unless mentioned otherwise, the following standard notation and terminology will be used. Bold letters represent vectors or matrices and other variables are scalars. R denotes the field of real numbers, R^+ is the set of non-negative real numbers, i.e., $R^+ := [0, +\infty)$, R^n denotes the usual n-dimensional vector space with real-valued elements (R), $R^{n\times m}$ is the set of all real-valued $(n \times m)$ matrices in the set R, and C^p is the set of p-times continuously differentiable function. And the vector norm $\|\mathbf{x}\|$ (or $\|\mathbf{x}(t)\|$) is the Euclidean one of vector $\mathbf{x}$ at time t, i.e.,

$$\|\mathbf{x}\| = \left[\sum_{i=1}^{n} |x_i|^2\right]^{1/2}, \forall \mathbf{x} \in R^n$$

where $\|\mathbf{x}\| \geq 0$, and $\|\mathbf{x}\| = 0$ *iff* $\mathbf{x} = \mathbf{0}$. The matrix norm is taken to be the corresponding induced one, i.e., for a real matrix $\mathbf{A} \in R^{n\times n}$,

$$\|\mathbf{A}\| = \left[\sigma_{\max}(\mathbf{A}^T\mathbf{A})\right]^{1/2},$$

where $\sigma_{\max}(\bullet)$ (or $\sigma_{\min}(\bullet)$) denotes the maximum (or minimum) eigenvalue of the designated matrix if all its eigenvalues are real, i.e., $\sigma_{\max}(\bullet) = \max_i\{\sigma_i(\bullet)\}$ and $\sigma_{\min}(\bullet) = \min_i\{\sigma_i(\bullet)\}$, where $\sigma_i(\bullet)$ is the ith eigenvalue of real matrix. And $(\bullet)^T$ denotes the transpose of $(\bullet)$ and $\mathbf{A} > \mathbf{0}$ $(\mathbf{A} < \mathbf{0})$ denotes a positive (negative) definite matrix $\mathbf{A}$. Here, a norm is a generalization of the idea of length and magnitude.

Definition 1: L_p and L_∞ Function Norms [20]

Let $\mathbf{f}(t): R^+ \rightarrow R^n$ be Lebesgue measurable function and $\mathbf{f}(t) = \mathbf{0}$ for $t < 0$, then the L_p-norm $\|\mathbf{f}\|_p$ is defined as

$$\|\mathbf{f}\|_p = \left[\int_0^\infty \|\mathbf{f}(t)\|^p dt\right]^{1/p} < \infty, \text{ for any fixed } p \in [1, \infty).$$

When $p = \infty$, $\mathbf{f} \in L_\infty$ if and only if

$$\|\mathbf{f}\|_\infty = ess\sup_{t\in[0,\infty)}\|\mathbf{f}(t)\| < \infty. \quad \Delta\Delta$$

Lemma 1: Barbalst's Lemma [20]

Let $f(\bullet): R^+ \to R$ be a scalar differentiable function of t. If $f(t)$ has a finite lower limit as $t \to \infty$, i.e., $\exists c, \forall t \geq 0, \quad \lim_{t\to\infty} f(t) \geq c$. Moreover if $\dot{f}(t)$ is uniformly continuous and a non-positive, then $\dot{f}(t) \to 0$ as $t \to \infty$. $\Delta\Delta$

Geometrically, the above result implies that a lower-bounded, nonincreasing, and smooth function necessarily has a vanishing derivative function.

Proof: The proof of this lemma can be founded in Sastry and Bodson [20].

Corollary 1: If $g, \dot{g} \in L_\infty$ and $g \in L_p$ for some $p \in [1,\infty)$, then $g(t) \to 0$ as $t \to \infty$.

This corollary follows immediately from Lemma 1. $\Delta\Delta$

The mathematical model of the system is obtained from the physical laws. From the control point of view, the Euler-Lagrangian formulation of motion for natural systems is very useful. In the following, we use Lagrangian dynamics to obtain the mathematical model of the robot system. The robot manipulator system under consideration is a set of n moving rigid bodies connected in a serial open chain mechanism with all revolute joints (a pure rotational motion with respect to the inertial frame). In addition, the robot moves in a singularity-free region of workspace. To derive the differential form of the robot dynamics, first, define the Lagrangian, $L = K - P$, where the Lagrangian (L) is difference between the kinetic and potential energies. Actually, the total energy of the robot arm is sum of the kinetic energy (K) and potential energy (P) of the linkages.

Consider Lagrange's equations for a conservative system described by

$$\frac{d}{dt}\left(\frac{\partial L}{\partial \dot{\mathbf{q}}}\right) - \frac{\partial L}{\partial \mathbf{q}} = \mathbf{T},$$

where $\mathbf{q} \in R^n$ is the vector of generalized coordinates and $\mathbf{T} \in R^n$ is the vector of generalized forces. Then, it can be shown that the dynamic model of a robot manipulator is compactly given in vector and matrix form as (see, e.g., Refs [1], [8], [16-18])

$$\mathbf{M}(\mathbf{q};\Theta)\ddot{\mathbf{q}} + \mathbf{C}(\mathbf{q},\dot{\mathbf{q}};\Theta)\dot{\mathbf{q}} + \mathbf{G}(\mathbf{q};\Theta) = \mathbf{T}, \quad \forall t \geq 0$$

where $\mathbf{q}, \dot{\mathbf{q}}$, and $\ddot{\mathbf{q}} \in R^n$ are the joint position, velocity, and acceleration vectors, respectively. Actually, all quantities in the above equation are functions of time (t) which is the independent variable; $\mathbf{M}(\mathbf{q};\Theta) \in R^{n\times n}$ is an inertia matrix whose elements are continuously differentiable; $\mathbf{C}(\mathbf{q},\dot{\mathbf{q}};\Theta) \in R^{n\times n}$ is a matrix valued function grouping the centrifugal and Coriolis terms and continuously differentiable functions of $\mathbf{q}$ and $\dot{\mathbf{q}}$ (i.e., C^{∞} function); $\mathbf{G}(\mathbf{q};\Theta) \in R^{n\times n}$ is the gravity force/torque vector; $\mathbf{T} \in R^n$ is the joint torque (or control input) vector supplied by the actuators. In reality, the robot manipulator system is always affected by various uncertainties. Thus the n-degree of freedom (DOF) robot dynamics under the uncertainties is written in a symbolic form [13, 19]

$$\mathbf{M}(\mathbf{q};\Theta)\ddot{\mathbf{q}} + \mathbf{C}(\mathbf{q},\dot{\mathbf{q}};\Theta)\dot{\mathbf{q}} + \mathbf{G}(\mathbf{q};\Theta) + \mathbf{T}_u(\mathbf{q},\dot{\mathbf{q}}) = \mathbf{T}, \ \forall t \geq 0 \qquad (1)$$

where the function $\mathbf{T}_u(\mathbf{q},\dot{\mathbf{q}}) \in R^n$ represents the vector of uncertain elements (or the unstructured uncertainties) which are difficult to characterize exactly or are totally unknown, such as friction, unmodelled dynamics, external disturbances, joint and link flexibilities, actuator and sensor noises, and the strengths of interactions from other subsystems. This term will be possibly time-varying and system state dependent vector; $\Theta \in R^m$ is the vector of bounded system parameters (manipulator link masses, link lengths, moments of inertia, etc.). In fact, the manipulator dynamics (1) is a set of second-order, coupled, and nonlinear differential equations. In the above dynamic formulation, we exclude the important case when the robot manipulator makes contact with an external environment (this topic will be discussed in Part II and III of this theses). Throughout this study, some arguments of the joint-space dynamics (1) are often omitted for brevity when possible.

To design advanced control algorithms, one must examine the physical properties of robot dynamics (1). Although the dynamic model (1) under consideration is complex and

highly nonlinear in nature, it has some fundamental structural properties which are actually inherent to rigid robot dynamics and can be summarized as follows [1, 6-8, 13, 16-19].

Property 1: $\mathbf{M(q)}$ is a symmetric and positive-definite matrix, i.e., $\mathbf{M(q;\Theta)} = \mathbf{M(q;\Theta)}^T > \mathbf{0}, \forall(\mathbf{q},\Theta)$, and $\mathbf{M}^{-1}$ exists for finite workspace which is a singular-free region. Furthermore $\mathbf{M(q;\Theta)}$ and $\mathbf{M(q;\Theta)}^{-1}$ are both differentiable matrix functions (C^{∞} in $\mathbf{q}$) and uniformly bounded above and below as

$$\eta_l \mathbf{E}_n \le \mathbf{M(q;\Theta)} \le \eta_u \mathbf{E}_n \text{ and } \frac{\mathbf{E}_n}{\eta_u} \le \mathbf{M(q;\Theta)}^{-1} \le \frac{\mathbf{E}_n}{\eta_l}, \text{ for all } \mathbf{q} \text{ and } \Theta.$$

Or the induced norms of the corresponding matrices satisfy

$$\delta_l \le \|\mathbf{M(q;\Theta)}\| \le \delta_u \text{ and } \frac{1}{\delta_u} \le \|\mathbf{M(q;\Theta)}^{-1}\| \le \frac{1}{\delta_l},$$

where $\mathbf{E}_n$ is an $n \times n$ identity matrix; η_l, η_u, δ_l, and δ_u $(< \infty)$ are positive constants for revolute joints and depend on the mass properties of the given manipulator.

Property 2: The dynamic model (1) is a linear relationship in the system parameters ($\Theta \in R^m$) of interest

$$\mathbf{M(q;\Theta)}\dot{\mathbf{x}} + \mathbf{C(q,\dot{q};\Theta)}\mathbf{x} + \mathbf{G(q;\Theta)} = \mathbf{R(q,\dot{q},x,\dot{x})}\Theta, \quad \forall \mathbf{q},\dot{\mathbf{q}},\mathbf{x},\dot{\mathbf{x}} \in R^n$$

where $\mathbf{R} \in R^{n \times m}$ is called the "regressor" matrix which consists of known functions of the joint-space variables and its elements are continuous (smooth) functions, and the parameter vector Θ belongs to a bounded set.

Remark: The known matrix ($\mathbf{R}$) is independent of system parameters, and the corresponding linear parameterization may not be unique since the dimensions of the parameter space depends on the specific choice of the parameters.

Property 3: $\mathbf{x}^T(\dot{\mathbf{M}} - 2\mathbf{C})\mathbf{x} = \mathbf{0}, \forall\, \mathbf{x} \in R^n$ with $\|\mathbf{x}\| < \infty$, that is, $(\dot{\mathbf{M}} - 2\mathbf{C})$ is a skew-symmetric matrix (or $\dot{\mathbf{M}} = \mathbf{C} + \mathbf{C}^T$) provided that $\mathbf{C}$ is properly defined as

$$\mathbf{C(q,\dot{q};\Theta)} = \left[\dot{\mathbf{q}}^T \mathbf{C}_k(\mathbf{q};\Theta)\right]_{k=1,\cdots,n},$$

where kth element of vector $\mathbf{C}(\mathbf{q},\dot{\mathbf{q}})\dot{\mathbf{q}}$ is given by $\dot{\mathbf{q}}^T\mathbf{C}_k(\mathbf{q})\dot{\mathbf{q}}$. In this formulation, $\mathbf{C}_k \in R^{n\times n}$ is symmetric and bounded matrix for all $(\mathbf{q},\Theta) \in R^n \times R^m$ (i.e., $\|\mathbf{C}_k\| < \infty$, $\forall k = 1,\cdots,n$), and this matrix may be defined as

$$\mathbf{C}_k = \tfrac{1}{2}[\frac{\partial \mathbf{m}_k}{\partial \mathbf{q}} + (\frac{\partial \mathbf{m}_k}{\partial \mathbf{q}})^T - \frac{\partial \mathbf{M}}{\partial q_k}],$$

where $\mathbf{m}_k$ denotes the kth column (or row) of $\mathbf{M}$ and q_k is the kth element of $\mathbf{q}$.

Property 4: $\mathbf{C}(\mathbf{q},\mathbf{x})\mathbf{y} = \mathbf{C}(\mathbf{q},\mathbf{y})\mathbf{x}$, $\forall(\mathbf{x},\mathbf{y},\mathbf{q}) \in R^n \times R^n \times R^n$, and it is known that the norm of $\mathbf{C}$ satisfies $\|\mathbf{C}\| \le \alpha_1\|\dot{\mathbf{q}}\|$ for any $(\mathbf{q},\dot{\mathbf{q}},\Theta)$, where α_1 is a positive constant number.

Property 5: There exists constant α_2 such that for any $\mathbf{q}$ and Θ, $\mathbf{G}$ is continuously differentiable (C^∞ function in $\mathbf{q}$) and bounded by $\|\mathbf{G}(\mathbf{q};\Theta)\| \le \alpha_2$. $\Delta\Delta$

Note that the fundamental properties mentioned above can be easily justified for a large class of manipulators. For example, the matrix $\mathbf{M}$ and vector $\mathbf{G}$ are bounded by constants, since they contain trigonometric terms in $\mathbf{q}$, and the skew-symmetric property $(\dot{\mathbf{M}} - 2\mathbf{C})$ can be obtained from the fact that the mapping $\mathbf{T} \rightarrow \dot{\mathbf{q}}$ from joint torque to joint velocity is passive. Also note that the vector $\mathbf{C}(\mathbf{q},\dot{\mathbf{q}};\Theta)\dot{\mathbf{q}} \in R^n$ is uniquely defined but the matrix $\mathbf{C}(\mathbf{q},\dot{\mathbf{q}};\Theta)$ is not.

For the system formulation, we make the following assumptions.

Assumption 1: Each degree of freedom of the robot manipulator is powered by an independent control input (or actuator).

Assumption 2: The nature of uncertainties ($\mathbf{T}_u$) strongly influences system performance. Note that the structure of $\mathbf{T}_u$ assumed here are bounded by higher-order polynomials in the system states rather than obeying either constant magnitude or first-order polynomials.

Assumption 3: The system state vectors ($\mathbf{q}$, $\dot{\mathbf{q}}$) are measurable (or available) for all $t \ge 0$ by using such as digital encoder and tachometers (or numerical differentiation in obtaining velocity estimates) and can therefore be utilized in the control synthesis; however, the information about the noise-prone joint acceleration ($\ddot{\mathbf{q}}$) is not necessary.

Assumption 4: The model-parameter vector, $\Theta = (\theta_1, \theta_2, \cdots, \theta_m)^T$, is unknown but assumed to be in between upper and lower bounds. That is, the variation of parameter θ_i is within the prescribed range (or the set) $\psi_i := [\underline{\theta}_i, \overline{\theta}_i] \subset R, \forall i \in [1, m]$, where $\underline{\theta}_i$ and $\overline{\theta}_i$ are known (or unknown) positive constants (i.e., parameter bounds). Therefore, we have $\psi := \psi_1 \times \psi_2 \times \cdots \times \psi_m$ and $\Theta \in \psi \subset R^m$. The set ψ is known (or unknown) but a non-empty compact set. $\Delta\Delta$

Notice that the only information assumed available on Θ is the knowledge of a non-empty set ψ to which it belongs.

Since we shall be mainly concerned with the trajectory tracking problem, a class of allowable desired joint trajectories (which describe the desired dynamic behavior and the motion control specifications) can be stated as follows (assuming that the inverse kinematics problem has been solved).

Assumption 5: For sufficiently smooth trajectories, the desired trajectory ($\mathbf{q}_d \in C^2$ function) and its derivatives are all continuous and uniformly bounded by constants as:

$$d_1 = \sup_{t \geq 0} \|\mathbf{q}_d\| < \infty, \; d_2 = \sup_{t \geq 0} \|\dot{\mathbf{q}}_d\| < \infty, \text{ and } d_3 = \sup_{t \geq 0} \|\ddot{\mathbf{q}}_d\| < \infty$$

where d_1, d_2, and d_3 are some positive constants.

As matter of fact, the above assumptions are neither restrictive nor unrealistic in robot dynamics.

Before proceeding, we introduce the following definitions for the desired system behavior.

Definition 2: Uniform boundedness and uniform ultimate boundedness (UUB).

See Appendix A for definitions [2-5].

Definition 3: Let $B_\zeta(\mathbf{x})$ represent the closed ball in R^n of radius $\zeta > 0$ centered at $\mathbf{x} = \mathbf{0}$:

$$B_\zeta(\mathbf{x}) := \left(\mathbf{x} \in R^n : \|\mathbf{x}\| \leq \zeta\right). \; \Delta\Delta$$

Actually, the UUB in Definition 2 means that the system responses (i.e., system state variables) will eventually enter some target ball, which is bounded by some positive constant $\overline{\zeta}$, around the origin after a finite interval of time $0 \le t_0 \le \overline{T} < \infty$ and remains thereafter $(\forall t{:}[t_0,\infty) \ge t_0 + \overline{T})$, that is, the norms of the system states are ultimately bounded by $\overline{\zeta}$. The required time $\overline{T}$ for target ball only depends on the magnitude of the initial ball (ζ_0) and the target ball ($\overline{\zeta}$) but not on t_0. In fact, the above definition describes the steady-state system performance. More detailed discussions of such a definition can be found in Refs. [2-5].

2.2 Problem Formulations

For the control objective (trajectory tracking problem), a number of joint-space tracking error vectors are defined. $\mathbf{e} \in R^n$ is the vector of the position tracking error defined as $\mathbf{e} = \mathbf{q} - \mathbf{q}_d$, where $\mathbf{q}_d \in R^n$ is the desired joint position vector. Then the reference tracking errors $\dot{\mathbf{e}}_r \in R^n$ are defined by $\dot{\mathbf{e}}_r = \dot{\mathbf{q}}_d - \mathbf{U}\mathbf{e}$, where $\mathbf{U} \in R^{n\times n}$ is a positive definite gain matrix chosen by the designer, $\mathbf{U} = diag(\mu)$, $\mu > 0$. Now define the sliding surface variable vector ($\mathbf{e}_s \in R^n$) as $\mathbf{e}_s(\mathbf{e},\dot{\mathbf{e}}) = \dot{\mathbf{q}} - \dot{\mathbf{e}}_r = \dot{\mathbf{e}} + \mathbf{U}\mathbf{e}$, which is commonly utilized in the sliding mode control method.

Lemma 3: If $\|\mathbf{e}_s(t)\| \le \gamma\ (< \infty)$ is satisfied for any $t \in [t_0,\infty)$ with a scalar constant γ and some t_0, then

$$\|\mathbf{e}(t)\| \le \exp[-\mu(t-t_0)]\left\{\|\mathbf{e}(t_0)\| - \frac{\gamma}{\mu}\right\} + \frac{\gamma}{\mu},$$

$$\|\dot{\mathbf{e}}(t)\| \le \gamma + \mu\|\mathbf{e}(t)\|.$$

Proof: The proof of this lemma is a straightforward.

In fact, this lemma shows that $\mathbf{e}(t)$ and $\dot{\mathbf{e}}(t)$ are also uniformly bounded and their ultimate bounds can be obtained from that of $\mathbf{e}_s$. That is, the corresponding ultimate bounds are given by

$$\lim_{t\to\infty}\|\mathbf{e}(t)\| = \frac{\gamma}{\mu} \text{ and } \lim_{t\to\infty}\|\dot{\mathbf{e}}(t)\| = 2\gamma$$

as long as the initial condition $\|\mathbf{e}(t_0)\|$ is bounded. In the special case, if $\gamma = 0$, then $\lim_{t\to\infty}\|\mathbf{e}(t)\| \to 0$ and $\lim_{t\to\infty}\|\dot{\mathbf{e}}(t)\| \to 0$.

With the above definitions, the next step is to formulate the problem of this study. Roughly speaking, this research presents a design methodology for robot controllers that guarantees the following problem statement (trajectory following problem), provided that some system states $(\mathbf{q}, \dot{\mathbf{q}})$ are available from measurements and also that the desired paths $(\mathbf{q}_d, \dot{\mathbf{q}}_d, \ddot{\mathbf{q}}_d)$ chosen by the user are all continuous and bounded functions of time $(\in L_\infty)$ within a finite workspace.

Problem Statement: For the given nonlinear uncertain dynamic model (1), derive realizable robust control law $\mathbf{T} = \mathbf{h}(t, \mathbf{q}, \dot{\mathbf{q}}, \mathbf{q}_d, \dot{\mathbf{q}}_d, \ddot{\mathbf{q}}_d; \Theta_0), t \geq 0$ by using dynamic compensation such that despite significant uncertainties (or a given class of uncertainties), every signal in the resulting closed-loop system remains bounded within the desired degree of accuracy after a finite time in some suitable sense (i.e., in the sense of Lyapunov stability), for example, uniform boundedness, UUB, and asymptotic stability. $\Delta\Delta$

In the above problem statement, Θ_0 are the estimates (nominal values) of the true values of Θ and $\mathbf{h}(\bullet): R^+ \times R^n \times R^n \times R^n \times R^n \times R^n \times R^m \to R^n$ are nonlinear functions in R^n.

Robust control approach for an uncertain mathematical model generally requires the knowledge of the possible upper bounds of uncertainties in order to implement a controller. Unfortunately, those uncertainties are usually unknown or poorly known. Therefore, some assumptions are made regarding the functional structures of the uncertainties. On the basis of the possible upper bounds of uncertainties, system designers implement a controller to

achieve some desired system responses. Here, the term robust means that the corresponding closed-loop system maintains the prescribed tracking properties under significant uncertainties. These robust control algorithms are usually developed by measuring the size of uncertainties which are typically characterized in terms of (appropriate) norms that enter the robustness conditions.

In what follows, we will present a class of control algorithms requiring minimal on-line computation while maintaining good robustness properties. As stated in the problem statement, the design objective is to formulate a control input vector so that the actual system responses track the desired quantities as closely and fast as possible irrespective of uncertainties. In this study, specifically, the general control structure takes the following form [13, 19],

$$\mathbf{T} = \mathbf{T}^{n/a} + \mathbf{T}^{r/a}, \quad t \geq 0 \tag{2}$$

for the uncertain system (1). Here the nominal control (or the primary controller) is chosen such that

$$\mathbf{T}^{n/a} = \mathbf{M}_0(\mathbf{q}_d;\Theta_0)\ddot{\mathbf{e}}_r + \mathbf{C}_0(\mathbf{q}_d,\dot{\mathbf{q}}_d;\Theta_0)\dot{\mathbf{e}}_r + \mathbf{G}_0(\mathbf{q}_d;\Theta_0) - \mathbf{k}_d\mathbf{e}_s,$$

where $\mathbf{M}_0, \mathbf{C}_0$, and $\mathbf{G}_0$ denote the estimates (or available values) of the true values $\mathbf{M}, \mathbf{C}$, and $\mathbf{G}$ via modeling, respectively; the feedback gain matrices $\mathbf{k}_d = k_d\mathbf{E}_n$ are chosen by the designer ($k_d > 0$). Thus the first part of the general control law consists of model-based feedforward dynamic compensation and PD feedback terms, and the second control term (the auxiliary control input) is given by $\mathbf{T}^{r/a} = -\mathbf{f}(\mathbf{e},\dot{\mathbf{e}},\mathbf{e}_s)$, where $\mathbf{f} \in R^n$ are some nonlinear functions on $(\mathbf{e}, \dot{\mathbf{e}}, \mathbf{e}_s)$ (i.e., nonlinear feedback structure). It is important to note that the control algorithm under consideration is the sum of two parts: the nominal control vector, $\mathbf{T}^{n/a} \in R^n$, is designed to stabilize the nominal system (system with no uncertainties), and the robust nonlinear control laws, $\mathbf{T}^{r/a} \in R^n$, are intended to account for both the resulting errors of the nominal control (or compensation error) and unstructured uncertainties which

are possibly time-varying. This two-stage control scheme is intended to achieve better robustness and tracking performance to significant uncertainties. The torque computation in the model-based portion can be performed off-line since the desired paths ($\mathbf{q}_d, \dot{\mathbf{q}}_d, \ddot{\mathbf{q}}_d$) and the nominal (or fixed) values of system parameters (Θ_0) are known in advance, while many other methods rely heavily on the on-line computations. That is, the quantities $\mathbf{M}_0$, $\mathbf{C}_0$, and $\mathbf{G}_0$ are not updated on-line (i.e., fixed parameters) since they are known values before control. A class of nonlinear feedback structures of robust control ($\mathbf{T}^{rn}$) will be specified later in details. In case of $\mathbf{M}_0 = \mathbf{C}_0 = \mathbf{G}_0 = \mathbf{0}$ in (2), the control structure is simply reduced to $\mathbf{T} = -\mathbf{k}_d\mathbf{e}_s + \mathbf{T}^{rn}$. If $\mathbf{T}^{rn} = \mathbf{0}$, then $\mathbf{T} = \mathbf{M}_0\ddot{\mathbf{e}}_r + \mathbf{C}_0\dot{\mathbf{e}}_r + \mathbf{G}_0 - \mathbf{k}_d\mathbf{e}_s$. In fact, the control scheme presented in (2) is a very general form and can be applied to a wide variety of important systems for motion control purposes.

Remark: Even if the true values ($\Theta \in R^m$) are not available, the possible ranges of parameter variations may be given in the control law (see Assumption 4). For example, the nominal value θ_{0i} may be selected as $\theta_{0i} = \frac{1}{2}(\underline{\theta}_i + \overline{\theta}_i)$, i.e., the mean value of the admissible range of θ_i, or any other manner by designer's convenience. Thus, instead of using the true parameter values ($\Theta \in R^m$) which are unknown, the control laws are designed by using the nominal values (Θ_0) which are known values in this study.

After substituting (2) into (1) and subtracting $\mathbf{M}\ddot{\mathbf{e}}_r + \mathbf{C}\dot{\mathbf{e}}_r + \mathbf{G}$ on both sides of the resulting equation, the error dynamics under the control law (2) can be expressed in the general form as

$$\mathbf{M}(\mathbf{q};\Theta)\dot{\mathbf{e}}_s = -\mathbf{C}(\mathbf{q},\dot{\mathbf{q}};\Theta)\mathbf{e}_s - (\mathbf{T}_u + \Delta\mathbf{R}_r) - \mathbf{k}_d\mathbf{e}_s + \mathbf{T}^{rn}, \tag{3}$$

where $\Delta\mathbf{R}_r \in R^n$ is of the form

$$\begin{aligned}\Delta\mathbf{R}_r = {} & [\mathbf{M}(\mathbf{q};\Theta) - \mathbf{M}_0(\mathbf{q}_d;\Theta_0)]\ddot{\mathbf{e}}_r + [\mathbf{C}(\mathbf{q},\dot{\mathbf{q}};\Theta) - \mathbf{C}_0(\mathbf{q}_d,\dot{\mathbf{q}}_d;\Theta_0)]\dot{\mathbf{e}}_r \\ & + [\mathbf{G}(\mathbf{q};\Theta) - \mathbf{G}_0(\mathbf{q}_d;\Theta_0)].\end{aligned} \tag{4}$$

Here the vector $\Delta\mathbf{R}_r(\mathbf{e},\dot{\mathbf{e}},\ddot{\mathbf{q}}_d;\Theta_0,\Theta)$ represents the structured uncertainties which are caused by modeling errors (or parameter variations) when the model structure is well known. It should be noted that $\Delta\mathbf{R}_r$ may be zero for the complete model-following of the control system. Unfortunately, in most real applications, the estimated parameters always differ from the actual ones, in other words, $\Delta\mathbf{R}_r$ is non-zero and even unknown (i.e., the nonlinear feedforward compensation is generally not perfect).

As stated before, robust control approaches usually require the evaluation of upper bounds on the system uncertainties for the implementation of controllers and the robustness (or stability) analysis. That is, the robust control synthesis will be based on a certain deterministic properties on the uncertainty bounds. Apparently, these bounds give insight to the strength and significance of uncertainties and may be used to judge whether complicated model-based control laws should be preferred rather than simple linear controllers. So far, only a few researchers discuss the evaluation of the norm bounds on the uncertainties. Since the conservative bounds make robustness criteria very restrictive, a successful application of any robust control methods is the development of these norm bounds by using suitable techniques. In what follows, the possible norm bounds on the uncertainties ($\Delta\mathbf{R}_r$ and $\mathbf{T}_u$) will be examined. As we shall see later, the only information assumed on $\Delta\mathbf{R}_r$ and $\mathbf{T}_u$ is bounded in magnitude, usually in their Euclidean norms. In deterministic control approach, the possible upper bounds on the system uncertainties ($\Delta\mathbf{R}_r$ and $\mathbf{T}_u$) can be expressed in the general form as

$$\|\Delta\mathbf{R}_r\| \le \phi_{ri}(t,\mathbf{e},\dot{\mathbf{e}}) \text{ and } \|\mathbf{T}_u\| \le \phi_{ui}(t,\mathbf{e},\dot{\mathbf{e}}),\ i=1,2$$

where $\phi_{ri}(\bullet): R^+ \times R^n \times R^n \to R^+$ and $\phi_{ui}(\bullet): R^+ \times R^n \times R^n \to R^+$ are the scalar bounding functions which are actually the functions of the Euclidean norms of the system states. For the specific purposes of the real applications, the scalar bounding functions can be given in many different forms.

First, the following assumptions are made on the dynamic model.

Assumption 6: There exist scalar constants $\rho_{11}, \rho_{12}, \rho_{13}$, and $\rho_{14} \in R^+, \forall t \in R^+$, such that

(i) $$\rho_{11} := \sup_{\Theta \in \Psi} \sup_{(\mathbf{q},\mathbf{q}_d) \in R^n \times R^n} \left\| \mathbf{M}(\mathbf{q};\Theta) - \mathbf{M}_0(\mathbf{q}_d;\Theta_0) \right\|,$$

(ii) $$\left\| \mathbf{C}(\mathbf{q},\dot{\mathbf{q}};\Theta) - \mathbf{C}_0(\mathbf{q}_d,\dot{\mathbf{q}}_d;\Theta_0) \right\| \le \rho_{12}\|\dot{\mathbf{q}}\| + \rho_{13}\|\dot{\mathbf{q}}_d\|,$$

in which

$$\rho_{12} := \sup_{\Theta \in \Psi} \sup_{\mathbf{q} \in R^n} \sum_{k=1}^{n} \left\| \mathbf{C}_k(\mathbf{q};\Theta) \right\|,$$

$$\rho_{13} := \sup_{\Theta_0 \in \Psi} \sup_{\mathbf{q}_d \in R^n} \sum_{k=1}^{n} \left\| \mathbf{C}_{0k}(\mathbf{q}_d;\Theta_0) \right\|,$$

(iii) $$\rho_{14} := \sup_{\Theta \in \Psi} \sup_{(\mathbf{q},\mathbf{q}_d) \in R^n \times R^n} \left\| \mathbf{G}(\mathbf{q};\Theta) - \mathbf{G}_0(\mathbf{q}_d;\Theta_0) \right\|,$$

where ρ_{1i} $(i = 1,\cdots,4)$ represent the bounds on the modeling errors. Now, we will provide quantitative information on the bounding properties of the uncertainties. The first step is to examine the bound of $\Delta\mathbf{R}_r$. Based on Assumptions 5 and 6, the following lemma provides the possible upper bound on $\Delta\mathbf{R}_r$ [6].

Lemma 4: The structured uncertainties ($\Delta\mathbf{R}_r$) is bounded in the norm as

$$\left\| \Delta\mathbf{R}_r \right\| \le c_0 + c_1\|\mathbf{e}\| + c_2\|\dot{\mathbf{e}}\| + c_3\|\mathbf{e}\|\|\dot{\mathbf{e}}\| = \phi_{r1},$$

where $c_i (i = 0,1,2,3)$ are finite constants that depend on the size of the uncertainties (i.e., the size of parametric variations and the upper bounds of the desired trajectories).

Proof: See Appendix B for the complete proof of this lemma.

As mentioned previously, the robust nonlinear controls ($\mathbf{T}^{rc}$) are intended to cope with the total uncertainties ($\mathbf{T}_u$ and $\Delta\mathbf{R}_r$) which are based on the certain deterministic properties. Generally speaking, the uncertainties are functions of the system states {i.e., $\mathbf{T}_u(\mathbf{e},\dot{\mathbf{e}})$ and $\Delta\mathbf{R}_r(\mathbf{e},\dot{\mathbf{e}},\ddot{\mathbf{q}}_d;\Theta_0,\Theta)$}, thus they may grow if the system states become unstable.

In this research, two general design schemes can be employed to compensate for the uncertainties in the closed-loop error dynamics (3) by suitable choices of robust nonlinear controls $\mathbf{T}^{rc}$: that is, nonadaptive and adaptive bounds of the robust nonlinear controllers.

The possible upper bounds on the uncertainties are assumed to be known for a class of nonadaptive robust control laws in Section 3. Without knowledge of these bounds, an adaptive version of a robust controller will be designed to directly identify these bounds in Section 4.

3. A CLASS OF NON-ADAPTIVE ROBUST CONTROL LAWS (DECENTRALIZED CONTROL SCHEMES)

In the rest of this section, given the general structure of control equation (2), the design procedure for a class of robust nonlinear control law ($\mathbf{T}^{rv}$) with nonadaptive bounds will be presented to cope with system uncertainties. In addition, the proposed controls can be implemented in a decentralized manner for real-time control purposes. The system uncertainties under consideration are assumed to be known.

3.1 Controller 1

Usually the system parameters are uncertain but so are the model structure. Thus, the following assumption is made on the unstructured uncertainties ($\mathbf{T}_u$) in this subsection.

Assumption 7: The unknown function $\mathbf{T}_u(t,\mathbf{e},\dot{\mathbf{e}}): R^+ \times R^n \times R^n \rightarrow R^n$ is bounded by

$$\|\mathbf{T}_u\| \le d_0 + d_1\|\mathbf{e}\| + d_2\|\dot{\mathbf{e}}\| + d_3\|\mathbf{e}\|\|\dot{\mathbf{e}}\| = \phi_{u1},$$

where $d_i (i = 0,1,2,3) \in R^+$ are known constants. $\Delta\Delta$

In the above assumption, the uncertainties are represented by a polynomial-type bounding function in the Euclidean norm with known coefficients.

In order to fulfill the requirements of designing a robust controller, *a priori* knowledge of possible bounds (or $\mathbf{c} \in R^4$ and $\mathbf{d} \in R^4$) in Lemma 4 and Assumption 7 are required.

In this subsection, the control law $\mathbf{T}^{rv}$ takes the following polynomial-type form

$$\mathbf{T}^{rv} = -\mathbf{k}_c\|\mathbf{e}\|^2\mathbf{e}_s. \tag{5}$$

Then the complete control law can be expressed as

$$\mathbf{T} = \mathbf{M}_0(\mathbf{q}_d;\Theta_0)\ddot{\mathbf{e}}_r + \mathbf{C}_0(\mathbf{q}_d,\dot{\mathbf{q}}_d;\Theta_0)\dot{\mathbf{e}}_r + \mathbf{G}_0(\mathbf{q}_d;\Theta_0) - \mathbf{k}_d\mathbf{e}_s - \mathbf{k}_c\|\mathbf{e}\|^2\mathbf{e}_s, \tag{6}$$

where the control gains $\mathbf{k}_a$ and $\mathbf{k}_c \in R^{n\times n}$ may be selected as diagonal matrices by the designer, that is, $\mathbf{k}_a = k_a\mathbf{E}_n$ and $\mathbf{k}_c = k_c\mathbf{E}_n$, ($k_a$ and $k_c > 0$).

Now, the stability and the tracking properties of the closed-loop system (3) with robust control law (5) are stated by the Lyapunov approach.

Theorem 1: Consider the closed-loop system dynamics (3) with known constants $\mathbf{c}$ and $\mathbf{d}$ on the uncertainty bounds in Lemma 4 and Assumption 7. Then the solutions $(\mathbf{e}(t),\mathbf{e}_s(t))$ under the control law (5) requiring only position and velocity measurements are globally uniformly ultimately bounded with respect to V_f. That is, there exists the compact set Ω_f such that for all $(\mathbf{e}(0),\mathbf{e}_s(0)) \in \overline{\Omega}$, the system responses globally converge to the following compact set:

$$\Omega_f = \left\{(\mathbf{e},\mathbf{e}_s) \in R^n \times R^n : V(\mathbf{e},\mathbf{e}_s) \le V_f\right\},$$

where the ultimate bound is given by $V_f = \dfrac{\gamma_3}{\gamma_0}$ and the set Ω_f is a subset of $\overline{\Omega}$ (i.e., $\Omega_f \subset \overline{\Omega}$). In other words, every solution starting at $t = t_0$ from the set $\overline{\Omega}$ crosses the target set Ω_f at $t = t_0 + \overline{T}$ and settles in Ω_f thereafter.

Proof: Consider the Lyapunov function candidate (a C^1 function), $V(\bullet): R^+ \times R^n \times R^n \to R^+$, for the closed-loop system as

$$V = \frac{1}{2}\mathbf{e}_s{}^T\mathbf{M}(\mathbf{q})\mathbf{e}_s + \frac{1}{2}\mathbf{e}^T\mathbf{F}\mathbf{e}, \tag{7}$$

where $\mathbf{F} = \varepsilon\mathbf{E}_n$, $\varepsilon > 0$. For a real, symmetric, and positive-definite matrix $\mathbf{A} \in R^{n\times n}$, the following inequality can be established by Rayleigh's principle

$$\sigma_{\min}(\mathbf{A})\|\mathbf{x}\|^2 \le \mathbf{x}^T\mathbf{A}\mathbf{x} \le \sigma_{\max}(\mathbf{A})\|\mathbf{x}\|^2, \ \forall \mathbf{x} \in R^n$$

It is clear that an upper and a lower bound on the Lyapunov function (7) can be estimated as

$$\frac{1}{2}\min\{\sigma_{\min}(\mathbf{M}),\varepsilon\}[\|\mathbf{e}_s\|^2 + \|\mathbf{e}\|^2] \le \frac{1}{2}\sigma_{\min}(\mathbf{M})\|\mathbf{e}_s\|^2 + \frac{1}{2}\varepsilon\|\mathbf{e}\|^2 \le V$$

$$\frac{1}{2}\sigma_{\max}(\mathbf{M})\|\mathbf{e}_s\|^2 + \frac{1}{2}\varepsilon\|\mathbf{e}\|^2 \le \frac{1}{2}\max\{\sigma_{\max}(\mathbf{M}),\varepsilon\}[\|\mathbf{e}_s\|^2 + \|\mathbf{e}\|^2]$$

which implies that V is clearly a legitimate Lyapunov function candidate and radially unbounded scalar function of $\mathbf{e}$ and $\mathbf{e}_s$, i.e., $V \to \infty$ as $\|\mathbf{e}\| \to \infty$ and $\|\mathbf{e}_s\| \to \infty$.

The total time derivative of V along the equation (3) is given by

$$\begin{aligned}\dot{V} &= \mathbf{e}_s^T \mathbf{M}\dot{\mathbf{e}}_s + \frac{1}{2}\mathbf{e}_s^T \dot{\mathbf{M}}\mathbf{e}_s + \mathbf{e}^T \mathbf{F}\dot{\mathbf{e}} \\ &= \mathbf{e}_s^T \{-\mathbf{C}(\mathbf{q},\dot{\mathbf{q}})\mathbf{e}_s - (\mathbf{T}_u + \Delta\mathbf{R}) - [\mathbf{k}_a + \mathbf{k}_c\|\mathbf{e}\|^2]\mathbf{e}_s\} + \frac{1}{2}\mathbf{e}_s^T \dot{\mathbf{M}}\mathbf{e}_s + \mathbf{e}^T \mathbf{F}\dot{\mathbf{e}} \end{aligned} \tag{8}$$

Utilizing Property 3, we obtain the upper bound on the time derivative of the Lyapunov function as

$$\begin{aligned}\dot{V} \le{}& \|\mathbf{e}_s\|\{c_0 + d_0 + (c_1 + d_1)\|\mathbf{e}\| + (c_2 + d_2)\|\dot{\mathbf{e}}\| + (c_3 + d_3)\|\mathbf{e}\|\|\dot{\mathbf{e}}\|\} \\ &-\{k_a + k_c\|\mathbf{e}\|^2\}\|\mathbf{e}_s\|^2 + \mathbf{e}^T \mathbf{F}(\mathbf{e}_s - \Lambda\mathbf{e})\end{aligned}$$

which leads to

$$\begin{aligned}&\le (c_0 + d_0)\|\mathbf{e}_s\| + (c_1 + d_1)\|\mathbf{e}\|\|\mathbf{e}_s\| + (c_2 + d_2)\|\mathbf{e}_s\|\|\dot{\mathbf{e}}\| + (c_3 + d_3)\|\mathbf{e}\|\|\mathbf{e}_s\|\|\dot{\mathbf{e}}\| \\ &\quad -k_a\|\mathbf{e}_s\|^2 - k_c\|\mathbf{e}\|^2\|\mathbf{e}_s\|^2 + \varepsilon\|\mathbf{e}\|\|\mathbf{e}_s\| - \varepsilon\mu\|\mathbf{e}\|^2 \end{aligned} \tag{9}$$

For further simplification, noting that $\|\dot{\mathbf{e}}\| \le \|\mathbf{e}_s\| + \mu\|\mathbf{e}\|$, then (9) satisfies

$$\begin{aligned}\dot{V} \le{}& (c_0 + d_0)\|\mathbf{e}_s\| + (c_1 + d_1)\|\mathbf{e}\|\|\mathbf{e}_s\| + (c_2 + d_2)\|\mathbf{e}_s\|\{\|\mathbf{e}_s\| + \mu\|\mathbf{e}\|\} \\ &+ (c_3 + d_3)\|\mathbf{e}\|\|\mathbf{e}_s\|\{\|\mathbf{e}_s\| + \mu\|\mathbf{e}\|\} - k_a\|\mathbf{e}_s\|^2 - k_c\|\mathbf{e}\|^2\|\mathbf{e}_s\|^2 + \varepsilon\|\mathbf{e}\|\|\mathbf{e}_s\| - \varepsilon\mu\|\mathbf{e}\|^2\end{aligned}$$

Further manipulation yields

$$\begin{aligned}\dot{V} \le{}& (c_0 + d_0)\|\mathbf{e}_s\| + (c_1 + d_1)\|\mathbf{e}\|\|\mathbf{e}_s\| + (c_2 + d_2)\|\mathbf{e}_s\|^2 + (c_2 + d_2)\mu\|\mathbf{e}\|\|\mathbf{e}_s\| \\ &+ (c_3 + d_3)\|\mathbf{e}\|\|\mathbf{e}_s\|^2 + (c_3 + d_3)\mu\|\mathbf{e}\|^2\|\mathbf{e}_s\| \\ &-k_a\|\mathbf{e}_s\|^2 - k_c\|\mathbf{e}\|^2\|\mathbf{e}_s\|^2 + \varepsilon\|\mathbf{e}\|\|\mathbf{e}_s\| - \varepsilon\mu\|\mathbf{e}\|^2. \end{aligned} \tag{10}$$

After grouping terms, the differential inequality (10) can be upper bounded by

$$\begin{aligned}\dot{V} \le{}& \{-k_a + (c_2 + d_2)\}\|\mathbf{e}_s\|^2 - k_c\|\mathbf{e}\|^2\|\mathbf{e}_s\|^2 + (c_3 + d_3)\|\mathbf{e}\|\|\mathbf{e}_s\|^2 \\ &+ (c_3 + d_3)\mu\|\mathbf{e}\|^2\|\mathbf{e}_s\| \\ &+\{(c_1 + d_1) + (c_2 + d_2)\mu + \varepsilon\}\|\mathbf{e}\|\|\mathbf{e}_s\| - \varepsilon\mu\|\mathbf{e}\|^2 + (c_0 + d_0)\|\mathbf{e}_s\| \end{aligned} \tag{11}$$

Completing squares and regrouping terms by using inequality $abc \le \frac{1}{4}b^2 + a^2c^2$ $(a,b,c \in R^+)$ in (11), we have

$$\dot{V} \le -\left\{\frac{k_a}{2} - (c_2 + d_2) - \frac{(c_3 + d_3)^2}{2k_c} - \left[(c_1 + d_1) + (c_2 + d_2)\mu + \varepsilon\right]^2\right\}\|\mathbf{e}_s\|^2$$
$$-\left\{\varepsilon\mu - \frac{\mu^2(c_3 + d_3)^2}{2k_c} - \frac{1}{4}\right\}\|\mathbf{e}\|^2 + \frac{(c_0 + d_0)^2}{2k_a}$$
$$-\frac{k_c}{2}\|\mathbf{e}_s\|^2\left\{\|\mathbf{e}\| - \frac{(c_3 + d_3)}{k_c}\right\}^2 - \frac{k_c}{2}\|\mathbf{e}\|^2\left\{\|\mathbf{e}_s\| - \frac{(c_3 + d_3)\mu}{k_c}\right\}^2 \tag{12}$$
$$-\frac{k_a}{2}\left\{\|\mathbf{e}_s\| - \frac{(c_0 + d_0)}{k_a}\right\}^2$$

Dropping the last three negative terms in (12) yields

$$\dot{V} \le -\left\{\frac{k_a}{2} - (c_2 + d_2) - \frac{(c_3 + d_3)^2}{2k_c} - \left[(c_1 + d_1) + (c_2 + d_2)\mu + \varepsilon\right]^2\right\}\|\mathbf{e}_s\|^2$$
$$-\left\{\varepsilon\mu - \frac{(c_3 + d_3)^2\mu^2}{2k_c} - \frac{1}{4}\right\}\|\mathbf{e}\|^2 + \frac{(c_0 + d_0)^2}{2k_a} \tag{13}$$

Letting

$$\gamma_1 = \frac{k_a}{2} - (c_2 + d_2) - \frac{(c_3 + d_3)^2}{2k_c} - \left[(c_1 + d_1) + (c_2 + d_2)\mu + \varepsilon\right]^2$$
$$\gamma_2 = \varepsilon\mu - \frac{(c_3 + d_3)^2\mu^2}{2k_c} - \frac{1}{4}$$
$$\gamma_3 = \frac{(c_0 + d_0)^2}{2k_a},$$

where γ_1, γ_2, and γ_3 can be positive constants with proper choices of design parameters (k_a, k_c, and μ), we can express the differential inequality (13) in the more compact form as

$$\dot{V} \le -\gamma_1\|\mathbf{e}_s\|^2 - \gamma_2\|\mathbf{e}\|^2 + \gamma_3 \tag{14}$$

Let $\gamma_0 = \min\left\{\frac{2\gamma_1}{\sigma_{\max}(\mathbf{M})}, \frac{2\gamma_2}{\varepsilon}\right\}$, then

$$\dot{V} \le -\gamma_0 V + \gamma_3 \tag{15}$$

Therefore, for $V_f = \frac{\gamma_3}{\gamma_0} \ge 0$, one have $\dot{V} < 0$ if $V > V_f$ (or $V \subset \Omega_f'$), where Ω_f' denotes the complement of Ω_f, i.e.,

$$\lim_{t\to\infty}\int_0^t \dot{V}(\tau)d\tau = V_f - V_0 \text{ and } |V_f - V_0| < \infty, \text{ with } V_0 = V_{t=0}(\mathbf{e},\mathbf{e}_s).$$

It can be concluded that the closed-loop system is globally bounded. A detailed solution of (15) for all $t \geq 0$ can be expressed as

$$V(\mathbf{e},\mathbf{e}_s) \leq \exp(-\gamma_0 t)\left\{V_0 - \frac{\gamma_3}{\gamma_0}\right\} + \frac{\gamma_3}{\gamma_0},\ t \geq 0 \tag{16}$$

where $V_0 \leq \frac{1}{2}\max\{\sigma_{\max}(\mathbf{M},\varepsilon)\}[\|\mathbf{e}_s(0)\|^2 + \|\mathbf{e}(0)\|^2]$, and the function $V(\mathbf{e},\mathbf{e}_s)$ decreases monotonically at rate of $\exp(-\gamma_0 t)$ until the solution reaches the target ball (or the residual set) Ω_f in a finite time. Therefore V is uniformly bounded and its ultimate bound (V_f) can be given by $0 \leq \lim_{t\to\infty} V = \inf_t V = V_f \leq V_0 < \infty$. In other words, the system state variables are uniformly bounded for all time. Moreover, the norm bounds of tracking errors ($\mathbf{e}$ and $\mathbf{e}_s$) can be shown to be as

$$\|\mathbf{e}_s\| \leq \frac{1}{\sqrt{\sigma_{\min}(\mathbf{M})}}\left\{\exp(-\gamma_0 t)\left[V_0 - \frac{\gamma_3}{\gamma_0}\right] + \frac{\gamma_3}{\gamma_0}\right\}^{1/2} \tag{17}$$

$$\|\mathbf{e}\| \leq \frac{1}{\sqrt{\varepsilon}}\left\{\exp(-\gamma_0 t)\left[V_0 - \frac{\gamma_3}{\gamma_0}\right] + \frac{\gamma_3}{\gamma_0}\right\}^{1/2}. \tag{18}$$

The above results also imply that the system responses converge to the following ball as $t \to \infty$:

$$B(\mathbf{e}) = \left\{\mathbf{e} \in R^n : \|\mathbf{e}\| \leq \frac{1}{\sqrt{\varepsilon}}\left(\frac{\gamma_3}{\gamma_0}\right)^{1/2}\right\}$$

and $$B(\mathbf{e}_s) = \left\{\mathbf{e}_s \in R^n : \|\mathbf{e}_s\| \leq \frac{1}{\sqrt{\sigma_{\min}(\mathbf{M})}}\left(\frac{\gamma_3}{\gamma_0}\right)^{1/2}\right\}.$$

As a consequence, the global ultimate boundedness results of all signals (or tracking errors) were guaranteed with respect to V_f in this design. In other words, the Euclidean norms of the tracking errors never leave the closed ball after a finite interval of time. One can manipulate the design parameters to determine the size of the residual set. However, from the practical point of view, the system designer should determine the trade-off between the

minimization of size of the residual set (or better tracking performances) and practical control gains (or control energy).

Remark: From Lemma 3, the boundedness of the sliding surface vector ($\mathbf{e}_s$) guarantees that of $\dot{\mathbf{e}}$.

3.2 Controller 2

In this subsection, the uncertainties $\Delta\mathbf{R}_r$ and $\mathbf{T}_u$ under consideration are the same as those in the previous subsection given by polynomial bounds, that is, all uncertainties are bounded in magnitude (i.e., in their Euclidean norm). The information on the possible bounds of uncertainties are also required. Based on the polynomial bounds, the following saturation-type (or boundary layer) control scheme [12-14, 19] is synthesized as

$$\mathbf{T}^{rv} = -\kappa(\mathbf{e},\mathbf{e}_s)\frac{\mathbf{e}_s}{\|\mathbf{e}_s\|+\xi}, \tag{19}$$

where the gain factor $\kappa(\mathbf{e},\mathbf{e}_s)$ can be expressed as

$$\kappa(\mathbf{e},\mathbf{e}_s) = \mathbf{k}_c\|\mathbf{e}\|^2\|\mathbf{e}_s\|$$

and $\xi > 0$ is free parameter which can be chosen arbitrarily by the designer. The existence of ξ in $\mathbf{T}^{rv}$ guarantees the continuity of control input even when $\|\mathbf{e}_s\|$ becomes zero. Thus the control action is continuous everywhere. In case of $\xi = 0$, the control action $\mathbf{T}^{rv}$ becomes a purely VS control law (or min-max controller), i.e., signum (or sign) function. If the control law is discontinuous in the system state variables, it causes chattering problem which is undesirable in the practical implementations. In order to smooth the control input, the boundary layer is adopted (see Fig. 1).

Then the overall control algorithm can be represented by

$$\begin{aligned}\mathbf{T} = {} & \mathbf{M}_0(\mathbf{q}_d;\Theta_0)\ddot{\mathbf{e}}_r + \mathbf{C}_0(\mathbf{q}_d,\dot{\mathbf{q}}_d;\Theta_0)\dot{\mathbf{e}}_r + \mathbf{G}_0(\mathbf{q}_d;\Theta_0) \\ & - \mathbf{k}_d\mathbf{e}_s - \mathbf{k}_c\|\mathbf{e}\|^2\|\mathbf{e}_s\|\frac{\mathbf{e}_s}{\|\mathbf{e}_s\|+\xi}.\end{aligned} \tag{20}$$

Now the system responses under the robust control law (19) are summarized in the following theorem, and the corresponding proof is also presented to ascertain the stability of the closed-loop system (3).

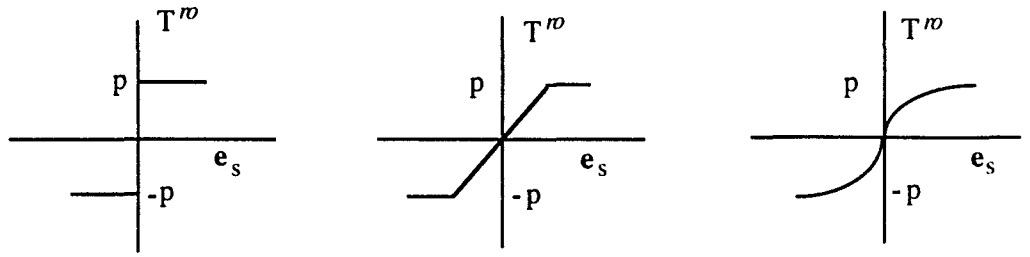

(1) (2) (3)

Figure 1. VS-type controllers ($\mathbf{T}^m = p\frac{\mathbf{e}_s}{\|\mathbf{e}_s\| + \xi}$): (1) Purely discontinuous control (or Bang-bang Control), (2) Saturation type control, (3) Smooth control.

Theorem 2: Consider the closed-loop system dynamics (3) with all bounded desired trajectories and with known constants c_i and d_i on the uncertainty bounds. Then the solutions $(\mathbf{e}(t), \mathbf{e}_s(t))$ in the closed-loop system are uniformly ultimately bounded. That is to say, there exists the compact set Ω_f such that the system responses globally converge to the residual set:

$$\Omega_f = \left\{(\mathbf{e}, \mathbf{e}_s) \in R^n \times R^n : V(\mathbf{e}, \mathbf{e}_s) \le V_f\right\}, \text{ where } V_f = \frac{\gamma_3}{\gamma_0}$$

Proof: The complete proof of this theorem follows the same procedure as that of Theorem 1. Choose the following Lyapunov-like function:

$$V = \tfrac{1}{2}\mathbf{e}_s^T\mathbf{M}(\mathbf{q})\mathbf{e}_s + \tfrac{1}{2}\mathbf{e}^T\mathbf{F}\mathbf{e} \tag{21}$$

Computing its time derivative (21) with respect to the closed-loop system (3), we get

$$\dot{V} = \mathbf{e}_s^T\mathbf{M}\dot{\mathbf{e}}_s + \frac{1}{2}\mathbf{e}_s^T\dot{\mathbf{M}}\mathbf{e}_s + \mathbf{e}^T\mathbf{F}\dot{\mathbf{e}}$$

$$= \mathbf{e}_s^T\left\{-\mathbf{C}(\mathbf{q},\dot{\mathbf{q}})\mathbf{e}_s - (\mathbf{T}_u + \Delta\mathbf{R}) - \mathbf{k}_d\mathbf{e}_s - \kappa(\mathbf{e},\mathbf{e}_s)\frac{\mathbf{e}_s}{\|\mathbf{e}_s\| + \xi}\right\} + \frac{1}{2}\mathbf{e}_s^T\dot{\mathbf{M}}\mathbf{e}_s + \mathbf{e}^T\mathbf{F}\dot{\mathbf{e}} \tag{22}$$

The upper bound on $\dot{V}$ is given by

$$\dot{V} \le \|\mathbf{e}_s\|\{c_0 + d_0 + (c_1 + d_1)\|\mathbf{e}\| + (c_2 + d_2)\|\dot{\mathbf{e}}\| + (c_3 + d_3)\|\mathbf{e}\|\|\dot{\mathbf{e}}\|\}$$
$$- \mathbf{k}_a\|\mathbf{e}_s\|^2 - \kappa(\mathbf{e},\mathbf{e}_s)\frac{\|\mathbf{e}_s\|^2}{\|\mathbf{e}_s\| + \xi} + \mathbf{e}^T\mathbf{F}(\mathbf{e}_s - \Lambda\mathbf{e}) \tag{23}$$

Note the fact that $\dfrac{\|\mathbf{e}_s\|^2}{\|\mathbf{e}_s\| + \xi} \ge \|\mathbf{e}_s\| - \xi$ and $\|\dot{\mathbf{e}}\| \le \|\mathbf{e}_s\| + \mu\|\mathbf{e}\|$. Hence, it is bounded by

$$\dot{V} \le (c_0 + d_0)\|\mathbf{e}_s\| + (c_1 + d_1)\|\mathbf{e}\|\|\mathbf{e}_s\| + (c_2 + d_2)\|\mathbf{e}_s\|\{\|\mathbf{e}_s\| + \mu\|\mathbf{e}\|\}$$
$$+ (c_3 + d_3)\|\mathbf{e}\|\|\mathbf{e}_s\|\{\|\mathbf{e}_s\| + \mu\|\mathbf{e}\|\}$$
$$-k_a\|\mathbf{e}_s\|^2 - k_c\|\mathbf{e}\|^2\|\mathbf{e}_s\|[\|\mathbf{e}_s\| - \xi] + \mu^2\|\mathbf{e}\|\|\mathbf{e}_s\| - \mu^3\|\mathbf{e}\|^2 \tag{24}$$

After some algebraic manipulations and grouping terms, one can obtain

$$\dot{V} \le \{-k_a + (c_2 + d_2)\}\|\mathbf{e}_s\|^2 - k_c\|\mathbf{e}\|^2\|\mathbf{e}_s\|^2 + (c_3 + d_3)\|\mathbf{e}\|\|\mathbf{e}_s\|^2$$
$$+ \{(c_3 + d_3)\mu + k_c\xi\}\|\mathbf{e}\|^2\|\mathbf{e}_s\|$$
$$+\{(c_1 + d_1) + (c_2 + d_2)\mu + \mu^2\}\|\mathbf{e}\|\|\mathbf{e}_s\| - \mu^3\|\mathbf{e}\|^2 + (c_0 + d_0)\|\mathbf{e}_s\|. \tag{25}$$

Use the inequality $abc \le \frac{1}{4}b^2 + a^2c^2$ for completing squares (25), then it follow that

$$\dot{V} \le -\left\{\frac{k_a}{2} - (c_2 + d_2) - \frac{(c_3 + d_3)^2}{2k_c} - [(c_1 + d_1) + (c_2 + d_2)\mu + \varepsilon]^2\right\}\|\mathbf{e}_s\|^2$$
$$-\left\{\varepsilon\mu - \frac{[(c_3 + d_3)\mu + k_c\xi]^2}{2k_c} - \frac{1}{4}\right\}\|\mathbf{e}\|^2 + \frac{(c_0 + d_0)^2}{2k_a}$$
$$-\frac{k_c}{2}\|\mathbf{e}_s\|^2\left\{\|\mathbf{e}\| - \frac{(c_3 + d_3)}{k_c}\right\}^2 - \frac{k_c}{2}\|\mathbf{e}\|^2\left\{\|\mathbf{e}_s\| - \frac{[(c_3 + d_3)\mu + k_c\xi]}{k_c}\right\}^2$$
$$-\frac{k_a}{2}\left\{\|\mathbf{e}_s\| - \frac{(c_0 + d_0)}{k_a}\right\}^2 \tag{26}$$

Letting

$$\gamma_1 = \frac{k_a}{2} - (c_2 + d_2) - \frac{(c_3 + d_3)^2}{2k_c} - [(c_1 + d_1) + (c_2 + d_2)\mu + \varepsilon]^2$$

$$\gamma_2 = \varepsilon\mu - \frac{[(c_3 + d_3)\mu + k_c\xi]^2}{2k_c} - \frac{1}{4}$$

$$\gamma_3 = \frac{(c_0 + d_0)^2}{2k_a}.$$

Then $\dot{V}$ satisfies the following inequality:

$$\dot{V} \le -\gamma_1 \|\mathbf{e}_s\|^2 - \gamma_2 \|\mathbf{e}\|^2 + \gamma_3, \tag{27}$$

where γ_1, γ_2, and γ_3 can be positive constants with proper choices of design parameters (k_a, k_c, and μ). Or more compactly,

$$\dot{V} \le -\gamma_0 V + \gamma_3, \tag{28}$$

where $\gamma_0 = \min\left\{\frac{\gamma_1}{\sigma_{\max}(\mathbf{M})}, \frac{\gamma_2}{\varepsilon}\right\}$. Therefore, for some $V_f = \frac{\gamma_3}{\gamma_0} \ge 0$, one have $\dot{V} < 0$ whenever $V > V_f$ ($or\ V \subset \Omega_f^c$), i.e., $\forall \mathbf{e}, \mathbf{e}_s \in \Omega_f^c$, where Ω_f^c is the complement of Ω_f.

A solution of (28) is written as

$$V(\mathbf{e}, \mathbf{e}_s) \le \exp(-\gamma_0 t)\left\{V_0(\mathbf{e}(0), \mathbf{e}_s(0)) - \frac{\gamma_3}{\gamma_0}\right\} + \frac{\gamma_3}{\gamma_0}. \tag{29}$$

The function $V(\mathbf{e}, \mathbf{e}_s)$ decreases at rate of $\exp(-\gamma_0 t)$ until the solution reaches the ball (or the residual set) Ω_f in a finite time. It also can be further shown to be as

$$\|\mathbf{e}_s\| \le \frac{1}{\sqrt{\sigma_{\min}(\mathbf{M})}}\left\{\exp(-\gamma_0 t)\left[V_0 - \frac{\gamma_3}{\gamma_0}\right] + \frac{\gamma_3}{\gamma_0}\right\}^{1/2} \tag{30}$$

$$\|\mathbf{e}\| \le \frac{1}{\sqrt{\varepsilon}}\left\{\exp(-\gamma_0 t)\left[V_0 - \frac{\gamma_3}{\gamma_0}\right] + \frac{\gamma_3}{\gamma_0}\right\}^{1/2}. \tag{31}$$

The above inequalities imply that the system responses converge to the following ball as $t \to \infty$:

$$B(\mathbf{e}) = \left\{\mathbf{e} \in R^n : \|\mathbf{e}\| \le \frac{1}{\sqrt{\varepsilon}}\left(\frac{\gamma_3}{\gamma_0}\right)^{1/2}\right\}$$

and $$B(\mathbf{e}_s) = \left\{\mathbf{e}_s \in R^n : \|\mathbf{e}_s\| \le \frac{1}{\sqrt{\sigma_{\min}(\mathbf{M})}}\left(\frac{\gamma_3}{\gamma_0}\right)^{1/2}\right\}. \tag{32}$$

Using the same reasoning as in the previous subsection, we can prove that all signals are globally bounded for all $t \ge 0$ as long as initial condition (V_0) is bounded. As a consequence, the global boundedness of all signals were established for all $t \ge 0$.

3.3 Controller 3

Introduce the augmented state error vector $\mathbf{x}_e \in R^{2n}$ as $\mathbf{x}_e(\mathbf{e},\dot{\mathbf{e}}) = \left[\mathbf{e}^T, \dot{\mathbf{e}}^T\right]^T$. Now new assumptions are made regarding the uncertainty bounds on $\mathbf{T}_u$ and $\Delta\mathbf{R}_r$ with known scalar bounding functions $\phi_{u2}(\geq \|\mathbf{T}_u\|)$ and $\phi_{r2}(\geq \|\Delta\mathbf{R}_r\|)$, and these new bounding functions will be the extension to those in Assumption 7 and the Lemma 4.

Assumption 8: The strength of the uncertainties ($\mathbf{T}_u$) satisfy the following norm bounds

$$\|\mathbf{T}_u\| \leq b_0 + b_1\|\mathbf{x}_e\| + \cdots + b_p\|\mathbf{x}_e\|^p = \sum_{i=0}^{p} b_i\|\mathbf{x}_e\|^i =: \phi_{u2},$$

where $b_i (i = 0, \cdots, p)$ are some known positive constants, and p is the highest order of $\mathbf{x}_e$ in the system uncertainties.

Lemma 5: The structured uncertainties ($\Delta\mathbf{R}_r$) are bounded in the form

$$\|\Delta\mathbf{R}_r\| \leq a_0 + a_1\|\mathbf{x}_e\| + a_2\|\mathbf{x}_e\|^2 =: \phi_{r2},$$

where $a_i (i = 0,1,2)$ are known positive constants.

Proof: See Appendix C.

The uncertainties ($\mathbf{T}_u$) assumed are bounded by higher-order polynomials in the norm [10, 13, 19], while the modeling error ($\Delta\mathbf{R}_r$) is at most quadratically bounded in the norms of the system states [6, 13, 19].

The primary objective of robust control law is to guarantee the desired system performance under significant uncertainties. To fulfill the requirements of designing a robust controller, *a priori* knowledge of possible uncertainty bounds on $\mathbf{T}_u$ and $\Delta\mathbf{R}_r$ are required. Consider a continuous VS-type controller [12-13, 19]

$$\mathbf{T}''' = -\frac{\phi_{r2}{}^2\mathbf{e}_s}{\|\mathbf{e}_s\|\phi_{r2} + \xi(t)} - \frac{\phi_{u2}{}^2\mathbf{e}_s}{\|\mathbf{e}_s\|\phi_{u2} + \xi(t)} \tag{33}$$

with $\xi(t) = \alpha\exp(-\beta t)$, where α and β are non-negative constants which can be arbitrarily selected by a designer. The major feature of this algorithm is that very conservative bounds (and functional structures) on $\mathbf{T}_u$ and $\Delta\mathbf{R}$ may be chosen to cope with

any higher-order uncertainties. As discussed in the controller 2 (see Fig. 1), there are some alternative structures for $\xi(t)$. The existence of ξ in $\mathbf{T}^{m}$ guarantees the continuity of control input even when $\|\mathbf{e}_s\|$ becomes zero. In case of $\xi = 0\,(or\ \alpha = 0)$, $\mathbf{T}^{m}$ becomes a purely VS control law and it is discontinuous on the surface $\mathbf{e}_s = 0$. The drawback of discontinuous control law is that it causes undesirable phenomena in practice such as chattering associated with excessive control activity and exciting high-frequency unmodelled dynamics in the system.

Remarks: (i) As shown in (33), the continuous VS-type controller ($\xi \neq 0$) can be discontinuous as $t \to \infty$, i.e., $\xi \to 0$ (or $\exp(-\beta t) \to 0$) $t \to \infty$, however, we are mainly concerned with the tracking properties in a finite time. (ii) From Assumption 8 and Lemma 5, the scalar bounding functions are bounded if $\mathbf{x}_e(\mathbf{e},\dot{\mathbf{e}})$ is bounded. Then the robust control vector also remains bounded. (iii) If all uncertainties are at most quadratically bounded, i.e., $p \leq 2$, then we can combine ϕ_{r2} and ϕ_{u2} to obtain one simple term by choosing more conservative bounds, i.e., $\phi_{r2} + \phi_{u2} = \bar{\phi}$ with $\bar{\phi} \in R^{+}$. $\Delta\Delta$

Now, we are ready to state the stability and the tracking properties of the closed-loop system (3) under robust control law (33).

Theorem 3: For bounded desired trajectories and with known constants **a** and **b** on the uncertainty bounds in Lemma 5 and Assumption 8, the solutions of the closed-loop system (3) under the control law (33) are at least uniformly ultimately bounded. That is, there exists the compact set Λ such that every trajectory of the system states, with $\xi \neq 0$ ($\alpha > 0, \beta = 0$), globally converges to the following residual set (with ultimate bound V_r):

$$\Lambda = \{\mathbf{e}_s \in R^{n}: V(t,\mathbf{e}_s) \leq V_r\},\ \text{with}\ V_r = \frac{2\alpha}{\gamma_0}\ \text{and}\ \gamma_0 = \frac{2k_d}{\sigma_{\max}(\mathbf{M})}$$

Otherwise, all signals, with $\xi \neq 0$ ($\alpha > 0$, $\beta > 0$) or $\xi = 0$ ($\alpha = 0$), are globally exponentially (or asymptotically) stable, i.e., $\lim_{t\to\infty}(\mathbf{e},\dot{\mathbf{e}},\mathbf{e}_s) \to 0$.

Proof: Choose a Lyapunov-like function, $V{:}(t,\mathbf{e}_s) \in R^{+} \times R^{n} \to R^{+}$, as

$$V = \tfrac{1}{2}\mathbf{e}_s^T\mathbf{M}\mathbf{e}_s. \tag{34}$$

Moreover, we observe that

$$\tfrac{1}{2}\sigma_{\min}(\mathbf{M})\|\mathbf{e}_s\|^2 \le V \le \tfrac{1}{2}\sigma_{\max}(\mathbf{M})\|\mathbf{e}_s\|^2, \text{ with } \sigma_{\min}(\mathbf{M}) > 0$$

where $\sigma_{\min}$ and $\sigma_{\max}$ account for the possible lower and upper bounds of $\mathbf{M}(\mathbf{q})$ in $\mathbf{q}$.

Taking its time derivative (34) along with the closed-loop system (3) yields

$$\begin{aligned}\dot{V} &= \mathbf{e}_s^T\mathbf{M}\dot{\mathbf{e}}_s + \tfrac{1}{2}\mathbf{e}_s^T\dot{\mathbf{M}}\mathbf{e}_s \\ &= \mathbf{e}_s^T\{-\mathbf{C}(\mathbf{q},\dot{\mathbf{q}})\mathbf{e}_s - (\mathbf{T}_u + \Delta\mathbf{R}_r) - \mathbf{k}_a\mathbf{e}_s \\ &\quad - \frac{\phi_{r2}^2\mathbf{e}_s}{\|\mathbf{e}_s\|\phi_{r2} + \xi(t)} - \frac{\phi_{u2}^2\mathbf{e}_s}{\|\mathbf{e}_s\|\phi_{u2} + \xi(t)}\} + \tfrac{1}{2}\mathbf{e}_s^T\dot{\mathbf{M}}\mathbf{e}_s\end{aligned} \tag{35}$$

By introducing Property 2, we then have

$$\dot{V} \le \|\mathbf{e}_s\|(\phi_{r2} + \phi_{u2}) - \mathbf{e}_s^T\mathbf{k}_a\mathbf{e}_s - \frac{\phi_{r2}^2\|\mathbf{e}_s\|^2}{\|\mathbf{e}_s\|\phi_{r2} + \xi(t)} - \frac{\phi_{u2}^2\|\mathbf{e}_s\|^2}{\|\mathbf{e}_s\|\phi_{u2} + \xi(t)} \tag{36}$$

from which

$$\begin{aligned}\dot{V} &\le -\mathbf{e}_s^T\mathbf{k}_a\mathbf{e}_s + \frac{\xi\|\mathbf{e}_s\|\phi_{r2}}{\|\mathbf{e}_s\|\phi_{r2} + \xi} + \frac{\xi\|\mathbf{e}_s\|\phi_{u2}}{\|\mathbf{e}_s\|\phi_{u2} + \xi} \\ &\le -k_a\|\mathbf{e}_s\|^2 + 2\xi.\end{aligned} \tag{37}$$

Then, $\dot{V}$ satisfies the following inequality

$$\dot{V} \le -\gamma_0 V + 2\xi, \tag{38}$$

where $\gamma_0 = \dfrac{2k_a}{\sigma_{\max}(\mathbf{M})} \ge 0$. It is easily verified that the solution of Eq. (38), with $\xi \ne 0$ ($\alpha > 0$, $\beta > 0$), can be written as

$$V(t,\mathbf{e}_s)\begin{cases} \le \exp(-\gamma_0 t)\{V_0(0,\mathbf{e}_s(0)) - \dfrac{2\alpha}{\gamma_0 - \beta}\} + \exp(-\beta t)\dfrac{2\alpha}{\gamma_0 - \beta}, & \gamma_0 \ne \beta \\ \le \exp(-\gamma_0 t)V_0(0,\mathbf{e}_s(0)) + 2\alpha t\exp(-\gamma_0 t), & \gamma_0 = \beta \end{cases} \tag{39}$$

A straightforward calculation shows that

$$\|\mathbf{e}_s\|\begin{cases} \le \sqrt{\dfrac{2}{\sigma_{\min}(\mathbf{M})}}\left\{\exp(-\gamma_0 t)\left[\sigma_{\max}(\mathbf{M})\|\mathbf{e}_s(0)\|^2 - \dfrac{2\alpha}{\gamma_0 - \beta}\right] + \exp(-\beta t)\dfrac{2\alpha}{\gamma_0 - \beta}\right\}^{\frac{1}{2}}, & \gamma_0 \ne \beta \\ \le \sqrt{\dfrac{2}{\sigma_{\min}(\mathbf{M})}}\left\{\exp(-\gamma_0 t)\left[\sigma_{\max}(\mathbf{M})\|\mathbf{e}_s(0)\|^2\right] + 2\alpha\exp(-\gamma_0 t)\right\}^{\frac{1}{2}}, & \gamma_0 = \beta \end{cases}$$

(40)

where $V_0 \le \sigma_{max}(\mathbf{M})\|\mathbf{e}_s(0)\|$. As shown in Lemma 3, the boundedness of $\mathbf{e}_s$ also guarantees those of $\mathbf{e}$ and $\dot{\mathbf{e}}$. Therefore, from (39) and (40), one can conclude that the solutions $(\mathbf{e},\dot{\mathbf{e}},\mathbf{e}_s)$ are globally exponentially stable for any bounded initial values. If $\xi \neq 0$ ($\alpha > 0, \beta = 0$), i.e., saturation (or boundary layer) type controller, then

$$V \le \exp(-\gamma_0 t)\{V_0 - \frac{2\alpha}{\gamma_0}\} + \frac{2\alpha}{\gamma_0}. \tag{41}$$

Therefore, the UUB of system responses are achieved with respect to V_r. In other words, for $V_r = \frac{2\alpha}{\gamma_0} \ge 0$, the function V is nonincreasing, that is, $\dot{V} < 0$ for all $(t,\mathbf{e}_s) \in R^+ \times R^n$ such that $V > V_r$ (or $V \subset \Lambda^c$), and the ultimate bound is given as $0 \le \lim_{t\to\infty} V = \inf_t V = V_r \le V_0$. Furthermore, the norm of joint tracking errors converge to the following ball:

$$B(\mathbf{e}_s) = \{\mathbf{e}_s \in R^n : \|\mathbf{e}_s\| \le \sqrt{\frac{2}{\sigma_{min}(\mathbf{M})}}\left(\frac{2\alpha}{\gamma_0}\right)^{1/2}\},$$

we can in turn show that $\|\mathbf{e}\|$ and $\|\dot{\mathbf{e}}\|$ are also ultimately bounded employing Lemma 3

$$B(\mathbf{e}) = \{\mathbf{e} \in R^n : \|\mathbf{e}\| \le \frac{1}{\mu}\sqrt{\frac{2}{\sigma_{min}(\mathbf{M})}}\left(\frac{2\alpha}{\gamma_0}\right)^{1/2}\}$$

$$B(\dot{\mathbf{e}}) = \{\dot{\mathbf{e}} \in R^n : \|\dot{\mathbf{e}}\| \le 2\sqrt{\frac{2}{\sigma_{min}(\mathbf{M})}}\left(\frac{2\alpha}{\gamma_0}\right)^{1/2}\}.$$

It is shown that the tracking errors (or all system states) in closed-loop system are uniformly ultimately bounded. The design parameters can be chosen to balance the conflicting demands of good control performance and limited control energy.

Remarks: (i) For the specific value $\xi = 0$ (or $\alpha = 0$) in (33) and (38), i.e., a purely discontinuous VS control law, it is readily shown that the closed-loop system is also exponentially stable. Since V is nonincreasing function which is upper bounded by V_0 and lower bounded by zero (i.e., $\mathbf{e}_s \in L_\infty$), we have

$$0 \le k_a \int_0^\infty \|\mathbf{e}_s\|^2 d\tau \le V_0 - \lim_{t\to\infty} V < \infty,$$

which implies that $\mathbf{e}_s \in L_2$ (i.e., square integrability of signals). Now, one obtain $\dot{\mathbf{e}}_s \in L_\infty$ from Eq. (3) because $\mathbf{M}^{-1}$ exists and is bounded. Hence $\mathbf{e}_s \in L_2 \cap L_\infty$ and $\dot{\mathbf{e}}_s \in L_\infty$. As a result, by Lemma 1 (or Corollary 2), we draw a conclusion that $\mathbf{e}_s \to 0$, which in turn implies that both $\mathbf{e} \to 0$ and $\dot{\mathbf{e}} \to 0$ as $t \to \infty$. (ii) Therefore, we have achieved stronger stability results of the tracking errors in both $\xi = 0$ (or $\alpha = 0$) and $\xi \neq 0$ ($\alpha > 0, \beta > 0$), i.e., global exponential (or asymptotic) stability, than those achieved in $\xi \neq 0$ ($\alpha \neq 0, \beta = 0$), i.e., UUB.

4. ADAPTIVE VERSION OF ROBUST CONTROLLER (DECENTRALIZED ROBUST ADAPTIVE CONTROL)

In the previous section, *a priori* knowledge of the uncertainty bounds is a crucial factor. Since the uncertainties are unknown or poorly known, sometimes the least upper bounds may not be easily obtained nor feasible to draw for a variety of reasons in practice. Thus for safety, one may choose some very conservative bounds, but that choice requires excessively large control energy. In this section, the prerequisites of the uncertainty bounds can be relaxed. Instead of estimating manipulator parameters, we directly update the unknown bounds of the uncertainties. This methodology is called adaptive bounds of the robust controller (or decentralized robust adaptive controller) [5, 9-10, 19]. Thus, we will develop a approach that combines robust control and adaptive control techniques.

The structural properties of the uncertainty bounds on the $\mathbf{T}_u$ and $\Delta\mathbf{R}_r$ are the same as those given in Lemma 5 and Assumption 8, which are based on the deterministic properties, i.e., $\|\Delta\mathbf{R}_r\| \le \phi_{r2}$ and $\|\mathbf{T}_u\| \le \phi_{u2}$. However, the uncertainty bounds ($\mathbf{a}$ and $\mathbf{b}$) are completely unknown rather than being assumed known in the previous subsection (Section 3.3).

Now, in order to develop the adaptation mechanism on the uncertainty bounds, we can define the regressor-like functions $\mathbf{R}_r(\mathbf{x}_e)$ and $\mathbf{R}_u(\mathbf{x}_e)$ as

$$\mathbf{R}_r := \begin{bmatrix} 1 & \|\mathbf{x}_e\| & \|\mathbf{x}_e\|^2 \end{bmatrix} \text{ and } \mathbf{R}_u := \begin{bmatrix} 1 & \|\mathbf{x}_e\| & \cdots & \|\mathbf{x}_e\|^p \end{bmatrix},$$

and the unknown vectors $\mathbf{a} \in R^3$ and $\mathbf{b} \in R^{p+1}$ are given as

$$\mathbf{a} = \begin{bmatrix} a_0 & a_1 & a_2 \end{bmatrix}^T \text{ and } \mathbf{b} = \begin{bmatrix} b_0 & b_1 & \cdots & b_p \end{bmatrix}^T.$$

Then the uncertainty bounds given in Lemma 5 and Assumption 8 are further expressed as

$$a_0 + a_1\|\mathbf{x}_e\| + a_2\|\mathbf{x}_e\|^2 =: \mathbf{R}_r\mathbf{a} =: \phi_{r2},$$

$$b_0 + b_1\|\mathbf{x}_e\| + \cdots + b_p\|\mathbf{x}_e\|^p = \sum_{i=0}^{p} b_i\|\mathbf{x}_e\|^i := \mathbf{R}_u\mathbf{b} =: \phi_{u2},$$

respectively, where ϕ_{r2} and ϕ_{u2} are now unknown scalar bounding functions. The above formulations represent the linear parameterization of the unknown bounding function. The corresponding estimated versions of the bounding functions via adaptive law can be expressed as

$$\hat{\phi}_{r2} = \mathbf{R}_r\hat{\mathbf{a}} \text{ and } \hat{\phi}_{u2} = \mathbf{R}_u\hat{\mathbf{b}},$$

where $\hat{\mathbf{a}}$ and $\hat{\mathbf{b}}$ are the estimated vectors of the unknown constant coefficients $\mathbf{a}$ and $\mathbf{b}$, respectively. In this study, the circumflex ($\hat{\bullet}$) represents the estimated value of ($\bullet$) provided by the adaptation law. Let $\tilde{\mathbf{a}} \in R^3$ and $\tilde{\mathbf{b}} \in R^{p+1}$ be the vectors of uncertainty bound errors with $\tilde{\mathbf{a}} = \mathbf{a} - \hat{\mathbf{a}}$ and $\tilde{\mathbf{b}} = \mathbf{b} - \hat{\mathbf{b}}$. Then the unknown gains are estimated by the following update schemes:

$$\dot{\hat{\mathbf{a}}} = \Gamma_r(\mathbf{R}_r^T\|\mathbf{e}_s\| - \omega_r\hat{\mathbf{a}}), \tag{42a}$$

$$\dot{\hat{\mathbf{b}}} = \Gamma_u(\mathbf{R}_u^T\|\mathbf{e}_s\| - \omega_u\hat{\mathbf{b}}), \tag{42b}$$

where the adaptation gains $\Gamma_r \in R^{3\times3}$ and $\Gamma_u \in R^{(p+1)\times(p+1)}$ may be selected as diagonal matrices, i.e., $\Gamma_r = \lambda_r\mathbf{E}, \lambda_r > 0$ and $\Gamma_u = \lambda_u\mathbf{E}, \lambda_u > 0$, respectively. The "leakage" terms $\omega_r(>0)$ and $\omega_u(>0)$ in the update laws in (42a) and (42b) belong to a class of σ-modification [3, 5, 15, 19] which are designed to improve robustness of adaptive schemes to uncertainties.

As mentioned before, the robust control ($\mathbf{T}^{rc}$) is primarily intended to cope with the total uncertainties ($\Delta\mathbf{R}_r$ and $\mathbf{T}_u$) and to ensure desired stability of the closed-loop system.

To achieve this, an adaptive version of robust control algorithm (controller 4) is expressed as [19]

$$\hat{\mathbf{T}}^{rc} = -\frac{(\hat{\phi}_{r2})^2\mathbf{e}_s}{\|\mathbf{e}_s\|(\hat{\phi}_{r2}) + \xi} - \frac{(\hat{\phi}_{u2})^2\mathbf{e}_s}{\|\mathbf{e}_s\|(\hat{\phi}_{u2}) + \xi}, \tag{43}$$

where $\xi = \alpha\exp(-\beta t)$, and the specific structures of $\xi(t)$ in the control law (43) are chosen as depicted in Eq. (33) (see Fig. 1). Then the complete controller has the form as

$$\mathbf{T} = \mathbf{M}_0(\mathbf{q}_d;\Theta)\ddot{\mathbf{e}}_r + \mathbf{C}_0(\mathbf{q}_d,\dot{\mathbf{q}}_d;\Theta)\dot{\mathbf{e}}_r + \mathbf{G}_0(\mathbf{q}_d;\Theta)$$
$$-\mathbf{k}_d\mathbf{e}_s - \frac{(\hat{\phi}_{r2})^2\mathbf{e}_s}{\|\mathbf{e}_s\|\hat{\phi}_{r2} + \xi} - \frac{(\hat{\phi}_{u2})^2\mathbf{e}_s}{\|\mathbf{e}_s\|\hat{\phi}_{u2} + \xi}$$

Now the closed-loop system (3) with the nonlinear control law (43) gives the following tracking properties with properly chosen design parameters.

Theorem 4: With the unknown constants **a** and **b** on the uncertainty bounds in Lemma 5 and Assumption 8, the solutions of the closed-loop system (3) under the robust control law (43) along with the adaptive scheme (42a) and (42b) are uniformly ultimately bounded; that is, every solution starting in Ψ^c enters the residual set Ψ and thereafter remains in Ψ (where Ψ^c denotes the complement of Ψ):

$$\Psi = \left\{(\mathbf{e}_s, \tilde{\mathbf{a}}, \tilde{\mathbf{b}}) \in R^n \times R^3 \times R^{(p+1)}: V \le V_r\right\},$$

where the ultimate bounds are given by

$$\xi \neq 0 \quad (\alpha > 0, \beta = 0);\ V_r = \frac{2\alpha + \gamma}{\gamma_0}$$

and $$\xi \neq 0 \quad (\alpha > 0, \beta > 0);\ V_r = \begin{cases} \dfrac{\gamma}{\gamma_0}, & \gamma_0 \neq \beta \\ \gamma, & \gamma_0 = \beta \end{cases}$$

with

$$\gamma = \frac{\omega_r}{2}\|\mathbf{a}\|^2 + \frac{\omega_u}{2}\|\mathbf{b}\|^2 \text{ and } \gamma_0 = \min\left\{\frac{2k_u}{\overline{\sigma}}, \frac{\omega_r}{\overline{\sigma}}, \frac{\omega_u}{\overline{\sigma}}\right\}.$$

Proof: To show the stability of the closed-loop system, define the Lyapunov-like function (a C^1 function), $V:(\mathbf{e}_s, \tilde{\mathbf{a}}, \tilde{\mathbf{b}}) \in R^n \times R^3 \times R^{p+1} \to R^+$, such that

$$V = \tfrac{1}{2}\tilde{\mathbf{x}}^T Q(\mathbf{q})\,\tilde{\mathbf{x}}, \tag{44}$$

where $\tilde{\mathbf{x}}^T = [\mathbf{e}_s^T\ \tilde{\mathbf{a}}^T\ \tilde{\mathbf{b}}^T]$ denotes the generalized state error vector and $Q(\mathbf{q}) = Block\ diag[\mathbf{M}(\mathbf{q}), \Gamma_r^{-1}, \Gamma_u^{-1}]$. Noting that $\mathbf{M}$, Γ_r, and Γ_u are all positive definite matrices, we have

$$\tfrac{1}{2}\underline{\sigma}\|\tilde{\mathbf{x}}\|^2 \le V \le \tfrac{1}{2}\overline{\sigma}\|\tilde{\mathbf{x}}\|^2,$$

where $\underline{\sigma} = \sigma_{\min}(Q) > 0$ since Q is positive definite and $\overline{\sigma} = \sigma_{\max}(Q)$. Thus, V is a legitimate Lyapunov function candidate.

Evaluating its time derivative (44) along with the closed-loop system (3) gives

$$\dot{V} = \mathbf{e}_s^T \mathbf{M}\dot{\mathbf{e}}_s + \tfrac{1}{2}\mathbf{e}_s^T \dot{\mathbf{M}}\mathbf{e}_s + \tilde{\mathbf{a}}^T \Gamma_r^{-1}\dot{\tilde{\mathbf{a}}} + \tilde{\mathbf{b}}^T \Gamma_u^{-1}\dot{\tilde{\mathbf{b}}}.$$

If the adaptation laws with leakage presented in (42a) and (42b) are chosen, then

$$\begin{aligned}\dot{V} = \mathbf{e}_s^T &\left\{-\mathbf{C}(\mathbf{q},\dot{\mathbf{q}})\mathbf{e}_s - (\mathbf{T}_u + \Delta\mathbf{R}) - \mathbf{k}_u\mathbf{e}_s - \frac{(\hat{\phi}_{r2})^2\mathbf{e}_s}{\|\mathbf{e}_s\|(\hat{\phi}_{r2}) + \xi} - \frac{(\hat{\phi}_{u2})^2\mathbf{e}_s}{\|\mathbf{e}_s\|(\hat{\phi}_{u2}) + \xi}\right\} \\ &+ \frac{1}{2}\mathbf{e}_s^T \dot{\mathbf{M}}\mathbf{e}_s - \tilde{\mathbf{a}}^T(\mathbf{R}_r^T\|\mathbf{e}_s\| - \omega_r\hat{\mathbf{a}}) - \tilde{\mathbf{b}}^T(\mathbf{R}_u^T\|\mathbf{e}_s\| - \omega_u\hat{\mathbf{b}})\end{aligned} \tag{45}$$

Here, $\dot{\tilde{\mathbf{a}}} = -\dot{\hat{\mathbf{a}}}$ and $\dot{\tilde{\mathbf{b}}} = -\dot{\hat{\mathbf{b}}}$ (assuming that $\dot{\mathbf{a}} = \dot{\mathbf{b}} = \mathbf{0}$). Applying Property 3 on Eq. (45) gives

$$\begin{aligned}\dot{V} \le &-\mathbf{e}_s^T\mathbf{k}_u\mathbf{e}_s + \|\mathbf{e}_s\|\mathbf{R}_r\mathbf{a} + \|\mathbf{e}_s\|\mathbf{R}_u\mathbf{b} - \frac{(\hat{\phi}_{r2})^2\|\mathbf{e}_s\|^2}{\|\mathbf{e}_s\|(\hat{\phi}_{r2}) + \xi} - \frac{(\hat{\phi}_{u2})^2\|\mathbf{e}_s\|^2}{\|\mathbf{e}_s\|(\hat{\phi}_{u2}) + \xi} \\ &- \tilde{\mathbf{a}}^T\mathbf{R}_r^T\|\mathbf{e}_s\| + \tilde{\mathbf{a}}^T\omega_r\hat{\mathbf{a}} - \tilde{\mathbf{b}}^T\mathbf{R}_u^T\|\mathbf{e}_s\| + \tilde{\mathbf{b}}^T\omega_u\hat{\mathbf{b}}\end{aligned}$$

Thus, it follows that

$$\begin{aligned}\dot{V} &\le -\mathbf{e}_s^T\mathbf{k}_u\mathbf{e}_s + \|\mathbf{e}_s\|\mathbf{R}_r\mathbf{a} + \|\mathbf{e}_s\|\mathbf{R}_u\mathbf{b} - (\mathbf{a}^T - \hat{\mathbf{a}}^T)\mathbf{R}_r^T\|\mathbf{e}_s\| - (\mathbf{b}^T - \hat{\mathbf{b}}^T)\mathbf{R}_u^T\|\mathbf{e}_s\| \\ &- \frac{(\hat{\phi}_{r2})^2\|\mathbf{e}_s\|^2}{\|\mathbf{e}_s\|(\hat{\phi}_{r2}) + \xi} - \frac{(\hat{\phi}_{u2})^2\|\mathbf{e}_s\|^2}{\|\mathbf{e}_s\|(\hat{\phi}_{u2}) + \xi} + \tilde{\mathbf{a}}^T\omega_r(\mathbf{a} - \tilde{\mathbf{a}}) + \tilde{\mathbf{b}}^T\omega_u(\mathbf{b} - \tilde{\mathbf{b}}) \\ &\le -\mathbf{e}_s^T\mathbf{k}_u\mathbf{e}_s + \|\mathbf{e}_s\|\hat{\phi}_{r2} + \|\mathbf{e}_s\|\hat{\phi}_{u2} - \frac{(\hat{\phi}_{r2})^2\|\mathbf{e}_s\|^2}{\|\mathbf{e}_s\|(\hat{\phi}_{r2}) + \xi} - \frac{(\hat{\phi}_{u2})^2\|\mathbf{e}_s\|^2}{\|\mathbf{e}_s\|(\hat{\phi}_{u2}) + \xi} \\ &- \omega_r\|\tilde{\mathbf{a}}\|^2 + \tilde{\mathbf{a}}^T\omega_r\mathbf{a} - \omega_u\|\tilde{\mathbf{b}}\|^2 + \tilde{\mathbf{b}}^T\omega_u\mathbf{b} \\ &\le -\mathbf{e}_s^T\mathbf{k}_u\mathbf{e}_s + \frac{\xi(\hat{\phi}_{r2})\|\mathbf{e}_s\|}{\|\mathbf{e}_s\|(\hat{\phi}_{r2}) + \xi} + \frac{\xi(\hat{\phi}_{u2})\|\mathbf{e}_s\|}{\|\mathbf{e}_s\|(\hat{\phi}_{u2}) + \xi} \\ &- \omega_r\|\tilde{\mathbf{a}}\|^2 + \omega_r\|\tilde{\mathbf{a}}\|\|\mathbf{a}\| - \omega_u\|\tilde{\mathbf{b}}\|^2 + \omega_u\|\tilde{\mathbf{b}}\|\|\mathbf{b}\|\end{aligned} \tag{46}$$

Noting that the following inequality

$$-\omega_r\|\tilde{\mathbf{a}}\|^2 + \omega_r\|\tilde{\mathbf{a}}\|\|\mathbf{a}\| - \omega_u\|\tilde{\mathbf{b}}\|^2 + \omega_u\|\tilde{\mathbf{b}}\|\|\mathbf{b}\| \le -\frac{\omega_r}{2}\|\tilde{\mathbf{a}}\|^2 + \frac{\omega_r}{2}\|\mathbf{a}\|^2 - \frac{\omega_u}{2}\|\tilde{\mathbf{b}}\|^2 + \frac{\omega_u}{2}\|\mathbf{b}\|^2,$$

we rewrite the differential inequality (46) as

$$\dot{V} \le -k_u \|\mathbf{e}_s\|^2 - \frac{\omega_r}{2}\|\tilde{\mathbf{a}}\|^2 - \frac{\omega_u}{2}\|\tilde{\mathbf{b}}\|^2 + 2\xi + \frac{\omega_r}{2}\|\mathbf{a}\|^2 + \frac{\omega_u}{2}\|\mathbf{b}\|^2. \tag{47}$$

Let

$$\gamma = \frac{\omega_r}{2}\|\mathbf{a}\|^2 + \frac{\omega_u}{2}\|\mathbf{b}\|^2 \text{ and } \gamma_0 = \min\left\{\frac{2k_u}{\overline{\sigma}}, \frac{\omega_r}{\overline{\sigma}}, \frac{\omega_u}{\overline{\sigma}}\right\}$$

for more compact notation, where $\gamma \in R^+$ and $\gamma_0 > 0$. It then follows from (47) that

$$\dot{V} \le -\gamma_0 V + 2\xi + \gamma. \tag{48}$$

If $\xi \neq 0$ ($\alpha > 0, \beta = 0$), i.e., a saturation-type controller, then, for $V_r = \frac{2\alpha + \gamma}{\gamma_0} \ge 0$, one have $\dot{V} < 0$ whenever $V > V_r$ (or $V \subset \Psi^c$), i.e., $\forall (\mathbf{e}_s, \tilde{\mathbf{a}}, \tilde{\mathbf{b}}) \in \Psi^c$. A detailed solution of Eq. (48) is given by

$$V \le \exp(-\gamma_0 t)[V_0 - \frac{2\alpha + \gamma}{\gamma_0}] + \frac{2\alpha + \gamma}{\gamma_0}, \ t \ge 0 \tag{49}$$

where $V_0 = V_{t=0}(\bullet)$ and the ultimate bound is given by

$$0 \le \lim_{t\to\infty} V = \inf_t V = V_r = \frac{2\alpha + \gamma}{\gamma_0} \le V_0 < \infty.$$

If $\xi \neq 0$ ($\alpha > 0, \beta > 0$), then the boundedness of V can be obtained by, for all $t \ge 0$

$$V(\mathbf{e}_s, \tilde{\mathbf{a}}, \tilde{\mathbf{b}}) \begin{cases} \le \exp(-\gamma_0 t)\left[V_0 - \dfrac{2\alpha}{\gamma_0 - \beta} - \dfrac{\gamma}{\gamma_0}\right] + \exp(-\beta t)\dfrac{2\alpha}{\gamma_0 - \beta} + \dfrac{\gamma}{\gamma_0}, \ \gamma_0 \neq \beta \\ \le \exp(-\gamma_0 t)[V_0 - \gamma] + 2\alpha t \exp(-\gamma_0 t) + \gamma, \ \gamma_0 = \beta \end{cases} \tag{50}$$

where the ultimate bounds are given by

$$0 \le \lim_{t\to\infty} V = \inf_t V = V_r = \frac{2\alpha + \gamma}{\gamma_0} \le V_0, \ \gamma_0 \neq \beta$$

and $0 \le \lim_{t\to\infty} V = \inf_t V = V_r = \gamma, \ \gamma_0 = \beta.$

The rate of convergence depends on the values of γ_0 and β. Thus V converge to the compact set Ψ exponentially. Moreover, from (49) and (50), the norm bounds of joint-space tracking errors can be estimated as follows:

In case of $\xi \neq 0$ $(\alpha > 0, \beta = 0)$,

$$\|\mathbf{e}_s\| \le \sqrt{\frac{2}{\bar{\sigma}}}\left[\exp(-\gamma_0 t)(V_0 - \frac{2\alpha+\gamma}{\gamma_0}) + \frac{2\alpha+\gamma}{\gamma_0}\right]^{1/2}, \tag{51}$$

and in case of $\xi \neq 0 \quad (\alpha > 0, \beta > 0)$,

$$\|\mathbf{e}_s\| \le \begin{cases} \sqrt{\frac{2}{\bar{\sigma}}}\left[\exp(-\gamma_0 t)(V_0 - \frac{2\alpha}{\gamma_0-\beta} - \frac{\gamma}{\gamma_0}) + \exp(-\beta t)\frac{2\alpha}{\gamma_0-\beta} + \frac{\gamma}{\gamma_0}\right]^{1/2}, \gamma_0 \neq \beta \\ \sqrt{\frac{2}{\bar{\sigma}}}\left[\exp(-\gamma_0 t)(V_0 - \gamma) + 2\alpha t \exp(-\gamma_0 t) + \gamma\right]^{1/2}, \gamma_0 = \beta \end{cases} \tag{52}$$

Finally, it can be shown from (51) and (52) that the norms of tracking errors converge to (or are attracted into) the following compact set as $t \to \infty$:

If $\xi \neq 0 \quad (\alpha > 0, \beta = 0)$, then

$$B(\mathbf{e}_s) = \left\{\mathbf{e}_s \in R^n : \|\mathbf{e}_s\| \le \sqrt{\frac{2(2\alpha+\gamma)}{\bar{\sigma}\gamma_0}}\right\}.$$

If $\xi \neq 0 \quad (\alpha > 0, \beta > 0)$, then

$$B(\mathbf{e}_s) = \begin{cases} \mathbf{e}_s \in R^n : \|\mathbf{e}_s\| \le \sqrt{\frac{2\gamma}{\bar{\sigma}\gamma_0}}, \gamma_0 \neq \beta \\ \mathbf{e}_s \in R^n : \|\mathbf{e}_s\| \le \sqrt{\frac{2\gamma}{\bar{\sigma}}}, \gamma_0 = \beta \end{cases}$$

In above results, the radius of the closed balls depend on the types of control structures. As a consequence, the uniform ultimate boundedness of tracking error ($\mathbf{e}_s$) can be easily established by using Definitions 2 and 3. The uniform ultimate boundednesses of other signals ($\tilde{\mathbf{a}}, \tilde{\mathbf{b}}$) are also guaranteed in similar fashions. Therefore, the robust control law (43) with the adaptive laws in Eqs. (42a) and (42b) renders the closed-loop system (3) uniformly ultimately bounded. In other words, all signals in the closed-loop dynamics are finally attracted into the target ball (Ψ) in finite time regardless of the uncertainties, and the UUB of system responses ($\mathbf{e}_s, \tilde{\mathbf{a}}, \tilde{\mathbf{b}}$) are established with respect to V_r in this design. Moreover, the size of the tracking errors can be reduced by manipulating the design

parameters. However, trade-off should be made between control energy (control gains) and system performances (the sizes of the residual set).

Remarks: (i) By the result of lemma 3, the uniform ultimate boundednesses of the (position/velocity) tracking errors ($\mathbf{e}$ and $\dot{\mathbf{e}}$) can be deduced from the boundedness of the sliding surface vector ($\mathbf{e}_s$). (ii) For the specific value $\xi = 0$ (or $\alpha = 0$) in (48), i.e., a purely discontinuous VS control law, it is readily shown that the closed-loop system is also uniformly ultimately bounded. Furthermore, if $\xi = 0$ and $\gamma = 0$, then the global exponential stability result can be obtained, i.e., $\lim_{t\to\infty}\|\mathbf{e}_s(t)\| = 0 \rightarrow \lim_{t\to\infty}\|\mathbf{e}(t)\| = 0$ and $\lim_{t\to\infty}\|\dot{\mathbf{e}}(t)\| = 0$. (iii) Even if α and β may be selected arbitrarily, provided that the system is stable, they must be chosen carefully to ensure the desired system performances in practice.

5. NUMERICAL SIMULATIONS

Computer simulation are conducted to test the performance of the proposed control laws using a 4th order Runge-Kutta method with a step size 0.005 sec. A class of control algorithms are applied to a simple two-link robotic manipulator (see Fig. 2) whose dynamic model can be expressed as [17]

$$\begin{aligned} T_1 &= m_2 l_2^2(\ddot{q}_1+\ddot{q}_2)+m_2 l_1 l_2\cos(q_2)(2\ddot{q}_1+\ddot{q}_2)+(m_1+m_2)l_1^2\ddot{q}_1-m_2 l_1 l_2\sin(q_2)\dot{q}_2^2 \\ &\quad -2m_2 l_1 l_2\sin(q_2)\dot{q}_1\dot{q}_2+m_2 l_2 g\cos(q_1+q_2)+(m_1+m_2)l_1 g\cos(q_1)+T_{u1} \\ T_2 &= m_2 l_1 l_2\cos(q_2)\ddot{q}_1+m_2 l_2^2(\ddot{q}_1+\ddot{q}_2)+m_2 l_1 l_2\sin(q_2)\dot{q}_1^2 \\ &\quad +m_2 l_2 g\cos(q_1+q_2)+T_{u2} \end{aligned}$$

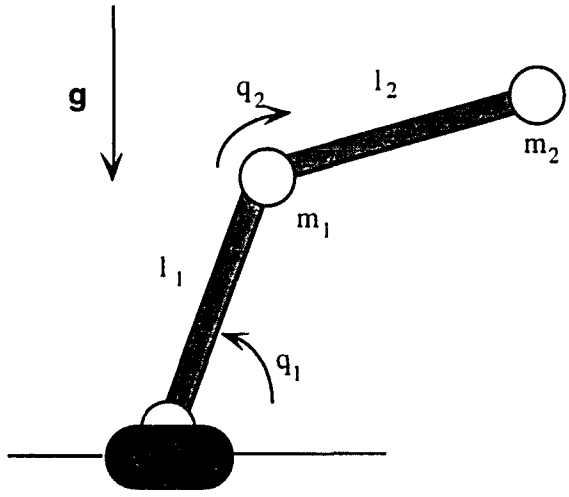

Figure 2. A two-link planer robotic manipulator model.

The above equation can also be written in vector and matrix form as

$$\mathbf{M}(\mathbf{q};\Theta)\ddot{\mathbf{q}}+\mathbf{C}(\mathbf{q},\dot{\mathbf{q}};\Theta)\dot{\mathbf{q}}+\mathbf{G}(\mathbf{q};\Theta)+\mathbf{T}_u=\mathbf{T},$$

where

$$\mathbf{M}(\mathbf{q};\Theta)=\begin{bmatrix} m_2 l_2^2 + 2m_2 l_1 l_2 \cos(q_2) + (m_1+m_2) l_1^2 & m_2 l_2^2 + m_2 l_1 l_2 \cos(q_2) \\ m_2 l_2^2 + m_2 l_1 l_2 \cos(q_2) & m_2 l_2^2 \end{bmatrix}$$

$$\mathbf{C}(\mathbf{q},\dot{\mathbf{q}};\Theta)=\begin{bmatrix} -2m_2 l_1 l_2 \sin(q_2)\dot{q}_2 & -m_2 l_1 l_2 \sin(q_2)\dot{q}_2 \\ m_2 l_1 l_2 \sin(q_2)\dot{q}_1 & 0 \end{bmatrix}$$

$$\mathbf{G}(\mathbf{q};\Theta)=\begin{bmatrix} m_2 l_2 g \cos(q_1+q_2) + (m_1+m_2) l_1 g \cos(q_1) \\ m_2 l_2 g \cos(q_1+q_2) \end{bmatrix}$$

$$\mathbf{T}_u=\begin{bmatrix} \mathrm{T}_{u1} \\ \mathrm{T}_{u2} \end{bmatrix},$$

where m_2 denotes the mass of the second link plus an unknown payload (i.e., the load considered as a part of the last link). The following choices of numerical values are used to carry out the computer simulations:

On defining the manipulator parameter vector Θ as

$$\Theta=[\theta_1 \quad \theta_2 \quad \theta_3 \quad \theta_4]^T=[l_1 \quad l_2 \quad m_1 \quad m_2]^T,$$

the actual values of manipulator parameters (Θ) are assumed to be $l_1 = l_2 = 1.0\,(m)$ and $m_1 = m_2 = 1.0\,(kg)$. Unfortunately, the true values of m_1 and m_2 are not available in the control laws, while l_1 and l_2 are assumed to be known exactly. Therefore, based on the possible bounds on m_1 and m_2, the corresponding estimated (or nominal) values of the robot parameters (Θ_0) are chosen by

$$\Theta_0=[1.0 \quad 1.0 \quad 1.5 \quad 1.25]^T.$$

Here, about 50% and 25% modeling errors were assumed for m_1 and m_2, respectively, that is, the assumed nominal values Θ_0 are deviated 50% and 25% from the actual values (Θ). The initial conditions of actual trajectories are given by

$$q_1(0)=q_2(0)=0.0\,(rad) \text{ and } \dot{q}_1(0)=\dot{q}_2(0)=0.0\,(rad/s).$$

The desired trajectories for the two joints are supposed to be

$$q_{d1}(t)=q_{d2}(t)=0.1*\cos(10t).$$

The unstructured uncertainties $\mathbf{T}_u$ are assumed to be

$T_{ui} = q_i + \dot{q}_i + q_i\dot{q}_i + \cos(\omega_f t)$ for controller 1-2, and

$T_{ui} = q_i + \dot{q}_i + q_i\dot{q}_i + q_i^2 + \dot{q}_i^2 + \cos(\omega_f t)$ for controller 3-4,

with $\omega_f = 1$ or $100\ (rad/\sec)$, where $i(=1, 2)$ represent the corresponding joints. For robust controller in Section 3.3, the known uncertainty bounds are given by

$$\mathbf{a} = [a_0 \quad a_1 \quad a_2]^T = [5.0 \quad 5.0 \quad 5.0]^T \text{ and } \mathbf{b} = [b_0 \quad b_1 \quad b_2]^T = [5.0 \quad 5.0 \quad 5.0]^T,$$

where the highest order of polynomial bound on the uncertainties $\mathbf{T}_u$ is selected to p=2 for demonstration purposes, i.e., quadratically bounded uncertainties. However, more significant uncertainties may also be assumed if necessary.

For adaptive bounds of the robust controller in Section 4, the initial conditions for unknown constants are given by

$$\mathbf{a}(0) = \mathbf{b}(0) = [0.0 \quad 0.0 \quad 0.0]^T.$$

The numerical values of some design parameters are selected as

$$k_a = 200,\ k_c = 150, \mu = 2.0.$$

For the adaptation scheme (in controller 4), some design parameters are chosen as

$$\Gamma_r = \Gamma_u = diag\ (15.0, 5.0, 5.0) \text{ and } \omega_r = \omega_u = 0.1.$$

The simulation results are depicted in figures 3-40. As shown in figures, the system responses ($\mathbf{e}, \dot{\mathbf{e}}, \mathbf{e}_s$) are all bounded. In adaptive bounds of robust controller (control law 4), the estimated values of unknown coefficients in the uncertainty bounds increase until satisfactory system performance is achieved as shown in Figs 35-36. In control law 3, the simulation results for specific values of ξ are provided to illustrate the chattering behavior in the control inputs, provided that other control gains are unchanged, that is, $\xi = 0.7$ (no chattering) and $\xi = 0.1$ (chattering phenomena), as shown in figures 21-26.

For the system uncertainties, the simulations at two different frequencies ($\omega_f = 1$ and $100\ rad/\sec$) are given to see the tracking performance of the control laws. The control torques are almost same except during starting periods. This is obvious because as time

goes on the tracking errors converge almost to zero. Then the control torques mainly depend on the nominal (or primary) control law which has the same form for all control laws in this study.

Simulation results are also given in Figs 37-40 to compare the performance of the proposed control laws with the PD controller ($\mathbf{T} = \mathbf{k}_p\mathbf{e} + \mathbf{k}_v\dot{\mathbf{e}}$), control gains being the same ($\mathbf{k}_p = k_p\mathbf{E}_2$ and $\mathbf{k}_v = k_v\mathbf{E}_2$, with $k_p = 400$ and $k_v = 200$).

Since the modeling error of m_1 is assumed to be greater than that of m_2, the tracking performances of joint 2 are slightly superior to those of joint 1. Therefore, one can conclude that the proposed controls are shown to be robust with respect to a given class of uncertainties.

Now extensive simulation results can be summarized as follows:

(i) All signals of the corresponding closed-loop system are guaranteed to be ultimately bounded. (ii) The designer has many alternatives in choosing design variables to meet the desired system specifications. (iii) The choices of ξ (or α and β) in (19), (33), and (43) affect the transient and overall system responses. (iv) Care should be taken in choosing the values of ξ (or α and β) to avoid chattering, that is, the values of $\xi(t)$ (or ξ) should be changed at a slower rate than those of $\phi_r\mathbf{e}_s$ and $\phi_u\mathbf{e}_s$ (or $\mathbf{e}_s$). In words, the chattering occurs with small values of ξ or with a rapidly decaying exponential term $\xi(t)$ (i.e., small α and high β). And the larger the control discontinuity the more severe the control chattering occurs. (v) The convergence of system responses can generally be rated from fastest to slowest in order as follows: $\xi = 0$ ($\alpha = 0$), $\xi \neq 0$ ($\alpha > 0, \beta > 0$), $\xi \neq 0$ ($\alpha > 0, \beta = 0$). (vi) As $\xi \to 0$, the system responses move toward being asymptotically stable and achieving a fast transient response, however, undesirable chattering may occur. (vii) Adaptive bound of robust controller gives generally better tracking performance. (viii) It is shown that a large amount of leakage (ω_r or ω_u) is needed as the system uncertainties

are significant. (ix) As expected, the presented control laws give better tracking properties than those of the PD control law.

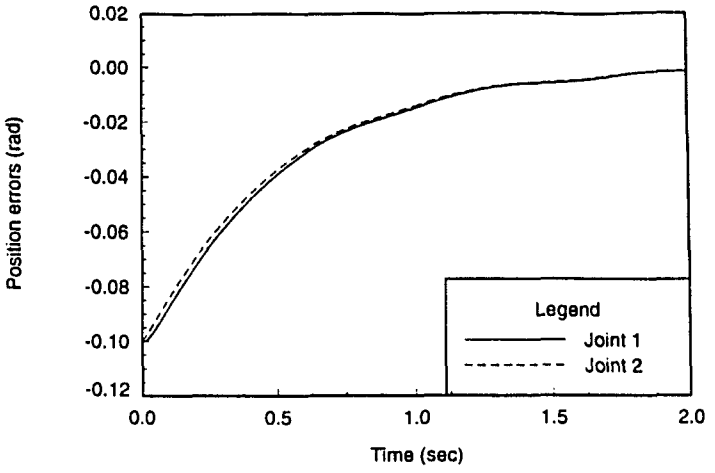

Figure 3. Joint position tracking errors under control law 1 ($\omega_f = 100$)

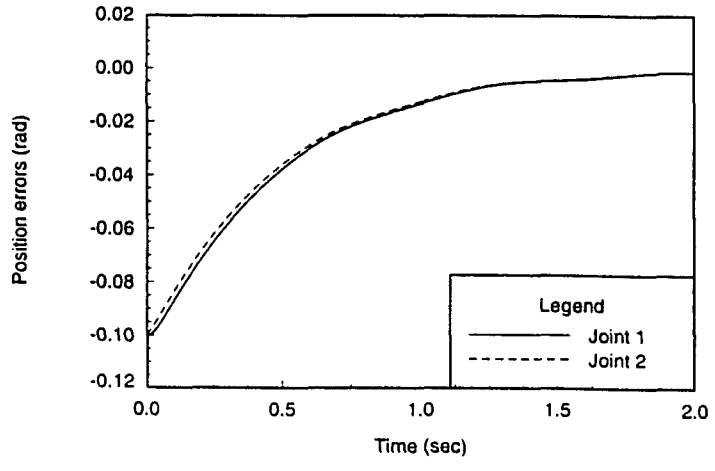

Figure 4. Joint position tracking errors under control law 1 ($\omega_f = 1$)

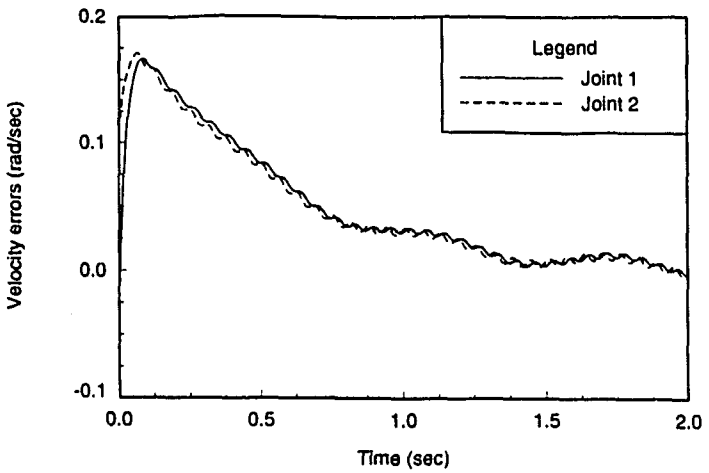

Figure 5. Joint velocity tracking errors under control law 1 ($\omega_f = 100$)

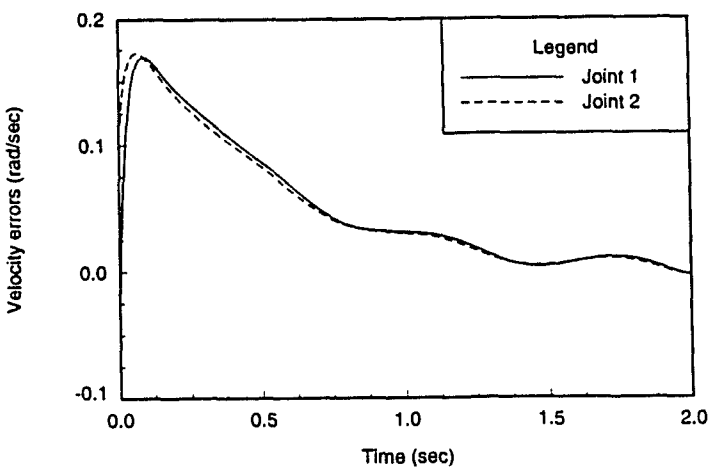

Figure 6. Joint velocity tracking errors under control law 1 ($\omega_f = 1$)

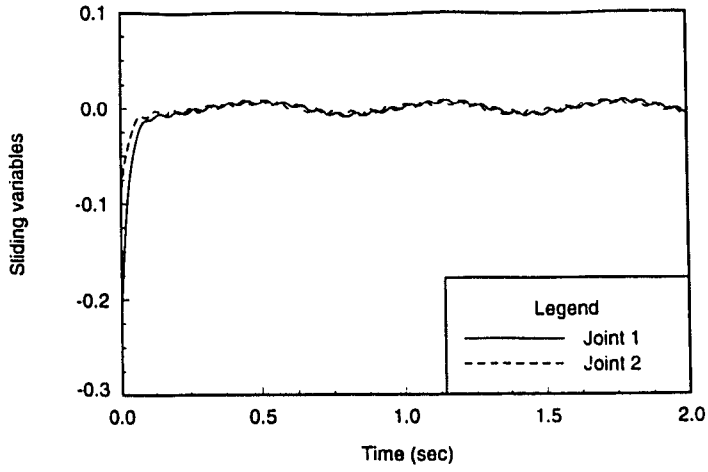

Figure 7. Sliding variables (tracking errors) under control law 1 ($\omega_f = 100$)

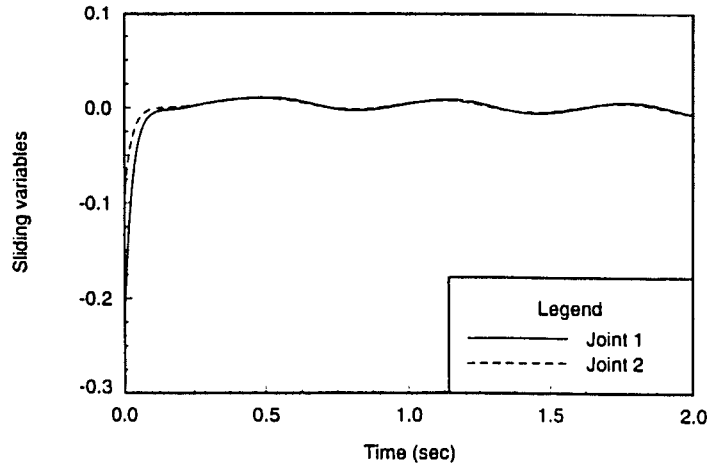

Figure 8. Sliding variables (tracking errors) under control law 1 ($\omega_f = 1$)

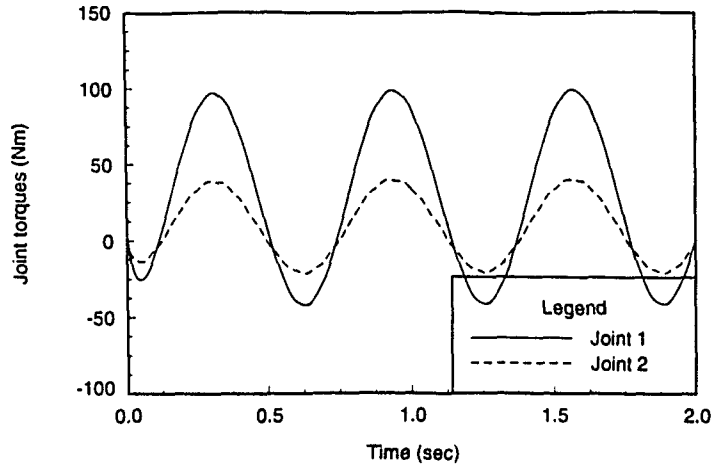

Figure 9. Joint torques under control law 1 ($\omega_f = 100$)

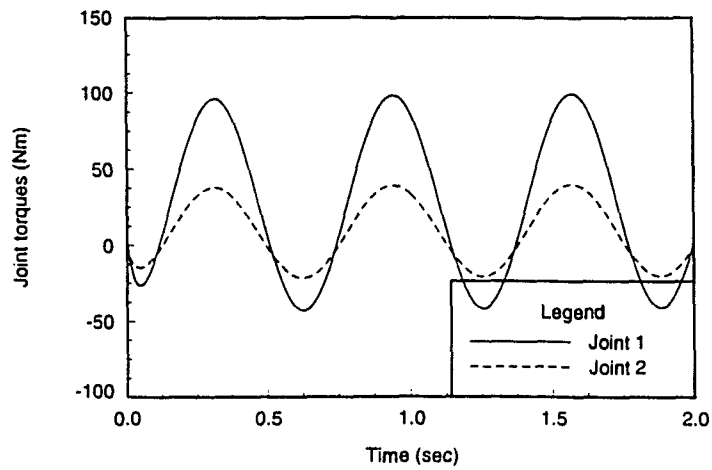

Figure 10. Joint torques under control law 1 ($\omega_f = 1$)

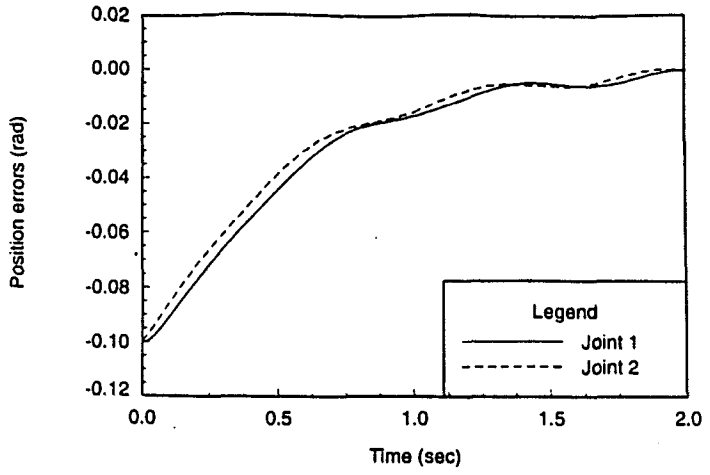

Figure 11. Joint position tracking errors under control law 2 ($\omega_f = 100, \xi = 0.1$)

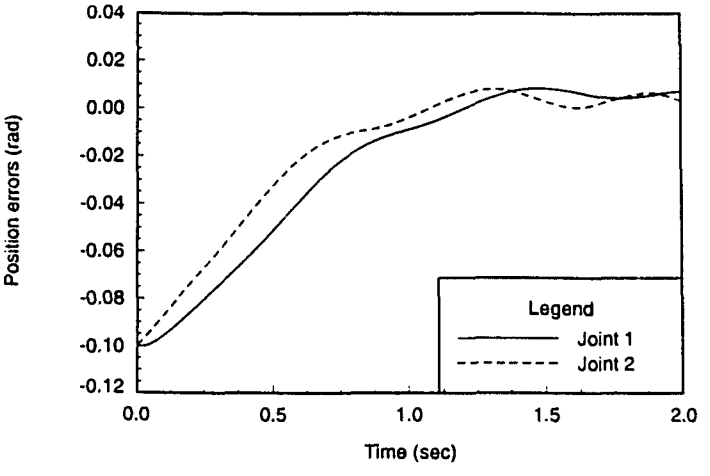

Figure 12. Joint position tracking errors under control law 2 ($\omega_f = 1, \xi = 0.5$)

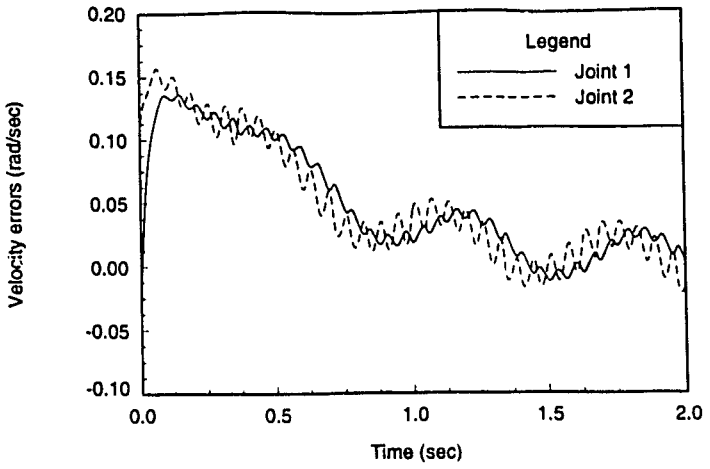

Figure 13. Joint velocity tracking errors under control law 2 ($\omega_j = 100, \xi = 0.1$)

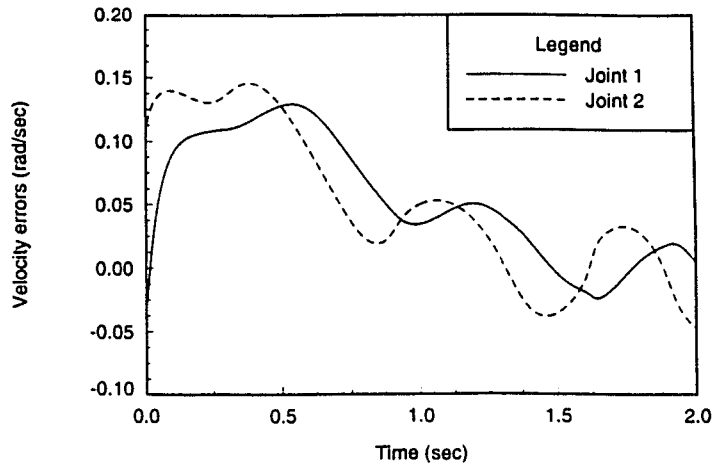

Figure 14. Joint velocity tracking errors under control law 2 ($\omega_j = 1, \xi = 0.5$)

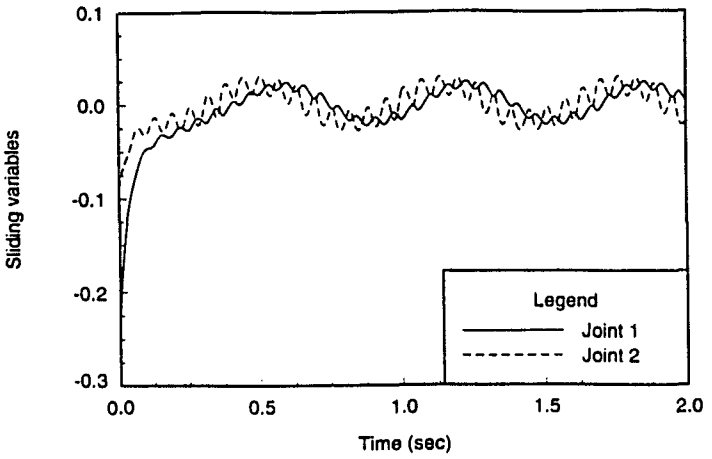

Figure 15. Sliding variables (tracking errors) under control law 2 ($\omega_f = 100, \xi = 0.1$)

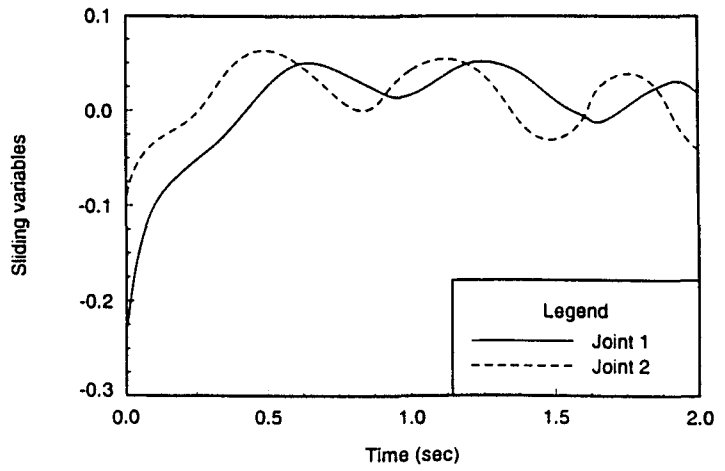

Figure 16. Sliding variables (tracking errors) under control law 2 ($\omega_f = 1, \xi = 0.5$)

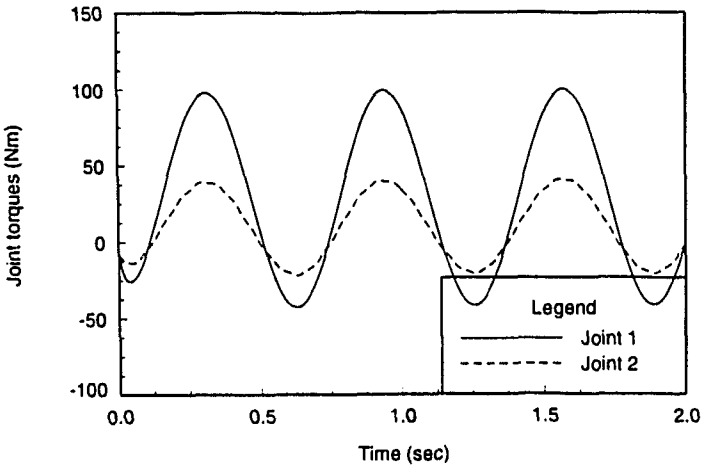

Figure 17. Joint torques under control law 2 ($\omega_f = 100, \xi = 0.1$)

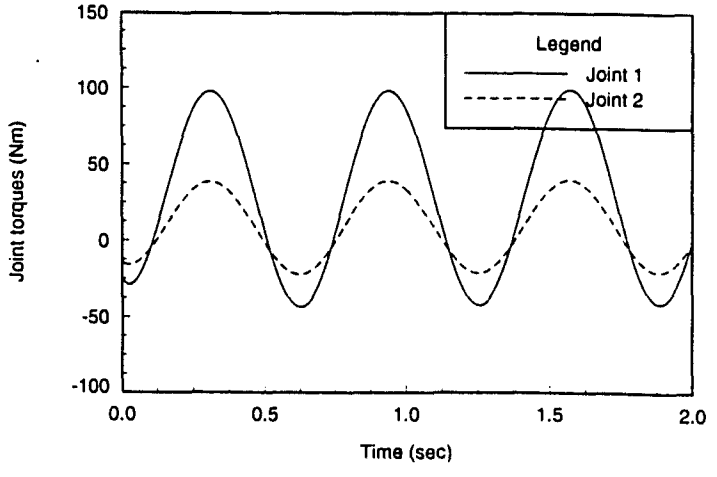

Figure 18. Joint torques under control law 2 ($\omega_f = 1, \xi = 0.5$)

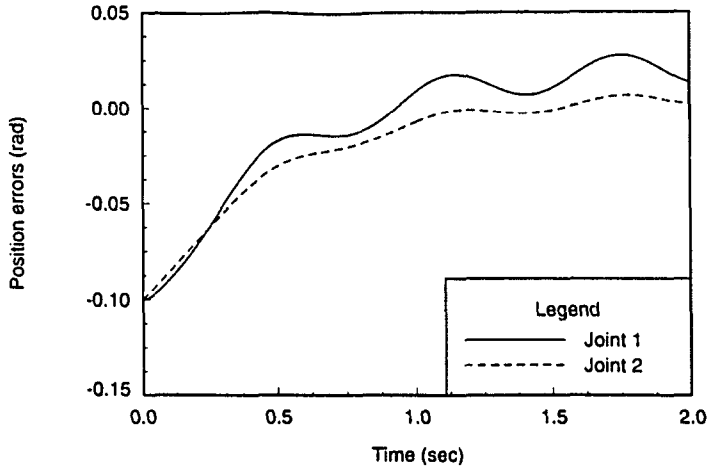

Figure 19. Joint position tracking errors under control law 3 ($\omega_j = 100, \xi = 0.7$)

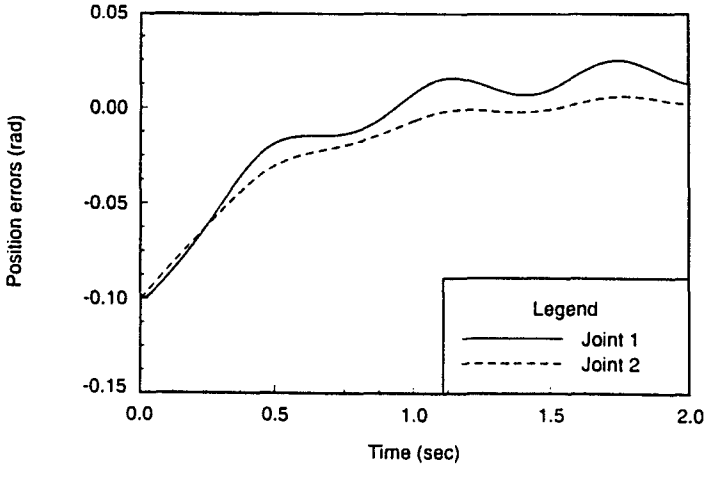

Figure 20. Joint position tracking errors under control law 3 ($\omega_j = 1, \xi = 0.1$)

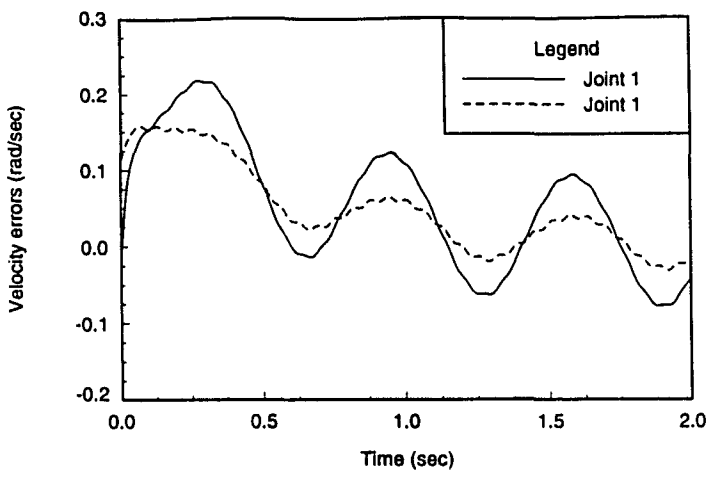

Figure 21. Joint velocity tracking errors under control law 3 ($\omega_f = 100, \xi = 0.7$)

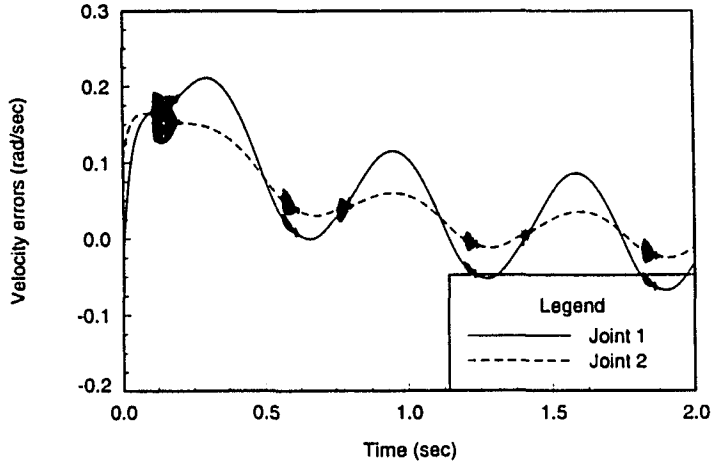

Figure 22. Joint velocity tracking errors under control law 3 ($\omega_f = 1, \xi = 0.1$)

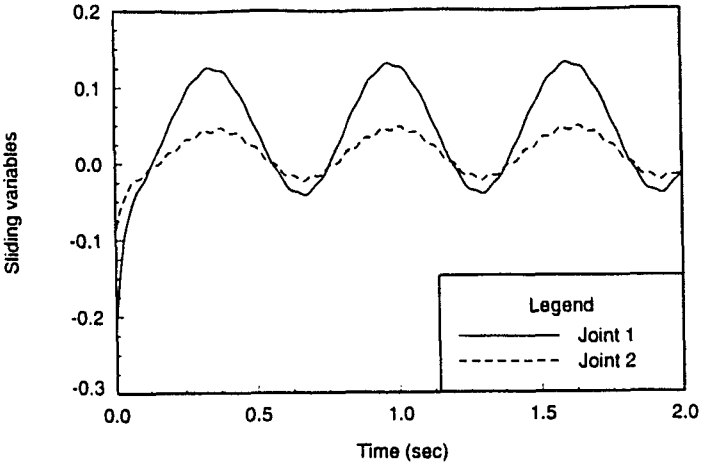

Figure 23. Sliding variables (tracking errors) under control law 3 ($\omega_f = 100, \xi = 0.7$)

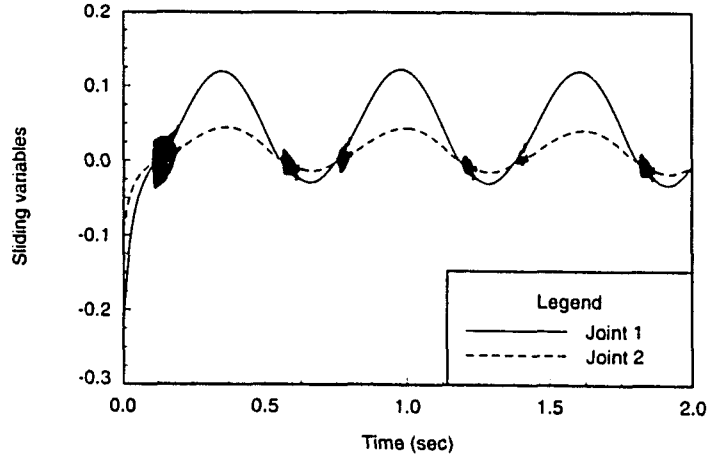

Figure 24. Sliding variables (tracking errors) under control law 3 ($\omega_f = 1, \xi = 0.1$)

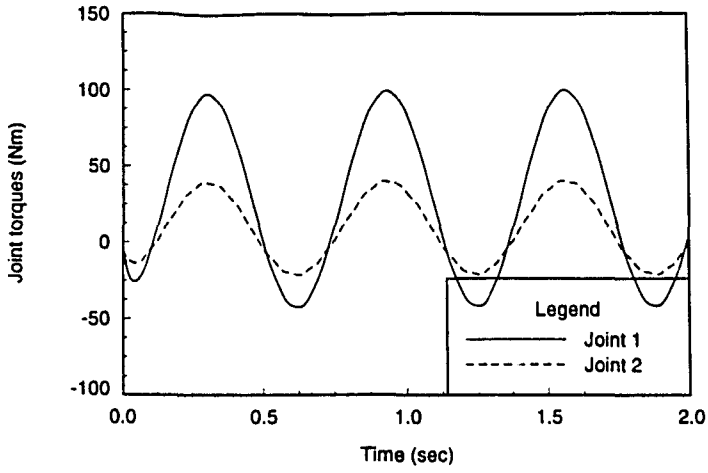

Figure 25. Joint torques under control law 3 ($\omega_f = 100, \xi = 0.7$)

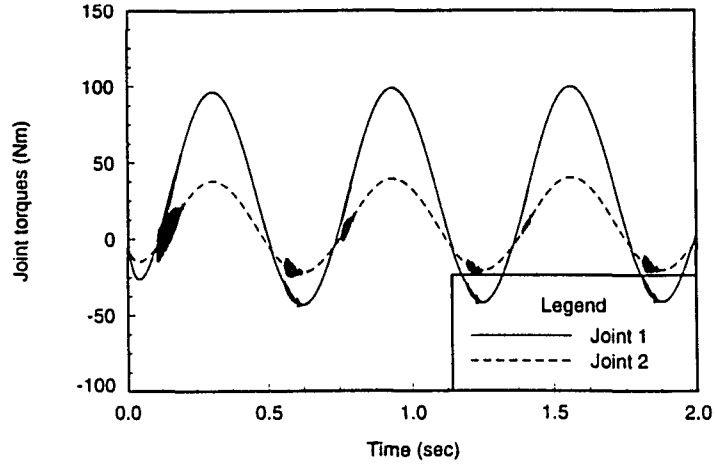

Figure 26. Joint torques under control law 3 ($\omega_f = 1, \xi = 0.1$)

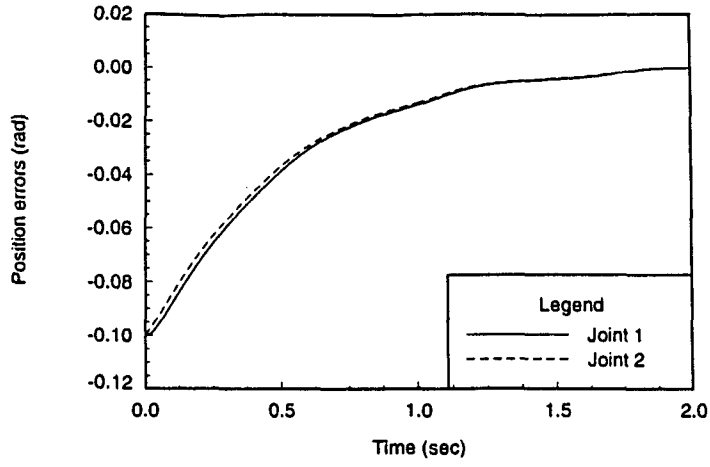

Figure 27. Joint position tracking errors under control law 4 ($\omega_j = 100, \xi = 0.1$)

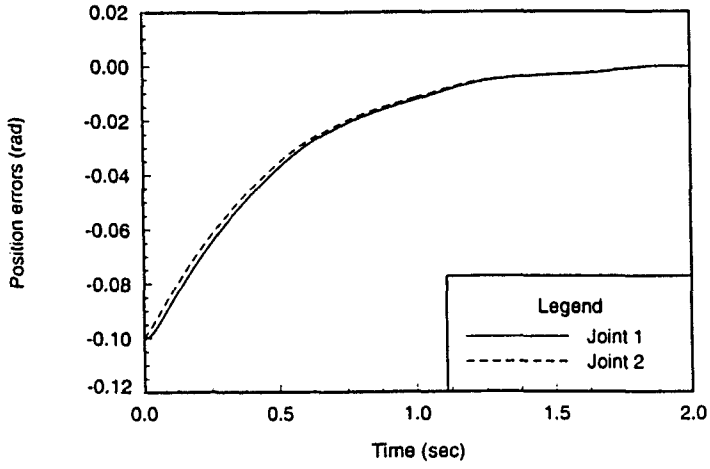

Figure 28. Joint position tracking errors under control law 4 ($\omega_j = 1, \xi = 0.1$)

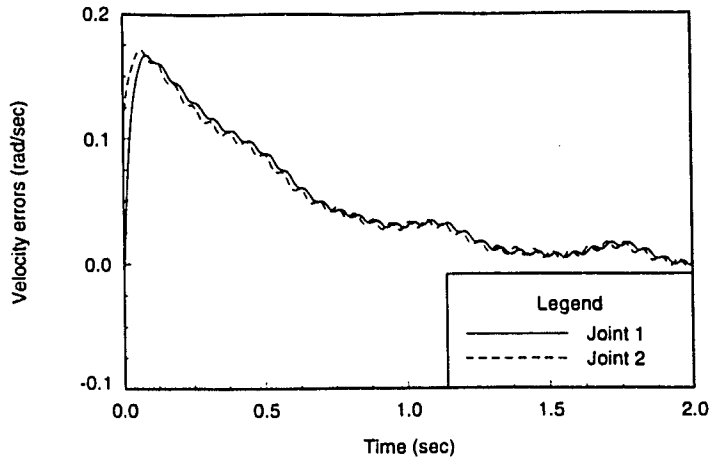

Figure 29. Joint velocity tracking errors under control law 4 ($\omega_l = 100, \xi = 0.1$)

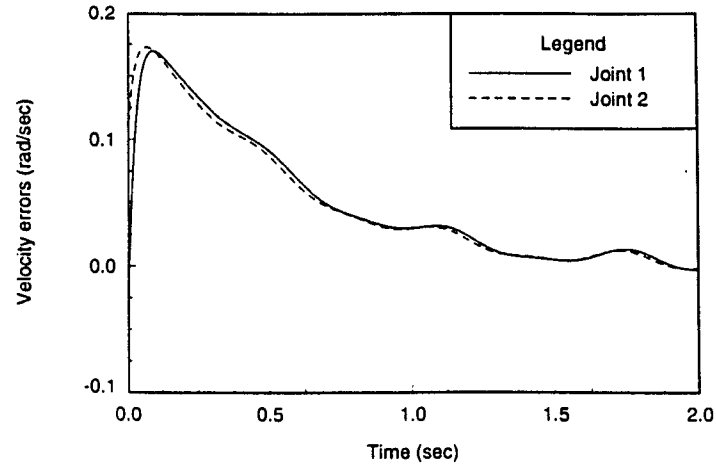

Figure 30. Joint velocity tracking errors under control law 4 ($\omega_l = 1, \xi = 0.1$)

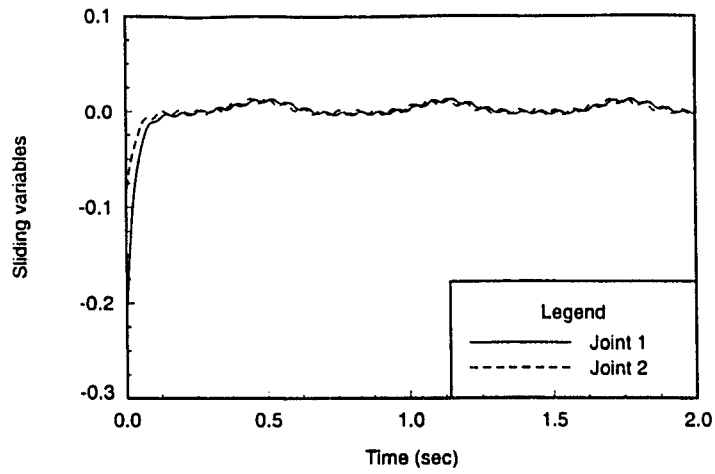

Figure 31. Sliding variables (tracking errors) under control law 4 ($\omega_f = 100, \xi = 0.1$)

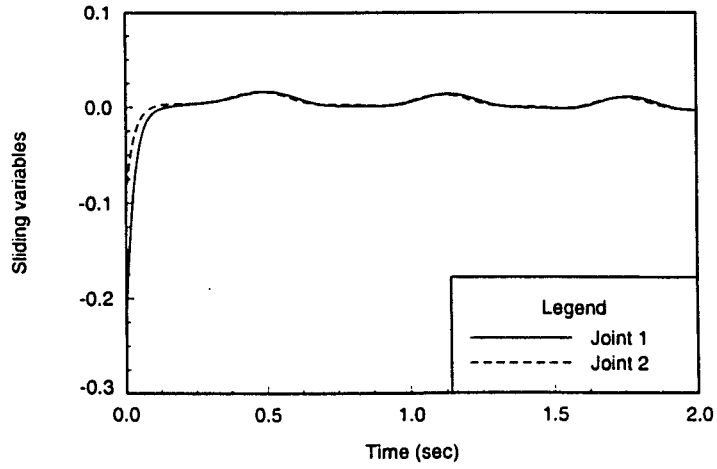

Figure 32. Sliding variables (tracking errors) under control law 4 ($\omega_f = 1, \xi = 0.1$)

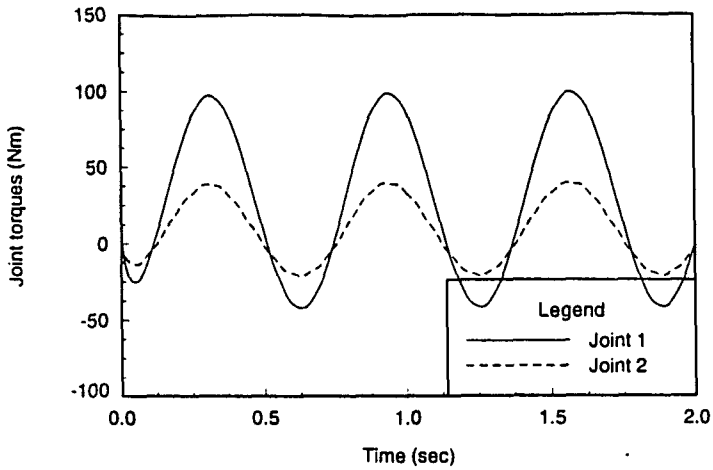

Figure 33. Joint torques under control law 4 ($\omega_f = 100, \xi = 0.1$)

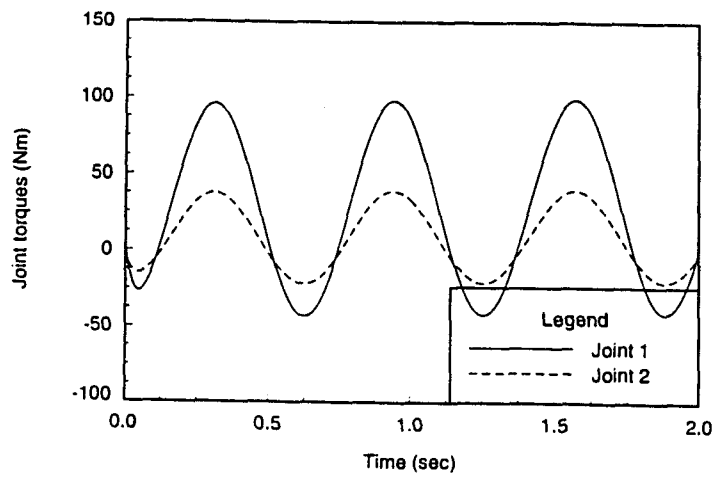

Figure 34. Joint torques under control law 4 ($\omega_f = 1, \xi = 0.1$)

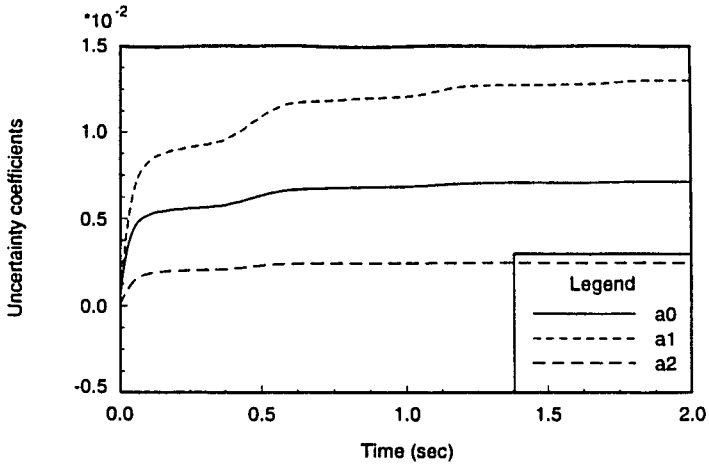

Figure 35. Uncertainty bound estimates under control law 4 ($\omega_f = 100, \xi = 0.1$)

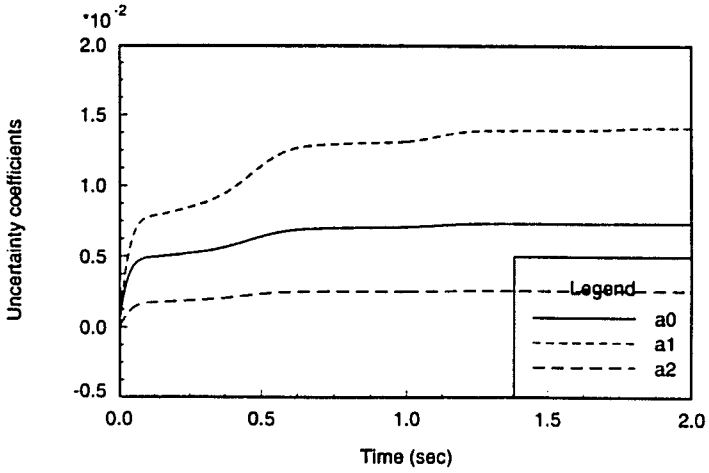

Figure 36. Uncertainty bound estimates under control law 4 ($\omega_f = 1, \xi = 0.1$)

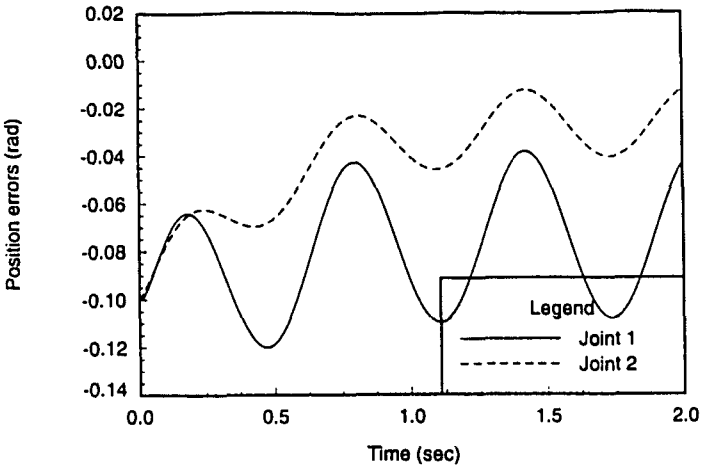

Figure 37. Joint position tracking errors under PD control law

$(\omega_f = 100, k_p = 400, k_v = 200)$

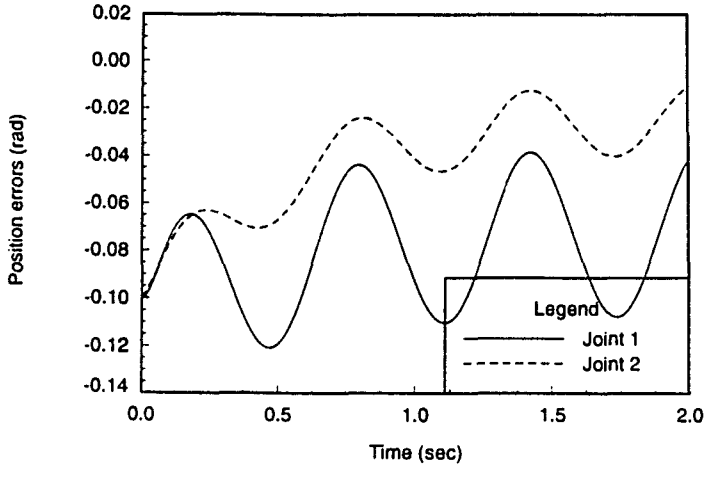

Figure 38. Joint position tracking errors under PD control law

$(\omega_f = 1, k_p = 400, k_v = 200)$

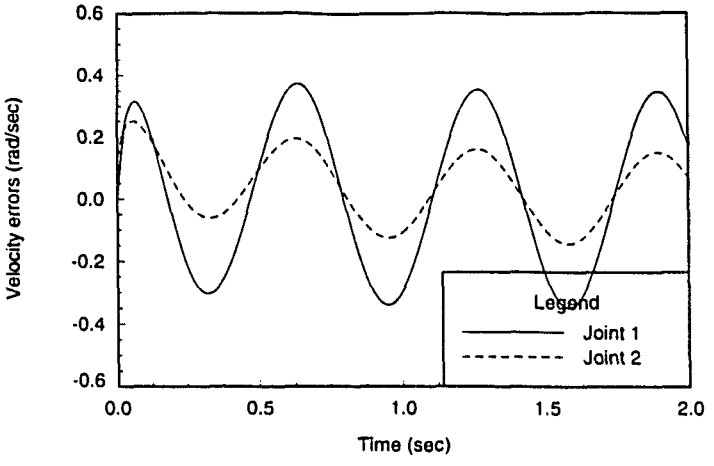

Figure 39. Joint velocity tracking errors under PD control law

$(\omega_f = 100, k_p = 400, k_v = 200)$

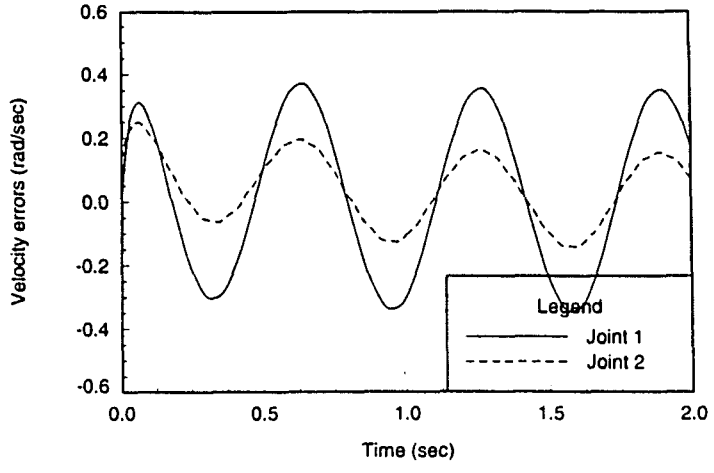

Figure 40. Joint velocity tracking errors under PD control law

$(\omega_f = 1, k_p = 400, k_v = 200)$

6. CONCLUSIONS

This research has presented dynamic compensation methodology for the robust trajectory tracking control of an uncertain robot model. The proposed control scheme consists of two major parts, that is, fully model-based feedforward control plus PD compensation and robust nonlinear controllers. The robust control synthesis adopted is based on the deterministic approach. Furthermore, the presented controllers can be implemented in decentralized manners. Both theoretical and simulation analysis are performed to ascertain the effectiveness of the proposed control algorithms. Stability and robustness issues of control laws have been investigated extensively and rigorously by the Lyapunov stability method. The outstanding contributions of the proposed control algorithms are summarized as follows: (i) The joint accelerations are not required in the control law; (ii) The presented control laws do not require the exact information about the system parameters and dynamics; (iii) Torque computations in the model-based portion can be calculated off-line if the desired trajectories and the nominal values of dynamic parameters are known in advance. This has high promise for real-time control; (iv) The robust control parts are designed to cope with the effect of higher-order uncertainties in the system; (v) Finally, it is shown that the proposed control laws can guarantee at least the UUB of all signals under significant uncertainties. Future works on this research should include extensive experimental results.

REFERENCES

[1] Craig, J.J., Hsu, P., and Sastry, S.S., "Adaptive control of mechanical manipulators," *Int. J. Robotics Res.*, 1987, 6(2), 16-28.

[2] Corless, M.J. and Leitmann, G., "Continuous state feedback guaranteeing uniform ultimate boundedness for uncertain dynamical systems," *IEEE Trans. Autom. Contrl.*, 1981, 26(5), 1139-1144.

[3] Corless, M.J. and Leitmann, G., "Adaptive control of systems containing uncertain functions and unknown functions with uncertain bounds," *J. Optim. Theory Appl.*, 1983, 41(1), 155-168.

[4] Chen, Y.H., "On the deterministic performance of uncertain dynamical systems," *Int. J. Contrl.*, 1986, 43(5), 1557-1579.

[5] Chen, Y.H., "Robust control system design: non-adaptive versus adaptive," *Int. J. Contrl.*, 1990, 51(6), 1457-1477.

[6] Dawson, D.M., Qu, Z., Lewis, F.L., and Dorsey, J.F., "Robust control for the tracking of robot motion," *Int. J. Control*, 1990, 52, 581-595.

[7] Abdallah, C., Dawson, D., Dorato, P., and Jamshidi, M., "Survey of robust control for rigid robots," 1991, *IEEE Contrl. Syst.*, 11, 24-30.

[8] Spong, M.W., "On the robust control of robot manipulators," *IEEE Trans. Autom. Contrl.*, 1992, 37(11), 1782-1786.

[9] Fu, L. C., "Robust adaptive decentralized control of robot manipulators," *IEEE Trans. Autom. Contrl.*, 1992, 37(1), 106-110.

[10] Shi, L. and Singh, S.K., "Decentralized adaptive controller design for large-scale systems with higher order interconnections," *IEEE Trans. Autom. Contrl.*, 1992, 37(8), 1106-1118.

[11] Qu, Z., "Robust control of a class of nonlinear uncertain systems," *IEEE Trans. Autom. Contrl.*, 1992, 37(9), 1437-1442.

[12] Qu, Z., "Global stabilization of nonlinear systems with a class of unmatched uncertainties," *Syst. & Contrl. Letters*, 1992, 18, 301-307.

[13] You, S.S. and Hall, J.L., "Robust tracking control for robot manipulators with significant uncertainties," *Proc. Midwest Electro-Tech.*, Ames, Iowa, 1994, 81-85.

[14] Young (ed), K.K.D., "Variable structure control for robotics and aerospace applications," Elsevier Science Publishers B.V., Amsterdam, Netherlands, 1993.

[15] Ioannou, P.A. and Kokotovic, P.V., "Instability analysis and the improvement of robustness of adaptive control," *Automatica*, 1984, 20(5), 583-594.

[16] Slotine, J.J. and Li, W., "On the adaptive control of robot manipulators," *Int. J. Robotics Research*, 1987, 6(3), 49-59.

[17] Ortega, R. and Spong, M.W., "Adaptive motion control of rigid robots: a tutorial," *Automatica*, 1989, 25(6), 877-888.

[18] Sadegh, N. and Horowitz, R., "Stability and robustness analysis of a class of adaptive controllers for robotic manipulators," *Int. J. Robotics Res.*, 1990, 9(3), 74-92.

[19] You, S.S. and Hall, J.L., "Model-based approach with adaptive bounds of robust controllers for robot manipulators," *Proc. IEEE Int. SMC*, 1994, 2, 1279-1284.

[20] Sastry, S. and Bodson, M., "Adaptive control, stability, convergence, and robustness," Prentice Hall, Englewood Cliffs, New Jersey, 1989.

APPENDIX

Appendix A

Consider an uncertain dynamical model described by

$$\dot{\mathbf{x}}(t) = \mathbf{f}(t, \mathbf{x}(t), \mathbf{u}(t), \mathbf{w}(t)), \quad \mathbf{x}(t_0) = \mathbf{x}_0, \tag{A1}$$

where $\mathbf{x}(t) \in R^n$ is the system state vector with $t \in R^+$; $\mathbf{u}(t) \in R^m$ is the control input vector; $\mathbf{w}(t) \in R^r$ is the uncertainties in the system and its values lie within a prescribed compact set (closed and bounded) $\Pi \subset R^r, \forall t \in R^+$ and $\mathbf{w} \in \Pi$, i.e., $\mathbf{w}(\bullet): R^+ \to \Pi \subset R^r$. The uncertainty bounding set Π may be known or unknown. Given a initial condition $(t_0, \mathbf{x}_0) \in R^+ \times R^n$, there exists a state feedback control function $\mathbf{p}(t, \mathbf{x}(t)): R^+ \times R^n \to R^m$. Then the corresponding closed-loop system is given by

$$\dot{\mathbf{x}}(t) = \bar{\mathbf{f}}(t, \mathbf{x}, \mathbf{p}(t, \mathbf{x}), \mathbf{w}). \tag{A2}$$

The solutions of the uncertain dynamical system $\mathbf{x}(t)$ with $\mathbf{x}_0 = \mathbf{x}(t_0)$ have the following properties:

(i) Uniform boundedness

Given any $\zeta_0[0, \infty)$, there exists a bound $d(\zeta_0) < \infty$, possibly dependent on ζ_0 but not on t_0, such that for any t_0 , all solutions $\mathbf{x}(\bullet): [t_0, t_1] \to R^n$ of (A2),

$$\|\mathbf{x}_0\| \le \zeta_0 \text{ and } \|\mathbf{x}(t)\| \le d(\zeta_0) \text{ for all } t \ge t_0$$

(ii) Uniform ultimate boundedness

For any $\bar{\zeta}(\in R^+) \ge \underline{\zeta}(\in R^+)$ and $\zeta_0(\in R^+)$, there exists a finite time (a nonnegative constant) $\bar{T}(\bar{\zeta}, \zeta_0) < \infty$, such that if $\mathbf{x}(\bullet): [t_0, \infty) \to R^n$ is a solution of the system with $\|\mathbf{x}(t_0)\| \le \zeta_0$, then, $\|\mathbf{x}(t)\| \le \bar{\zeta}$, $\forall t > t_0 + \bar{T}$.

Appendix B

Proof of Lemma 4:

The modeling error $\Delta \mathbf{R}_r$ can be estimated as follows:

Taking the norms on both sides of (4) gives

$$\|\Delta \mathbf{R}_r\| \le \|\mathbf{M}-\mathbf{M}_0\|\|\ddot{\mathbf{e}}_r\| + \|\mathbf{C}-\mathbf{C}_0\|\|\dot{\mathbf{e}}_r\| + \|\mathbf{G}-\mathbf{G}_0\|.$$

Now, from Assumptions 5 and 6, the following inequality is obtained;

$$\begin{aligned}\|\Delta \mathbf{R}_r\| &\le \rho_{11}\|\ddot{\mathbf{e}}_r\| + (\rho_{12}\|\dot{\mathbf{q}}\| + \rho_{13}\|\dot{\mathbf{q}}_d\|)\|\dot{\mathbf{e}}_r\| + \rho_{14} \\ &\le \rho_{11}(\|\ddot{\mathbf{q}}_d\| + \mu\|\dot{\mathbf{e}}\|) + [\rho_{12}(\|\dot{\mathbf{q}}_d\| + \|\dot{\mathbf{e}}\|) + \rho_{13}\|\dot{\mathbf{q}}_d\|](\|\dot{\mathbf{q}}_d\| + \mu\|\mathbf{e}\|) + \rho_{14} \\ &\le [\rho_{11}d_3 + (\rho_{12}+\rho_{13})d_2^{\,2} + \rho_{14}] + (\rho_{12}+\rho_{13})\mu d_2\|\mathbf{e}\| + (\rho_{11}\mu + \rho_{12}d_2)\|\dot{\mathbf{e}}\| + \mu\rho_{12}\|\mathbf{e}\|\|\dot{\mathbf{e}}\|.\end{aligned}$$

Then, it follows that

$$\|\Delta \mathbf{R}_r\| \le c_0 + c_1\|\mathbf{e}\| + c_2\|\dot{\mathbf{e}}\| + c_3\|\mathbf{e}\|\|\dot{\mathbf{e}}\|,$$

where

$$c_0 = \rho_{11}d_3 + (\rho_{12}+\rho_{13})d_2^{\,2} + \rho_{14},\ c_1 = (\rho_{12}+\rho_{13})\mu d_2,$$
$$c_2 = \rho_{11}\mu + \rho_{12}d_2,\ c_3 = \mu\rho_{12}$$

QED.

Appendix C

Proof of Lemma 5:

Note that $\|\mathbf{e}\| \le \|\mathbf{x}_e\|$ and $\|\dot{\mathbf{e}}\| \le \|\mathbf{x}_e\|$. From the result of Lemma 4, the uncertainty bound can be given as

$$\|\Delta \mathbf{R}_r\| \le c_0 + (c_1 + c_2)\|\mathbf{x}_e\| + c_3\|\mathbf{x}_e\|^2.$$

Finally, the bounds on $\Delta \mathbf{R}_r$ can be expressed

$$\|\Delta \mathbf{R}_r\| \le a_0 + a_1\|\mathbf{x}_e\| + a_2\|\mathbf{x}_e\|^2,$$

where $a_0 = c_0$, $a_1 = c_1 + c_2$, and $a_2 = c_3$.

The proof is completed. $\Delta\Delta$

PART II

A CLASS OF HYBRID POSITION AND FORCE CONTROLLERS FOR A SINGLE ROBOT MANIPULATOR WITH CONSTRAINED MOTION TASKS

OVERVIEW

This part of the dissertation considers the efficient methodology of formulating system dynamics and hybrid position/force control for a single robot manipulator under geometric end-effector constraints (i.e., system with closed kinematic chain). In order to facilitate dynamic analysis and control synthesis, the original joint-space dynamics (or a set of DAEs) is transformed into the constraint-space model through nonlinear transformations in which the manipulator dynamics can be readily decomposed into two subsystems (or two sets of differential equations): the (reduced-order) position-controlled subsystem is specified in the direction tangential to the known constraint surfaces, and the force-controlled subsystem is specified in the normal (or orthogonal) direction. Employing the transformed dynamic model, a class of hybrid control laws are presented to manipulate the position and contact force at the end-effector simultaneously and accurately: the modified computed torque method, the robust adaptive controller, and adaptive hybrid impedance controller. The rigorous stability and performance properties of the corresponding closed-loop systems are established in the sense that the global asymptotic stability for the computed torque controller, the UUB stability result for the robust adaptive controller, and the global asymptotic stability for the adaptive hybrid impedance controller. A simple example is presented to demonstrate the design procedures developed in the study. The main contribution of this work is to show how the joint-space formulations (system dynamics and control synthesis) can be generally transformed and successfully applied to the task-space formulations.

1. INTRODUCTION

There has been considerable research on the control of a single robot manipulator moving through free space within an unconstrained environment, see for example Refs [1-4]. These schemes are mainly concerned with a purely motion control of the system in which the robotic manipulator is not significantly interacting with the external environment. However, many practical tasks require extensive physical contact of the robot end-effector with external objects (or environments) in the workspace in applications such as machining tasks (grinding, deburring, polishing, etc.), contour following tasks, assembly operations, turning a crank, inserting a peg into a hole, various material handlings, human-like operations, and others. Obviously, while performing such contact tasks, the motion of the robot end-effector is kinematically constrained. In these cases, a position or motion control alone could lead to excessive contact forces or loss of contact with environments. In addition, the interactions generally affect the performance of the overall system and may degrade (even destroy) the stability of its control system. Since the end-effector contact with the external environment results in a robotic system as a closed-chain mechanism, certain degrees of freedom (often abbreviated DOF) are lost due to geometric constraints imposed on the system. In general, it is necessary to control both the position of the end-effector and the contact forces exerted by the end-effector on the environment if a high-performance robot system is to be achieved. In this sense, the primary aim of this research is to provide a unified and compact approach to dynamic analysis and control synthesis for robotic manipulator with closed kinematic chain.

The kinematics and dynamics of constrained robot system are widely discussed in Refs [5-8] and numerous others. Among various approaches within the hybrid control architecture, the impedance control and the position/force control (or hybrid control for short) have been extensively suggested. In the impedance control [9-11], the external

environment is modeled as a mechanical impedance to produce compliant motion, and contact force is controlled indirectly as a result of position control. In the area of hybrid position/force control, the position/force can be directly controlled to achieve accurate tracking performance.

In Ref. [5], the author identified the task constraints represented by natural and artificial constraints. Raibert and Craig [6] developed a hybrid controller based on the decomposition of the task space in the manner proposed by Mason [5]. Without parametric uncertainties and external disturbances in the robotic system, several hybrid control strategies have been proposed (Yoshikawa [12], and Mcclamroch and Wang [13]). From a practical point of view, these assumptions are unrealistic in many applications. The robot system contains various uncertainties, such as the structured uncertainties (or parametric uncertainties) and the unstructured uncertainties (for example, friction, external disturbances, and unmodelled dynamics). Since the uncertainties affect the stability and performance of the overall system, the robustness issues should be considered in such cases. This problem motivates the adaptive control approach. Several hybrid adaptive control schemes for robot manipulators can be found in Refs [14-16], while a few authors have addressed robust hybrid adaptive control. Although there has been considerable research on these topics in recent years, there is still much research to be carried out.

The first task of this research is to develop a unified approach that transforms the original joint-space dynamics (i.e., differential-algebraic equations (DAEs)) into the constraint-space model. The constraint frame is set up as a direct sum of position-controlled subspace and force-controlled subspace: the position subspace spanned by tangential vectors and the force subspace generated by normal vectors. Then the system dynamics in the transformed frame can be readily decomposed into two orthogonal subsystems: one subsystem specifies the end-effector motion (or purely kinetic reduced-order system) and the other characterizes the constraint forces caused by external contact. The method of

decoupling the contact forces from the position dynamics based on the orthogonality condition is especially useful for dynamic analysis and controller design purposes. Next, based on new transformed dynamic model, a class of hybrid controllers are presented. In hybrid controllers, the generalized positions and forces of the gripper are simultaneously regulated in two orthogonal directions, i.e., the position control in the free directions (or along the surface) and the force control in the constrained directions (or normal to the surface). A modified computed torque is adopted on the basis of complete knowledge of dynamic model and asymptotic stability of the closed-loop system is guaranteed. In the presence of uncertainties, two types of adaptive control law are formulated: the robust hybrid controller guaranteeing the uniform ultimate boundedness (UUB) stability results and the hybrid impedance control ensuring the asymptotic stability by the Lyapunov approach. Therefore, it is shown that the robotic system can be globally stabilized by the proposed control algorithms.

The rest of this chapter is organized as follows. First, the dynamic models and problem formulation will be presented in Section 2. Next, a class of hybrid control laws are introduced in Section 3. After that, a two-link planer robot interacting with external surface is presented as an example in Section 4. Finally, Conclusions are given in Section 5.

2. MANIPULATOR DYNAMIC MODEL SUBJECT TO EXTERNAL CONSTRAINTS

Consider a single robot system interacting with external environments, as depicted in Fig. 1. Suppose that the robot manipulator moves in a singularity-free region of workspace with kinematically nonredundant mechanism and the surface-type constraints are imposed on the robotic system. The external environment is assumed to be either elastic (deformable) or rigid without friction. In addition, it is assumed that constrained motion involves a point contact between end-effector and external surface, where the contact point is required to move along surface in a specified way while exerting appropriate interaction forces. Therefore, a closed-chain mechanism is always formed through contact surface with internal and/or external constraints.

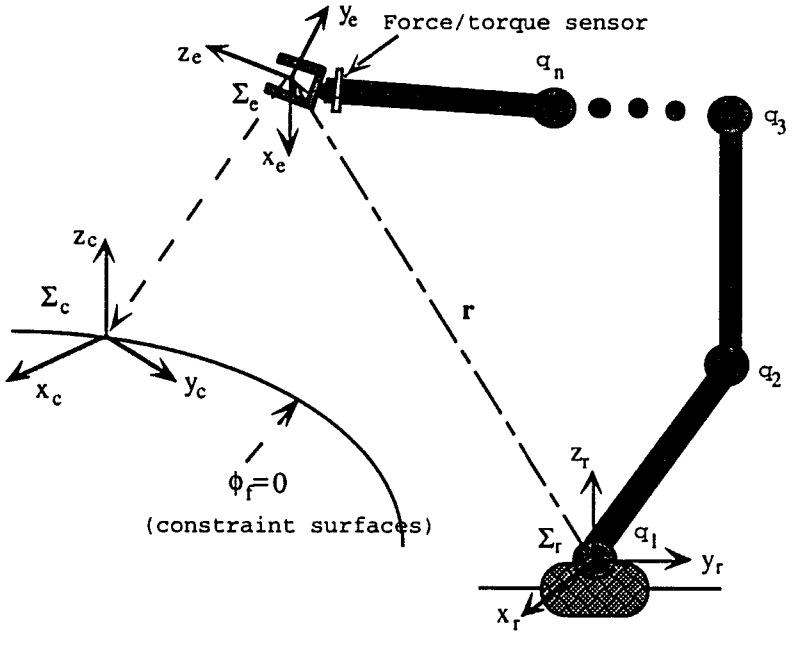

Figure 1. A schematic diagram of a single robot system subject to external constraints.

To describe the kinematic and dynamic relationships among the components of the closed-chain mechanism, a set of coordinate system are defined as follows: $\Sigma_r\{o_r - x_r y_r z_r\}$ is the world coordinate system which serves as a reference frame for the task space; $\Sigma_e\{o_e - x_e y_e z_e\}$ is the end-effector frame of the manipulator and its origin is at the contact point with the external environment; $\Sigma_c\{o_c - x_c y_c z_c\}$ is the constraint coordinate system in which the contact task to be accomplished is readily described. Here, all coordinate frames are right-handed and all bases in the frames will be orthonormal with the usual inner product in $\Re^3$.

The following notations and terminology will be utilized throughout this study. The vector norm $\|\mathbf{x}\|$ is the Euclidean norm of vector $\mathbf{x} \in \Re^n$ (the set of all n-dimensional Euclidean space), i.e., $\|\mathbf{x}\| = (\mathbf{x}^T\mathbf{x})^{1/2}$, and the matrix norm is the corresponding induced norm of matrix $\mathbf{A} \in \Re^{n\times n}$ (the set of all $n \times n$ real matrices), i.e., $\|\mathbf{A}\| = [\rho_{max}(\mathbf{A}^T\mathbf{A})]^{1/2}$, where $\rho_{max}(\bullet)[\rho_{min}(\bullet)]$ denotes the maximum (minimum) eigenvalue of the designated matrix, and superscript T stands for a transpose operation. In addition, $RS(\mathbf{A})$ (or $\mathrm{Im}(\mathbf{A})$) and $rk(\mathbf{A})$ denote the range (or image) space and the rank of matrix $\mathbf{A}$, respectively, while $NS(\mathbf{A})$ (or $Ker(\mathbf{A})$) represents the null space (or kernel) of $\mathbf{A}$. Throughout this study, the generalized positions in Cartesian space include both position and orientation (or rotation) information, and the generalized forces in Cartesian space imply force and torque.

In what follows, the concept of configuration space will be briefly discussed, that is, the configuration space for Cartesian positions and orientations of rigid bodies (or frames). First, consider an unconstrained motion operation of a robotic mechanism (or an open-chain structure) whose joint (or internal) position vector is denoted by $\mathbf{q} \in \Re^n$. Let $\mathbf{p} = [\mathbf{r}^T, \Psi^T]^T \in \Re^{n_0}$ $(n_0 \le n)$ be a generalized position vector of the manipulator end-effector (or gripper) with respect to frame Σ_r, which is composed of the Cartesian position vector $\mathbf{r}$ and the orientation vector (such as Euler angles) Ψ to define the end-effector

configuration. For an arbitrary position and orientation of the end-effector in $\Re^3$, $\mathbf{p}$ is typically chosen as some parameterization of 6-dimensional manifold (i.e., n_0=6, with $\mathbf{r} \in \Re^3$ and $\Psi \in \Re^3$). Thus, the robot end-effector moves towards the constraint surfaces with 6-DOF in position/orientation. Due to nonredundancy, it holds that $n_0 = n$ ($= 6$ for example) throughout the study. However, kinematic redundancy (i.e., $n_0 < n$, with "extra" DOF) can be utilized to improve the robot operations, such as dexterous manipulation, singularity and obstacle avoidance purposes.

There exist several methods of defining a set of independent parameters to represent an arbitrary orientation of a rigid body in the Euclidean space $\Re^3$. For example, the rotational motion Ψ can be described by three Euler angles, as shown pictorially in Fig. 2. More specifically, the Euler angles are specified in terms of the image of the three parameters (α, β, γ) obtained by performing three elementary rotations of body-attached frame (or rotating frame) Σ_e with respect to fixed frame Σ_r in a right-handed sense, that is, rotating α (yaw angle) about the z axis, then β (pitch angle) about the new y axis, and finally γ (roll angle) about the new x axis. Then the resulting overall transformation with Euler angles is given in a 3×3 matrix as

$$
\begin{aligned}
R(\alpha,\beta,\gamma) &= {}^r_e YPR(\alpha,\beta,\gamma) = [{}^r_e\mathbf{i} \;\vdots\; {}^r_e\mathbf{j} \;\vdots\; {}^r_e\mathbf{k}] \\
&= \begin{bmatrix} C\alpha C\beta & C\alpha S\beta S\gamma - S\alpha C\gamma & C\alpha S\beta C\gamma + S\alpha S\gamma \\ S\alpha C\beta & S\alpha S\beta S\gamma + C\alpha C\gamma & S\alpha S\beta C\gamma - C\alpha S\gamma \\ -S\beta & C\beta S\gamma & C\beta C\gamma \end{bmatrix},
\end{aligned} \tag{1}
$$

where ${}^r_e\mathbf{i}$, ${}^r_e\mathbf{j}$, and ${}^r_e\mathbf{k} \in \Re^3$ denote coordinate vectors of the principle axes of body frame Σ_e relative to frame Σ_r; For the notational convenience in the analysis, $C\alpha = \cos(\alpha)$, $S\beta = \sin(\beta)$, and $C\gamma = \cos(\gamma)$, and so on. Thus, the orthogonal rotation matrix $R(\bullet)$: $\Re^3 \rightarrow \Re^3$ (with $RR^T = R^T R = \mathbf{E}$ and $R^{-1} = R^T$) maps from coordinate system Σ_e into Σ_r, where $\mathbf{E}$ is an identity matrix with appropriate dimension.

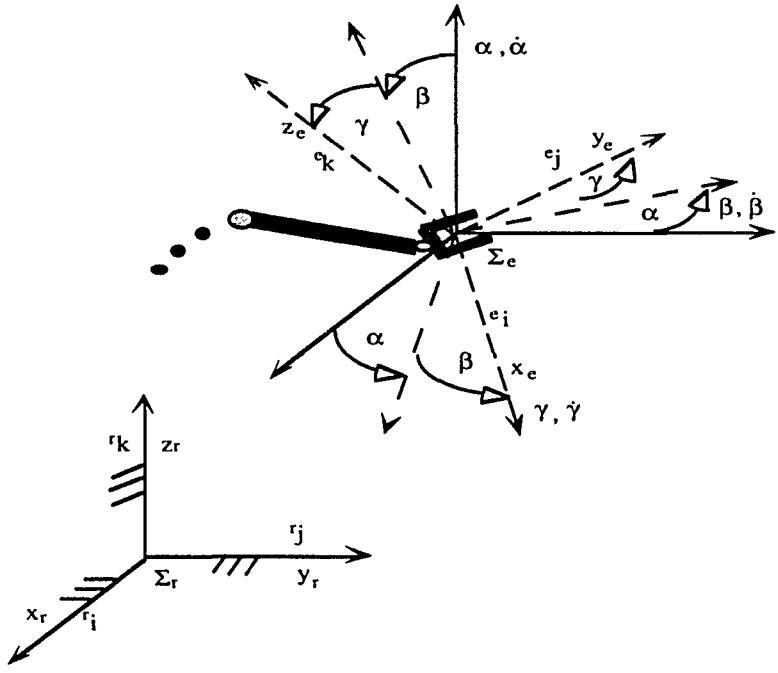

Figure 2. Geometrical description of Euler angles (yaw, pitch, and roll angles).

For the purpose of the present study, the motion of a rigid body (or frame) in a three-dimensional workspace is specified by

$$(\mathbf{r}, R) \in \Re^3 \times SO(3) = SE(3),$$

where the Special Orthogonal group of order 3, denoted by $SO(3)$ ($\subset \Re^{3\times 3}$), represents a set (or group) of all proper 3×3 rotational matrices on $\Re^3$, and is a three-dimensional differential submanifold of $\Re^9$. Here, $SO(3)$ can be more formally defined as

$$SO(3) = \{R \in \Re^{3\times 3} : \det(R) = +1,\ R^T R = R R^T = \mathbf{E}\}.$$

Consequently, it is clear that the motions (position and orientation) of a rigid body belong to 6-dimensional manifold. The Special Euclidean group, denoted by $SE(3)$, can be considered as the configuration space for rigid bodies, that is, the configuration of a rigid body with respect to reference frame is completely represented by $SE(3)$ with dimension 6. It is worth noting that the configuration space $SE(3)$ which consists of the translations and

proper rotations can also be expressed in a 4×4 matrix, often referred to as "homogeneous" (transformation) matrix in robotics literature. Based on this observations, $SE(3)$ is a group isomorphic to a group of 4×4 homogeneous matrices and also isomorphic to the set of frames in which the isomorphism may depend upon the choice of the reference frame. The 4×4 homogeneous matrix is defined as:

$$ {}^{r}_{e}T = \begin{bmatrix} Rotation & Position \\ Perspective & Scaling \end{bmatrix} = \begin{bmatrix} \underset{(3\times3)}{R} & \underset{(3\times1)}{\mathbf{r}} \\ 0\ \ 0\ \ 0 & 1 \end{bmatrix}. $$

In addition, $\omega \in \Re^3$ is the vector of the angular velocity of the frame Σ_e as viewed in Σ_r. The time derivative of orientation vector (or Euler angles) is called Euler rates and related as (see Fig. 2)

$$ \omega = (-\dot{\beta} S\alpha + \dot{\gamma} C\beta C\alpha)\,{}^{r}\mathbf{i} + (\dot{\beta} C\alpha + \dot{\gamma} C\beta S\alpha)\,{}^{r}\mathbf{j} + (\dot{\alpha} - \dot{\gamma} S\beta)\,{}^{r}\mathbf{k}, \tag{2} $$

where ${}^{r}\mathbf{i}$, ${}^{r}\mathbf{j}$, and ${}^{r}\mathbf{k} \in \Re^3$ represent the orthonormal vectors of the principle axes of Σ_r. As a result, the rotational velocity vector of the body frame (along with the relationship between the angular velocity ($\omega \in \Re^3$) and the rates of Euler angles ($\dot{\Psi}$)) is given in a compact form as

$$ \omega = \Delta(\Psi)\dot{\Psi}, \tag{3} $$

where the transformation matrix $\Delta \in \Re^{3\times3}$ is easily defined as

$$ \Delta(\Psi) = \begin{bmatrix} 0 & -S\alpha & C\beta C\alpha \\ 0 & C\alpha & C\beta S\alpha \\ 1 & 0 & -S\beta \end{bmatrix} $$

which maps the Euler rates into the angular velocity. Some comments are in order at this point. Since $\det(\Delta) = \cos(\beta)$, the singularity (or degeneracy) is likely to occur at $\det(\Delta) = 0$ in which the matrix Δ is rank deficient. Thus the Euler angles are not uniquely defined when a robot manipulator is operated near a singular point. In this study, Δ is assumed a nonsingular matrix over any Ψ of interest so that a singular point is eliminated, although the singularity is not avoided in any Euler angle representations with three independent parameters. And the mapping $\Psi \rightarrow R$ (or $SO(3)$) is surjective (onto) and the

reverse map $R \rightarrow \Psi$ is also surjective if $\cos\beta \neq 0$. Assume that R is time-varying, with $R \in SO(3)$, $\forall t \in \Re^+$. Then it is well known that $\dot{R} = \overline{\omega}(\omega)R$, where the skew-symmetric matrix function $\overline{\omega}(\omega)$ is given by

$$\overline{\omega} = [\omega\times] = \begin{bmatrix} 0 & -\omega_z & \omega_y \\ \omega_z & 0 & -\omega_x \\ -\omega_y & \omega_x & 0 \end{bmatrix},$$

where ω is an arbitrary three-dimensional vector, $\omega = col(\omega_x, \omega_y, \omega_z)$. More formally, $\overline{\omega} \in so(3) = \{\overline{\omega} \in \Re^{3\times3}: \overline{\omega}^T = -\overline{\omega}\}$, with $so(3) \subset \Re^{3\times3}$. As shown in (3), it is clear that ω is not the time derivative of any three-dimensional representation of rotation vector. In other words, the integral of $\dot{\Psi}$ is clearly given by Ψ, while that of ω has no physical meaning.

With the notation defined above, the two representations of the generalized velocity vector (or twists) of end-effector moving in space $\Re^3$ via Euler angles are related as

$$\mathbf{v} = \mathbf{N}(\mathbf{p})\dot{\mathbf{p}}, \text{ with } \mathbf{p} = (\mathbf{r}, R) \in SE(3), n = 6 \tag{4}$$

where $\mathbf{v} = [\dot{\mathbf{r}}^T, \omega^T]^T \in \Re^6$ and $\dot{\mathbf{p}} = [\dot{\mathbf{r}}^T, \dot{\Psi}^T]^T \in \Re^6$, with $\mathbf{N}(\mathbf{p}) = \begin{bmatrix} \mathbf{E}_{3\times3} & \mathbf{0}_{3\times3} \\ \mathbf{0}_{3\times3} & \Delta \end{bmatrix} \in \Re^{6\times6}$, and $\mathbf{E}_{n\times n}$ and $\mathbf{0}_{n\times n}$ represent $n \times n$ identity and null matrices, respectively. Of course, $\mathbf{N}$ is a nonsingular Jacobian matrix. As shown above, the motion space of an end-effector is a subset of the space $SE(3)$.

Now, the forward (or direct) kinematics under the assumption of a rigid manipulator is defined as

$$\mathbf{p} = \mathbf{h}(\mathbf{q}), \tag{5}$$

where $\mathbf{h}(\bullet): C^2$ ($\Re^n \rightarrow \Re^n$ (*or* $SE(3), n = 6$)) represents a mapping (or transformation) from joint space to end-effector space. This mapping is continuous, invertible, and twice differentiable (a C^2 function) whose elements are nonlinear functions of joint-space variables and kinematic parameters (such as link lengths and offsets). Thus this embodies the geometry of a given robot manipulator. By chain rule of differentiation, the corresponding velocity relation is then given by

$$\mathbf{v} = [\dot{\mathbf{r}}^T, \omega^T]^T = \mathbf{J}\dot{\mathbf{q}}, \tag{6}$$

with $\mathbf{J} = \mathbf{N}\dfrac{\partial \mathbf{h}(\mathbf{q})}{\partial \mathbf{q}}$, where $\mathbf{J} \in \Re^{n \times n}$ is the standard manipulator Jacobian which has full rank over any $\mathbf{q}$ of interest and contains important information concerning the performance characteristics of robotic mechanism. A unique inverse transformation exists in (6) if $\mathbf{J}$ is a square matrix with maximal rank or if and only if the mapping is bijective. In practice, the direct kinematics and its Jacobian matrix are fixed and *a priori* known for a given manipulator.

In case of a closed-chain mechanism, a robotic system is possibly internally and/or externally constrained. Thus, a suitable configuration space will be a submanifold of dimension of an unconstrained system. If $m\,(<n)$ mutually independent external constraints (or a set of m hypersurfaces) are imposed on the end-effector while robot in motion, then the constraint surfaces along which the end-effector should trace satisfy the constraint equations of the form

$$\phi_f(\mathbf{p}) = [\phi_{f1}(\mathbf{p}), \cdots, \phi_{fm}(\mathbf{p})]^T = \mathbf{0}_m \ \{\text{or } \phi_{fi}(\mathbf{p}) = 0 \ \ (i = 1, \cdots, m)\}, \tag{7}$$

where $\phi_f(\bullet) \in C^2\,(\Re^n\,(or\,SE(3)) \rightarrow \Re^m)$ $\{\text{or } \phi_{fi}(\bullet) \in C^2(\Re^n\,(or\,SE(3)) \rightarrow \Re^1)\}$ are the "natural" constraint functions resulting from geometric characteristics of task configuration to be performed (i.e., system constraints due to direct contact between bodies), and $\mathbf{0}_m$ denotes m-dimensional null vector. Depending upon the given task, the constraint surfaces can be stationary or nonstationary. The gripper motion restrictions described by (7) are commonly called "holonomic" (integrable) constraints in the literature [8, 12-13, 17]. Otherwise, the system constraints are "nonholonomic", for example, inequality and nonintegrable differential constraints. In order to specify the desired motion of the system, a set of "artificial" constraints along the surfaces are introduced as [5-8, 12, 17]

$$\phi_t(\mathbf{p}) = [\phi_{t1}(\mathbf{p}), \cdots, \phi_{t(n-m)}(\mathbf{p})]^T, \tag{8}$$

with $\phi_t(\bullet) \in C^2\ (\Re^n (or\, SE(3)) \rightarrow \Re^{(n-m)})$, in such a way that the constraint surface variables ($\phi_f(\mathbf{p})$ and $\phi_t(\mathbf{p})$), which are a subset of space $\Re^n$, are mutually independent over any $\mathbf{p}$ of interest and twice differentiable functions with respect to $\mathbf{p}$ and time. Later, for the purpose of this study, the natural and artificial constraints which are selected to be mutually orthogonal together form n-dimensional task-oriented space (in general, $n = 6$) to uniquely specify the end-effector configuration.

The robot manipulator under consideration consists of a series of rigid bodies with n revolute joints. On the basis of Euler-Lagrange formulation, the joint-space dynamics of constrained robot manipulator takes a set of mixed differential and algebraic equations (DAEs) of the general form [13]

$$\mathbf{M}(\mathbf{q};\Theta)\ddot{\mathbf{q}} + \mathbf{C}(\mathbf{q},\dot{\mathbf{q}};\Theta)\dot{\mathbf{q}} + \mathbf{G}(\mathbf{q};\Theta) + \mathbf{T}_u = \mathbf{T} - \mathbf{T}_c, \tag{9a}$$

$$\phi_f(\mathbf{p}) = \mathbf{0}_m, \text{ with } \mathbf{p} = \mathbf{h}(\mathbf{q}) \tag{9b}$$

where $\mathbf{q}, \dot{\mathbf{q}}$, and $\ddot{\mathbf{q}} \in \Re^n$ denote the vectors of joint displacement, velocity, and acceleration, respectively; $\mathbf{M}(\mathbf{q}) \in \Re^{n \times n}$ is an inertia matrix; the matrix $\mathbf{C}(\mathbf{q},\dot{\mathbf{q}}) \in \Re^{n \times n}$ represents the centripetal and Coriolis effects; $\mathbf{G}(\mathbf{q}) \in \Re^n$ is the vector containing gravitational torques; $\mathbf{T}_u \in \Re^n$ denotes the effect of unstructured uncertainties, such as friction, external disturbances, actuator noise, and unmodelled dynamics; $\mathbf{T} \in \Re^n$ is the control input vector supplied by the actuators; $\mathbf{T}_c \in \Re^n$ represents the vector of the generalized contact (or interaction) forces between the end-effector and the external environment, and its structure will be specified later in detail. And all robot dynamic parameters, such as link lengths, masses, and moments of inertia, are lumped together into a parameter vector $\Theta \in \Re^{\nu}$. In this formulation, both the joint-space variables and the Cartesian-space variables may not be independent due to system constraints. Generally, the function $\phi_f(\mathbf{p}) = \mathbf{0}$ constraining the gripper configuration are nonlinear in terms of $\mathbf{p}$. Also assume that the robotic system is equipped with joint position and velocity sensors (such as

digital encoders and tachometers), and a force sensor at its end-effector (e.g., a wrist force/torque sensor). Normally the dynamic synthesis of robots deal with only position specification. In many practical applications, however, force specifications are essential because of the interactions between the gripper and it environment. Hereafter, we will often omit the functional dependencies in the equations when it is clear. It is well known that the dynamic model (9a,b) has several fundamental properties that can be exploited to control system design (see Refs [1-4] for details).

Property 1: $\mathbf{M}$ is a symmetric and positive-definite matrix, i.e., $\mathbf{M} = \mathbf{M}^T > \mathbf{0}$. Further, $\mathbf{M}$ and $\mathbf{M}^{-1}$ are uniformly bounded above and below as a function of $\mathbf{q}$, for example,

$$\underline{\alpha}\mathbf{E} \le \mathbf{M} \le \overline{\alpha}\mathbf{E}, \quad \forall \mathbf{q} \in \Re^n,$$

where $\underline{\alpha}$ and $\overline{\alpha}$ are scalar constants ($0 < \underline{\alpha} \le \overline{\alpha} < \infty$, for all revolute joints).

Property 2: The matrix $(\dot{\mathbf{M}} - 2\mathbf{C})$ is a skew-symmetric with a suitable definition of the matrix $\mathbf{C}$, that is, $\mathbf{x}^T(\dot{\mathbf{M}} - 2\mathbf{C})\mathbf{x} = \mathbf{0}$, $\forall \mathbf{x} \in \Re^n$. Furthermore, $\mathbf{C}$ is linear in $\dot{\mathbf{q}}$ such that $\|\mathbf{C}\| \le a\|\dot{\mathbf{q}}\|$, where $a(> 0)$ is a scalar constant.

Property 3: A part of the dynamic structure (9a) is linear in terms of a suitably selected set of dynamic parameters, that is,

$$\mathbf{M}(\mathbf{q};\Theta)\mathbf{y} + \mathbf{C}(\mathbf{q},\dot{\mathbf{q}};\Theta)\mathbf{x} + \mathbf{G}(\mathbf{q};\Theta) = \mathbf{R}(\mathbf{q},\dot{\mathbf{q}},\mathbf{x},\mathbf{y})\Theta,$$

where $\mathbf{R} \in \Re^{n \times s_1}$ is a "regressor" matrix which depends on known functions of joint-space variables $(\mathbf{q},\dot{\mathbf{q}}, \mathbf{x}, \mathbf{y}) \in \Re^n$, and $\Theta \in \Re^{s_1}$ is the vector of known (or unknown) system parameters of interest.

Remark 1: In the above formulation, it is not necessary to satisfy $\mathbf{y} = \dot{\mathbf{x}}$. In addition, the choice of the vector of system parameters is not unique. Namely, the dimension of the parameter space depends on the particular choice of the robot manipulators. $\Delta\Delta$

However, task specifications of many practical tasks are best described in terms of the end-effector configurations in the Cartesian space, that is, the end-effector motions and

contact forces in the operational space are actually among the most important issues in the successful manipulation of constrained robot system. In addition, the governing equations (i.e., a set of DAEs) are not appropriate forms for dynamic analysis and control synthesis purposes (i.e., computationally inefficient formulations and singular system of differential equations in nature). The rest of this section provides an efficient approach to the problems of converting and extending the joint-space model to the task-oriented space model. This enables one to simplify the specifications of the tasks and reduce the original dynamics to the minimal sets. Thus the hybrid control problem can be solved more efficiently. Based on the above observations, introduce the constraint surface frame (Σ_c) where the constraint tasks to be performed are easily described (see Fig. 1). Let us combine the two subvectors ϕ_f and ϕ_t to generate a complete set of generalized position vector in the constraint-space frame as

$$\mathbf{x}_w = [\mathbf{x}_f{}^T, \mathbf{x}_t{}^T]^T, \ \mathbf{x}_w \in \Re^n \tag{10}$$

which is completely parameterized in terms of constraint-surface variables by

$$\mathbf{x}_f = \phi_f(\mathbf{p}) \text{ and } \mathbf{x}_t = \phi_t(\mathbf{p}),$$

with $\mathbf{x}_f \in \Re^m$ and $\mathbf{x}_t \in \Re^{(n-m)}$. For complex tasks, the constraint frame is generally time-varying and its origin is usually located at current end-effector configuration $\mathbf{p}$ (i.e., the contact point of the robot end-effector with the external environment). Since the natural constraints (or a set of environment configuration variables) are orthogonal to the artificial constraints (or a set of purely kinetic variables), n-dimensional task space can be split into two orthogonal subspaces: $(n-m)$-dimensional position subspace and m-dimensional contact force subspace. If the end-effector contacts with the constraint surface, then the system motion is restricted along normal directions. Thus a set of m curvilinear coordinates $\mathbf{x}_f$ equal to zeroes at each instant time of system's motion in the constraint-space. Now the corresponding velocity can be obtained by differentiating Eq. (10) with respect to time

$$\dot{\mathbf{x}}_w = \mathbf{J}_\phi \mathbf{v}, \text{ with } \mathbf{J}_\phi = [\mathbf{J}_f{}^T, \mathbf{J}_t{}^T]^T \in \Re^{n\times n} \tag{11}$$

where some matrices and vectors are defined as follows:

$$\mathbf{J}_f = \frac{\partial \phi_f}{\partial \mathbf{p}} = [\frac{\partial \phi_{f1}}{\partial \mathbf{p}}{}^T, \cdots, \frac{\partial \phi_{fm}}{\partial \mathbf{p}}{}^T]^T \in \Re^{m\times n}, \text{ with } \frac{\partial \phi_{fi}}{\partial \mathbf{p}}{}^T \in \Re^{n\times 1} \ (i = 1,\cdots,m),$$

$$\mathbf{J}_t = \frac{\partial \phi_t}{\partial \mathbf{p}} = [\frac{\partial \phi_{t1}}{\partial \mathbf{p}}{}^T, \cdots, \frac{\partial \phi_{t(n-m)}}{\partial \mathbf{p}}{}^T]^T \in \Re^{(n-m)\times n}, \text{ with } \frac{\partial \phi_{tj}}{\partial \mathbf{p}}{}^T \in \Re^{n\times 1} \ (j = 1,\cdots,n-m).$$

In this formulation, the square matrix $\mathbf{J}_\phi$ is the augmented constraint Jacobian transformation from the end-effector frame to the constraint frame. When the constraint frame is fixed on the workspace, $\mathbf{J}_\phi$ is just a rotation matrix. Since the constraint equations are mutually independent, the non-square submatrices $\mathbf{J}_f$ and $\mathbf{J}_t$ have full (maximal) rank over any $\mathbf{p}$ of interest, i.e., $rk(\mathbf{J}_f) = m$ and $rk(\mathbf{J}_t) = (n-m)$, respectively. And a vector $\frac{\partial \phi_{fi}}{\partial \mathbf{p}}{}^T$ specifies the normal (or orthogonal) direction to the local surface at $\mathbf{p}$, that is, $\frac{\partial \phi_{fi}}{\partial \mathbf{p}} \bullet \mathbf{v} = 0 \ (i = 1,\cdots,m)$, while $\dot{\mathbf{x}}_t = \mathbf{J}_t \dot{\mathbf{v}}$. Clearly, the motion vector $\mathbf{v}$ lies in the null space of the vector space spanned by $\{\frac{\partial \phi_{f1}}{\partial \mathbf{p}}{}^T, \cdots, \frac{\partial \phi_{fm}}{\partial \mathbf{p}}{}^T\}$. It is especially important to note that the row vectors of $\mathbf{J}_f$ and $\mathbf{J}_t$ span the normal subspace and its orthogonal complement (i.e., the tangential subspace) of $\Re^n$, respectively. Thus the following orthogonality condition holds:

$$\mathbf{J}_t \bullet \mathbf{J}_f{}^T = \mathbf{0}_{(n-m)\times m} \ (\text{or } \mathbf{J}_f \bullet \mathbf{J}_t{}^T = \mathbf{0}_{m\times(n-m)}). \tag{12a}$$

This is equivalent to

$$\frac{\partial \phi_{tj}}{\partial \mathbf{p}} \bullet \frac{\partial \phi_{fi}}{\partial \mathbf{p}}{}^T = 0 \ (\text{or } \frac{\partial \phi_{fi}}{\partial \mathbf{p}} \bullet \frac{\partial \phi_{tj}}{\partial \mathbf{p}}{}^T = 0) \ (i = 1,\cdots,m),(j = 1,\cdots,(n-m)) \tag{12b}$$

which also implies that $RS(\mathbf{J}_f{}^T) = NS(\mathbf{J}_t)$ or $RS(\mathbf{J}_t{}^T) = NS(\mathbf{J}_f)$. Since $RS(\mathbf{J}_f{}^T)$ and $RS(\mathbf{J}_t{}^T)$ (or the column spaces of $\mathbf{J}_f{}^T$ and $\mathbf{J}_t{}^T$) are the two subspaces and further orthogonal complements of each other in n-dimensional vector space, it is possible to show that the constraint space ($\Re^n$) can be decomposed into direct sum of two subspaces as

$$\Re^n = RS(\mathbf{J}_t^T) \oplus RS(\mathbf{J}_f^T), \text{ with } RS(\mathbf{J}_t^T) \cap RS(\mathbf{J}_f^T) = \{\mathbf{0}\}. \tag{13}$$

As shown above, the dimension of direct sum of two subspaces is given by

$$n = \dim\{RS(\mathbf{J}_t^T) \oplus RS(\mathbf{J}_f^T)\} = \dim\{RS(\mathbf{J}_t^T)\} + \dim\{RS(\mathbf{J}_f^T)\}$$

which implies that the two vector spaces completely generates (or spans) $\Re^n$. In other words, the constraint frame has the following set of vectors as its basis in the n-dimensional space

$$\{\frac{\partial \phi_{fi}}{\partial \mathbf{p}}^T \ (i = 1, \cdots, m); \frac{\partial \phi_{ij}}{\partial \mathbf{p}}^T \ (j = 1, \cdots, (n-m))\}. \tag{14}$$

By virtue of the above results, the $RS(\mathbf{J}_t^T)$ specifies the motion-controlled subspace, while the $RS(\mathbf{J}_f^T)$ represents the subspace of contact forces. Thus the submatrices $\mathbf{J}_f^T$ and $\mathbf{J}_t^T$ make the force and motion spaces independent. In case of infinitely rigid environment, the forces in $RS(\mathbf{J}_f^T)$ do not work and only affect the constraint forces.

Remark 2: To facilitate the subsequent design, we can define new submatrices by normalizing the row spaces of $\mathbf{J}_f$ and $\mathbf{J}_t$ to unit lengths in $\mathbf{J}_\phi$, namely,

$$\frac{\partial \phi_{fi}}{\partial \mathbf{p}} \Big/ \left\| \frac{\partial \phi_{fi}}{\partial \mathbf{p}} \right\| \ (i = 1, \cdots, m) \text{ and } \frac{\partial \phi_{ij}}{\partial \mathbf{p}} \Big/ \left\| \frac{\partial \phi_{ij}}{\partial \mathbf{p}} \right\| \ (i = 1, \cdots, n-m).$$

Then n-dimensional constraint space has a set of unit vectors as its new basis. $\Delta\Delta$

Now combining Eqs (5) and (7) gives

$$\Omega(\mathbf{q}) = \mathbf{0}_m, \tag{15}$$

where $\Omega(\bullet) = \phi_f(\mathbf{h}(\bullet)) : C^2(\Re^n \to \Re^m)$. Then the velocity constraint equation can be obtained in joint-space formulation as

$$\mathbf{J}_f \mathbf{v} = \mathbf{J}_\Omega \dot{\mathbf{q}} = \mathbf{0}_m, \tag{16}$$

where $\mathbf{J}_\Omega (= \mathbf{J}_f \mathbf{J} \in \Re^{m \times n})$ is the constraint Jacobian matrix with full row rank (since the constraint equations are independent). To maintain appropriate contact between robot end-effector and external environment, the joint-space variables cannot be in arbitrary directions but should satisfy the following constraint manifold

$$\overline{M}_J = \{(\mathbf{q},\dot{\mathbf{q}}) \in \Re^n \times \Re^n:\ \ \Omega(\mathbf{q}) = \mathbf{0}_m,\ \mathbf{J}_\Omega \dot{\mathbf{q}} = \mathbf{0}_m\},$$

or alternatively in the end-effector variables as

$$\overline{M}_E = \{(\mathbf{p},\dot{\mathbf{p}}) \in \Re^n \times \Re^n:\ \ \phi_f(\mathbf{p}) = \mathbf{0}_m,\ \mathbf{J}_f \mathbf{N}(\mathbf{p})\dot{\mathbf{p}} = \mathbf{0}_m\}.$$

As a result, the geometric constraints imposed on the robot end-effector can be considered as restricting its joint-space motion (or the end-effector configuration) to the specific constraint manifold only. This leads to dimension reduction of constrained robot dynamics, that is, the number of DOF of the system will be eventually reduced to $(n-m)$.

When the robot manipulator makes direct interaction with external environments, the system dynamics should include the dynamic behavior of environments. In the following, modeling of the environment is discussed and the corresponding contact forces (or wrenches represented as a force and moment pair) are also formulated. First, in case of frictionless rigid contact, the interaction forces are given only in terms of normal forces and can be expressed in the Cartesian space as

$$\mathbf{F}_p = \mathbf{J}_f{}^T \lambda, \tag{17}$$

where $\lambda \in \Re^m$ is a vector of "Lagrange" undetermined multipliers related with the holonomic constraints and can be actually regarded as the magnitude of contact forces if the row space of $\mathbf{J}_f$ is normalized as shown in Remark 2, while $\mathbf{J}_f$ only resolves λ into appropriate directions. As a matter of fact, the Lagrange multipliers uniquely characterize the constraint forces if $\mathbf{J}_f$ has full row rank. In this case, the generalized contact forces $\mathbf{F}_p$ do not generate power at the contact point, that is, $\mathbf{v}^T \bullet \mathbf{F}_p = 0$. However, a slight position error could lead to extremely large contact forces. Note that this contact force can be measured by a wrist-mounted force sensor. Secondly, in case of non-rigid contact (i.e., an elastic passive environment), the contact forces are ($\mathbf{f} \in \Re^m$) given by

$$\mathbf{f} = \begin{cases} \mathbf{0} & \text{if } \mathbf{x}_{fa} < \mathbf{x}_f \ (\textit{no contact}) \\ \mathbf{k}_e(\mathbf{x}_{fa} - \mathbf{x}_f) & \text{if } \mathbf{x}_{fa} \geq \mathbf{x}_f \ (\textit{during contact}) \end{cases} \tag{18}$$

where $\mathbf{x}_{fa} \in \Re^m$ indicates the actual end-effector position in the constraint coordinates which is aligned with the normal direction of environment, and $\mathbf{x}_f \in \Re^m$ is the location of environment (i.e., undeformed reference position) when the robot end-effector does not exert any force on the environment. The matrix $\mathbf{k}_e$ represents the $m \times m$ equivalent stiffness determined from a series of spring constants, such as the environment stiffness and the end-effector compliance. For example, $\mathbf{k}_e$ can be chosen as known positive-definite diagonal matrix, $\mathbf{k}_e = diag[k_{e1}, \cdots, k_{em}]$, where $k_{ei}\ (>0)$ specifies the stiffness along dimension i. As a matter of fact, it is difficult to exactly characterize the dynamic behavior of environment. In this study, the external environment is only modeled as a linear spring for simplicity, however, similar results can be obtained for any passive environmental mechanism (for example, mass-spring-damper model). Note that the contact forces can be computed by either a force/torque sensor mounted on the end-effector or the position error measurement. The contact forces corresponding to external constraints can be expressed in the operational space as

$$\mathbf{F}_p = \mathbf{J}_f{}^T \mathbf{f}, \tag{19}$$

where the elastic environment can generate the reaction forces only along the normal directions.

From now on, the contact forces representing the physical behavior of the environment at end-effector are expressed in the general form as

$$\overline{\mathbf{F}}_p = \mathbf{J}_f{}^T \bar{\mathbf{f}}, \text{ with } \bar{\mathbf{f}} = \lambda \text{ or } \mathbf{f} \tag{20}$$

where the generalized contact forces ($\overline{\mathbf{F}}_p \in \Re^n$) can be determined on the basis of the contact conditions between the end-effector and the environment, that is, a frictionless rigid contact and an elastic contact. As shown above, it is worth recalling that a knowledge of both the contact forces and the constraint Jocobian are required to compute the constraint forces. In this study, wrenches are dual to twists. Furthermore, a wrench and a twist are

reciprocal, i.e., $\overline{\mathbf{F}}_p \bullet \mathbf{v}^T = 0$. By the principle of virtual work, the generalized contact forces can be written in the joint-space (see Eq.(9a)) as

$$\mathbf{T}_c = \mathbf{J}^T \overline{\mathbf{F}}_p = \mathbf{J}_\Omega{}^T \bar{\mathbf{f}}. \tag{21}$$

In many typical force control applications, for example ($n = 6$ in general), the surface-type tasks have 5-dimensional space for motion (or $n - m = 5$), so that the contact force need only be controlled in 1-dimensional nominal direction (or $m = 1$). From Eqs (6) and (11), the velocity and acceleration relationship between the constraint frame and the joint space can be expressed as

$$\dot{\mathbf{x}}_w = \mathbf{J}_w \dot{\mathbf{q}}, \tag{22a}$$

$$\ddot{\mathbf{x}}_w = \dot{\mathbf{J}}_w \dot{\mathbf{q}} + \mathbf{J}_w \ddot{\mathbf{q}}, \tag{22b}$$

where $\mathbf{J}_w$ ($= \mathbf{J}_\phi \mathbf{J} \in \Re^{n \times n}$) has full rank. Thus the corresponding joint-space variables are given as

$$\dot{\mathbf{q}} = \mathbf{J}_w{}^{-1} \dot{\mathbf{x}}_w, \tag{23}$$

$$\ddot{\mathbf{q}} = \mathbf{J}_w{}^{-1} \ddot{\mathbf{x}}_w + \dot{\mathbf{J}}_w{}^{-1} \dot{\mathbf{x}}_w, \tag{24}$$

where the fact that $\dot{\mathbf{J}}_w{}^{-1} = -\mathbf{J}_w{}^{-1} \dot{\mathbf{J}}_w \mathbf{J}_w{}^{-1}$ has been utilized and the proof of this is given in Appendix A.

Next, substituting Eqs (21), (23), and (24) into Eq. (9a) and premultiplying both sides of the resultant equation by $\mathbf{J}_w{}^{-T}$ leads to

$$\mathbf{M}_w(\mathbf{x}_w)\ddot{\mathbf{x}}_w + \mathbf{C}_w(\mathbf{x}_w, \dot{\mathbf{x}}_w)\dot{\mathbf{x}}_w + \mathbf{G}_w(\mathbf{x}_w) + \mathbf{F}_u = \mathbf{F} - \mathbf{J}_w{}^{-T} \mathbf{J}_\Omega{}^T \bar{\mathbf{f}}, \tag{25}$$

where the relationships between the joint-space and the constraint-space formulations are symbolically defined as

$$\mathbf{M}_w(\mathbf{x}_w) = \mathbf{J}_w{}^{-T} \mathbf{M}(\mathbf{q}) \mathbf{J}_w{}^{-1},$$

$$\mathbf{C}_w(\mathbf{x}_w, \dot{\mathbf{x}}_w) = \mathbf{J}_w{}^{-T} \mathbf{C}(\mathbf{q}, \dot{\mathbf{q}}) \mathbf{J}_w{}^{-1} + \mathbf{J}_w{}^{-T} \mathbf{M}(\mathbf{q}) \dot{\mathbf{J}}_w{}^{-1},$$

$$\mathbf{G}_w(\mathbf{x}_w) = \mathbf{J}_w{}^{-T} \mathbf{G}(\mathbf{q}),$$

$$\mathbf{F}_u = \mathbf{J}_w{}^{-T} \mathbf{T}_u,$$

$$\mathbf{F} = \mathbf{J}_w^{-T}\mathbf{T}.$$

For the sake of further analysis, the identity matrix $\mathbf{E}_{n\times n}$ can be partitioned such that

$$\mathbf{E}_{n\times n} = [\mathbf{E}_f \vdots \mathbf{E}_t],$$

where

$$\mathbf{E}_f = [\mathbf{E}_{m\times m}{}^T, \mathbf{0}^T]^T, \quad \mathbf{E}_f \in \Re^{n\times m}$$

$$\mathbf{E}_t = [\mathbf{0}^T, \mathbf{E}_{(n-m)\times(n-m)}{}^T]^T, \quad \mathbf{E}_t \in \Re^{n\times(n-m)}$$

with $\mathbf{E}_t{}^T\mathbf{E}_f = \mathbf{0}$ and $\mathbf{E}_f{}^T\mathbf{E}_f = \mathbf{E}_{m\times m}$. By abuse of the above notations, we can easily obtain $\mathbf{J}_w^{-T}\mathbf{J}_\Omega{}^T = \mathbf{E}_f$.

Hence, the robot dynamics with holonomic constraints finally can be written in the constraint-space formulation as

$$\mathbf{M}_w(\mathbf{x}_w;\Theta)\ddot{\mathbf{x}}_w + \mathbf{C}_w(\mathbf{x}_w,\dot{\mathbf{x}}_w;\Theta)\dot{\mathbf{x}}_w + \mathbf{G}_w(\mathbf{x}_w;\Theta) + \mathbf{F}_u = \mathbf{F} - \mathbf{E}_f\bar{\mathbf{f}}, \tag{26a}$$

$$\mathbf{x}_f = \mathbf{0}, \tag{26b}$$

where $\mathbf{x}_w = [\mathbf{0}^T, \mathbf{x}_t{}^T]^T$ (or $\mathbf{x}_w = \mathbf{E}_t\mathbf{x}_t$) and all constraint-space variables are expressed in a reference frame. It should be noted that both constraint equations and the constraint forces are expressed in simple forms under a new coordinate system and the motions of the constrained robot are completely governed in terms of $(n-m)$ independent variables $\mathbf{x}_t$. A choice of $\mathbf{x}_t$ of $\mathbf{x}_w$ depends on the task geometry to be performed. Furthermore, the force-controlled subsystem and the position-controlled subsystem (or the force-free equations of motion) are separated by premultiplying $\mathbf{E}_f{}^T$ and $\mathbf{E}_t{}^T$ on both sides of (26a), respectively, that is,

$$\mathbf{F}_f = \mathbf{E}_f{}^T\mathbf{F} = \mathbf{E}_f{}^T\mathbf{M}_w\mathbf{E}_t\ddot{\mathbf{x}}_t + \mathbf{E}_f{}^T\mathbf{C}_w\mathbf{E}_t\dot{\mathbf{x}}_t + \mathbf{E}_f{}^T\mathbf{G}_w + \mathbf{E}_f{}^T\mathbf{F}_u + \bar{\mathbf{f}}, \tag{27a}$$

$$\mathbf{F}_t = \mathbf{E}_t{}^T\mathbf{F} = \mathbf{E}_t{}^T\mathbf{M}_w\mathbf{E}_t\ddot{\mathbf{x}}_t + \mathbf{E}_t{}^T\mathbf{C}_w\mathbf{E}_t\dot{\mathbf{x}}_t + \mathbf{E}_t{}^T\mathbf{G}_w + \mathbf{E}_t{}^T\mathbf{F}_u, \tag{27b}$$

$$\mathbf{x}_f = \mathbf{0}. \tag{27c}$$

Henceforth, the dynamic equations (26a,b) or equivalently (27a-c) form the basis for control synthesis in the subsequent section. Now, the design objective of constrained robot

system becomes a problem of controller design for the two subsystems to achieve the desired force and position trajectories during contact tasks.

Some essential properties of the transformed dynamics (26a) which are similar to its joint-space model are summarized as follows (similar to those in Refs [14-17]):

Property 1: $\mathbf{M}_w(\mathbf{x}_w)$ is a positive definite matrix. Furthermore, both $\mathbf{M}_w(\mathbf{x}_w)$ and $\mathbf{M}_w^{-1}(\mathbf{x}_w)$ are uniformly bounded functions.

Property 2: The matrix $\mathbf{N}_w(\mathbf{x}_w, \dot{\mathbf{x}}_w) = \dot{\mathbf{M}}_w(\mathbf{x}_w) - 2\mathbf{C}_w(\mathbf{x}_w, \dot{\mathbf{x}}_w)$ is a skew-symmetric matrix (i.e., $\mathbf{N}_w = -\mathbf{N}_w^T$), thus, $\mathbf{x}^T\mathbf{N}_w\mathbf{x} = \mathbf{0}, \forall\ \mathbf{x} \in \Re^n$.

Proof: The detailed proof is given in Appendix B.

Property 3: A part of the dynamics (26a) is still linear function in terms of some suitably selected set of parameter vector, $\Theta \in \Re^{s_2}$, that is,

$$\mathbf{M}_w(\mathbf{x}_w;\Theta)\mathbf{z} + \mathbf{C}_w(\mathbf{x}_w, \dot{\mathbf{x}}_w;\Theta)\mathbf{y} + \mathbf{G}_w(\mathbf{x}_w;\Theta) = \mathbf{R}_w(\mathbf{x}_w, \dot{\mathbf{x}}_w, \mathbf{y}, \mathbf{z})\Theta,$$

where $\mathbf{y}$ and $\mathbf{z}$ are the corresponding n-dimensional vectors; $\mathbf{R}_w \in \Re^{n \times s_2}$ is a regressor matrix of known functions; $\Theta \in \Re^{s_2}$ is the vector of robot physical parameters. $\Delta\Delta$

The controller design in the subsequent section will be based on the above fundamental properties of the dynamic model.

3. SYNTHESIS OF A CLASS OF HYBRID CONTROLLERS

Based on the dynamic model described by (26a,b), a class of hybrid controllers are formulated provided that joint-space variables (position and velocity) and contact forces are available for measurements. Also assume that the desired quantities $(\mathbf{x}_{td}, \dot{\mathbf{x}}_{td}, \ddot{\mathbf{x}}_{td}, \bar{\mathbf{f}}_d)$ to be tracked are continuous and bounded over all time. Realizing that the types of control schemes employed depend on the types of external environments, then the control objective is to determine a set of input torques such that the actual system states of interest $(\mathbf{x}_t, \bar{\mathbf{f}})$ simultaneously track the desired trajectories $(\mathbf{x}_{td}, \bar{\mathbf{f}}_d)$ as closely as possible. Since the control input vector $\mathbf{F}$ in Eq. (26a) is viewed as the hypothetical forces (or virtual forces) acting on the constraint space, then these forces are eventually converted to the joint torques by Jacobian transformation, namely, $\mathbf{T} = \mathbf{J}_w^T \mathbf{F}$.

3.1 A Class of Hybrid Position/Force Controllers

In this subsection, the external environments are infinitely rigid surfaces. Thus, the dynamic equations under consideration are specified by

$$\mathbf{M}_w(\mathbf{x}_w)\ddot{\mathbf{x}}_w + \mathbf{C}_w(\mathbf{x}_w, \dot{\mathbf{x}}_w)\dot{\mathbf{x}}_w + \mathbf{G}_w(\mathbf{x}_w) + \mathbf{F}_u = \mathbf{F} - \mathbf{E}_f \lambda, \tag{28a}$$

$$\mathbf{x}_f = \mathbf{0}. \tag{28b}$$

Based on this formulation, a class of hybrid controllers are now formulated.

3.1.1 Modified Computed Torque Approach

The control synthesis will be based on so-called computed torque method (or inverse dynamics) to decouple and linearize the system dynamics. Before controller design, a

number of tracking error vectors are defined as follows. The position tracking error, $\mathbf{e}_w \in \Re^n$, is given by

$$\mathbf{e}_w = \mathbf{x}_w - \mathbf{x}_{wd} = [\mathbf{0}^T, \mathbf{e}_t^T]^T, \tag{29}$$

with $\mathbf{e}_t = \mathbf{x}_t - \mathbf{x}_{td}$, where $\mathbf{x}_{wd} \in \Re^n$ (or $\mathbf{x}_{td} \in \Re^{(n-m)}$) is the vector of desired position trajectories. The contact force tracking errors are defined as

$$\mathbf{e}_\lambda = \lambda - \lambda_d, \tag{30a}$$

$$\mathbf{e}_\Lambda = \int_0^t \mathbf{e}_\lambda(\tau) d\tau, \tag{30b}$$

where $\lambda_d \in \Re^m$ is the desired force vector, and $\mathbf{e}_\Lambda$ is the vector of the accumulated force error.

In the absence of system uncertainties (i.e., $\mathbf{F}_u = \mathbf{0}$ as well as without parametric uncertainties), consider the modified computed torque in the form

$$\mathbf{F} = \mathbf{M}_w(\mathbf{x}_w)[\ddot{\mathbf{x}}_{wd} - \mathbf{k}_v\dot{\mathbf{e}}_w - \mathbf{k}_p\mathbf{e}_w] + \mathbf{C}_w(\mathbf{x}_w, \dot{\mathbf{x}}_w)\dot{\mathbf{x}}_w + \mathbf{G}_w(\mathbf{x}_w) + \mathbf{E}_f(\lambda_d - \mathbf{k}_f\mathbf{e}_\Lambda), \tag{31}$$

where the design parameters $\mathbf{k}_p \in \Re^{n\times n}$, $\mathbf{k}_v \in \Re^{n\times n}$, and $\mathbf{k}_f \in \Re^{m\times m}$ are proportional, derivative, and integral feedback gain matrices, respectively, which are chosen as positive-definite and diagonal matrices. As noted earlier, the control law (31) can be further written in two subsystems as

$$\mathbf{F}_f = \mathbf{E}_f{}^T\mathbf{F} = \mathbf{E}_f{}^T\mathbf{M}_w\mathbf{E}_t[\ddot{\mathbf{x}}_{td} - \bar{\mathbf{k}}_v\dot{\mathbf{e}}_t - \bar{\mathbf{k}}_p\mathbf{e}_t] + \mathbf{E}_f{}^T\mathbf{C}_w\mathbf{E}_t\dot{\mathbf{x}}_t + \mathbf{E}_f{}^T\mathbf{G}_w + (\lambda_d - \mathbf{k}_f\mathbf{e}_\Lambda), \tag{32a}$$

$$\mathbf{F}_t = \mathbf{E}_t{}^T\mathbf{F} = \mathbf{E}_t{}^T\mathbf{M}_w\mathbf{E}_t[\ddot{\mathbf{x}}_{td} - \bar{\mathbf{k}}_v\dot{\mathbf{e}}_t - \bar{\mathbf{k}}_p\mathbf{e}_t] + \mathbf{E}_t{}^T\mathbf{C}_w\mathbf{E}_t\dot{\mathbf{x}}_t + \mathbf{E}_t{}^T\mathbf{G}_w, \tag{32b}$$

where the relationships among some gain matrices are given as

$$\mathbf{k}_v = \mathbf{E}_t\bar{\mathbf{k}}_v\mathbf{E}_t{}^T \in \Re^{n\times n}, \quad \bar{\mathbf{k}}_v \in \Re^{(n-m)\times(n-m)},$$

$$\mathbf{k}_p = \mathbf{E}_t\bar{\mathbf{k}}_p\mathbf{E}_t{}^T \in \Re^{n\times n}, \quad \bar{\mathbf{k}}_p \in \Re^{(n-m)\times(n-m)},$$

and the feedback gain terms ($\bar{\mathbf{k}}_p$ and $\bar{\mathbf{k}}_v$) are also selected as positive-definite matrices. A block diagram of the proposed controller is shown in Fig. 3.

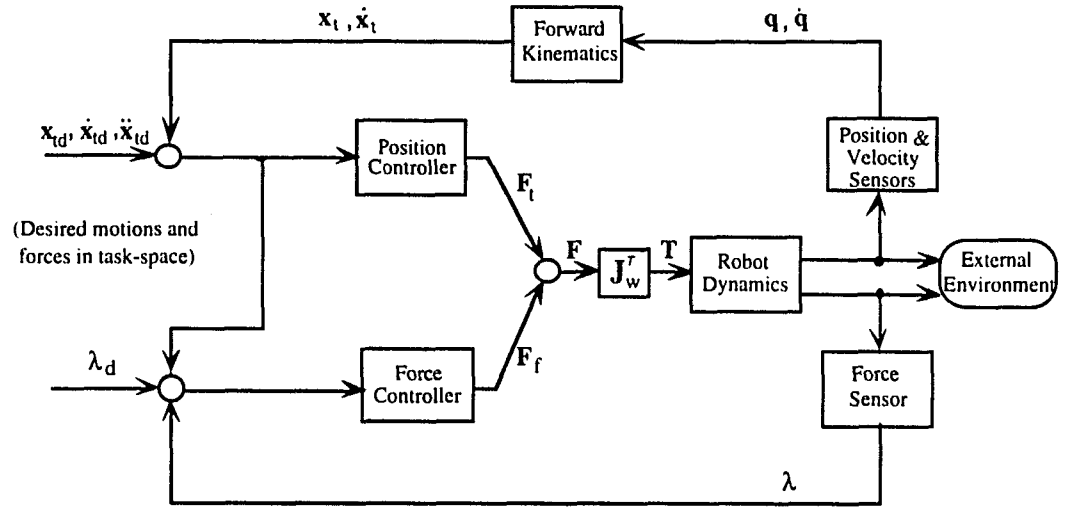

Figure 3. Block diagram of hybrid computed torque method.

In this case (i.e., ideal case), a control goal would be $(\mathbf{e}_t, \mathbf{e}_\lambda) \to 0$ as $t \to \infty$. Now the tracking properties of the robot system under the control law (31) are summarized as follows.

Theorem 1: Consider constrained robot dynamics (28a,b) assuming that Θ is well known in advance and $\mathbf{F}_u = \mathbf{0}$ (i.e., without uncertainties in the system dynamics). Then the control law (31) guarantees global asymptotic stability of the corresponding closed-loop system, i.e., $(\mathbf{x}_t, \lambda) \to (\mathbf{x}_{td}, \lambda_d)$ as $t \to \infty$.

Proof: For the stability of the closed-loop system, substituting (31) into (28a) yields

$$\mathbf{M}_w(\ddot{\mathbf{e}}_w + \mathbf{k}_v\dot{\mathbf{e}}_w + \mathbf{k}_p\mathbf{e}_w) = -\mathbf{E}_f(\mathbf{e}_\lambda + \mathbf{k}_f\mathbf{e}_\lambda). \tag{33}$$

Premultiplying $\mathbf{E}_t^T$ on both sides of (33) and using $\mathbf{E}_t^T\mathbf{E}_f = \mathbf{0}$ gives

$$\mathbf{E}_t^T\mathbf{M}_w(\ddot{\mathbf{e}}_w + \mathbf{k}_v\dot{\mathbf{e}}_w + \mathbf{k}_p\mathbf{e}_w) = \mathbf{0}.$$

It follows that

$$\mathbf{E}_t^T\mathbf{M}_w\mathbf{E}_t(\ddot{\mathbf{e}}_t + \bar{\mathbf{k}}_v\dot{\mathbf{e}}_t + \bar{\mathbf{k}}_p\mathbf{e}_t) = \mathbf{0}. \tag{34}$$

Since $\mathbf{E}_t^T \mathbf{M}_w \mathbf{E}_t \neq \mathbf{0}$, the closed-loop error equation for position-controlled subsystem is given by

$$(\ddot{\mathbf{e}}_t + \bar{\mathbf{k}}_v \dot{\mathbf{e}}_t + \bar{\mathbf{k}}_p \mathbf{e}_t) = \mathbf{0} \tag{35}$$

which guarantees that $\mathbf{e}_t \to \mathbf{0}$ as $t \to \infty$. On the other hand, in view of (35), the closed-loop error dynamics (33) is now equivalent to

$$\mathbf{E}_f^T \mathbf{E}_f (\mathbf{e}_\lambda + \mathbf{k}_f \mathbf{e}_\Lambda) = \mathbf{0}.$$

Since $\mathbf{E}_f^T \mathbf{E}_f = \mathbf{E}_{m \times m}$, the error dynamics for force-controlled subsystem is given by

$$(\mathbf{e}_\lambda + \mathbf{k}_f \mathbf{e}_\Lambda) = \mathbf{0} \tag{36}$$

which ensures that $\mathbf{e}_\lambda \to \mathbf{0}$ as $t \to \infty$. Obviously, as $\bar{\mathbf{k}}_v, \bar{\mathbf{k}}_p, \mathbf{k}_f > \mathbf{0}$, the global asymptotic stability results of the closed-loop system are readily established, i.e., $\lim_{t \to \infty} \mathbf{e}_t = \mathbf{0}$ and $\lim_{t \to \infty} \mathbf{e}_\lambda = \mathbf{0}$. The specific values of gain matrices are then selected such that the system responses meet designer's performance specifications. Note that, in force control loop, the accumulated force error signals are introduced. In addition, the control law provides an asymptotic tracking solution without contact force measurement ($\mathbf{k}_f = \mathbf{0}$).

3.1.2 Robust Adaptive Hybrid Control

In this subsection, some or all of dynamic parameters of the manipulator are supposed to be unknown rather than assumed to be exactly known as in the previous subsection. Furthermore, the external disturbance term is considered in the system dynamics. Then the adaptive hybrid control can be used to cope with modeling errors (or parametric uncertainties) and external disturbances.

Now, some system variables are introduced as follows. The "reference" tracking error is defined as

$$\dot{\mathbf{x}}_{wr} = [\dot{\mathbf{x}}_{fr}^T, \ \dot{\mathbf{x}}_{tr}^T]^T, \tag{37}$$

with $\dot{\mathbf{x}}_{fr} = \mathbf{0}$ and $\dot{\mathbf{x}}_{tr} = \dot{\mathbf{x}}_{td} - \mathbf{k}_a \mathbf{e}_t$, where $\mathbf{k}_a \in \Re^{(n-m)\times(n-m)}$ is selected as positive-definite and diagonal matrix, i.e., $\mathbf{k}_a = k_a \mathbf{E}$, with $k_a > 0$. The "sliding" variable vector used as a measure of tracking error is defined as

$$\mathbf{x}_{ws} = \dot{\mathbf{x}}_w - \dot{\mathbf{x}}_{wr} = [\mathbf{x}_{fs}^T,\ \mathbf{x}_{ts}^T]^T, \tag{38}$$

where $\mathbf{x}_{fs} = \mathbf{0}$ and $\mathbf{x}_{ts} = \dot{\mathbf{e}}_t + \mathbf{k}_a \mathbf{e}_t$.

Lemma 1: If $\|\mathbf{x}_{ts}\| \le \overline{\sigma} (< \infty)$ is satisfied for any $t \in [t_o, \infty)$ and some $t_o \in \Re^+$, then

$$\|\mathbf{e}_t(t)\| \le \exp[-k_a(t - t_o)]\{\|\mathbf{e}_t(t_o)\| - \frac{\overline{\sigma}}{k_a}\} + \frac{\overline{\sigma}}{k_a} \text{ and } \|\dot{\mathbf{e}}_t(t)\| \le \overline{\sigma} + k_a \|\mathbf{e}_t(t)\|.$$

Proof: The proof of this lemma is a straightforward.

Lemma 2: Let $\mathbf{f}(t): \Re^+ \to \Re^n$ be a uniformly continuous function, then for any $p_o > 0$, $\lim_{t\to\infty} \mathbf{f}(t) = \mathbf{0}$ iff $\lim_{t\to\infty} \int_t^{t+p} \mathbf{f}(\tau) d\tau = \mathbf{0}$ for all $0 < p \le p_o$.

Proof: See [20]. ΔΔ

Let $\tilde{\Theta}(t) = \hat{\Theta}(t) - \Theta$ be the parameter error vector, where $\hat{\Theta}(t)$ denotes the current estimate of Θ. In this study, the circumflex $(\hat{\bullet})$ represents the adaptive estimates of $(\bullet)$ and the notation $(\tilde{\bullet})$ refers to $(\tilde{\bullet}) = (\hat{\bullet}) - (\bullet)$. By Property 3 in (26a,b), define the following functions:

$$\mathbf{M}_w(\mathbf{x}_w;\Theta)\ddot{\mathbf{x}}_{wr} + \mathbf{C}_w(\mathbf{x}_w, \dot{\mathbf{x}}_w;\Theta)\dot{\mathbf{x}}_{wr} + \mathbf{G}_w(\mathbf{x}_w;\Theta) = \mathbf{R}_r(\mathbf{x}_w, \dot{\mathbf{x}}_w, \dot{\mathbf{x}}_{wr}, \ddot{\mathbf{x}}_{wr})\Theta, \tag{39a}$$

$$\hat{\mathbf{M}}_w(\mathbf{x}_w;\hat{\Theta})\ddot{\mathbf{x}}_{wr} + \hat{\mathbf{C}}_w(\mathbf{x}_w, \dot{\mathbf{x}}_w;\hat{\Theta})\dot{\mathbf{x}}_{wr} + \hat{\mathbf{G}}_w(\mathbf{x}_w;\hat{\Theta}) = \mathbf{R}_r(\mathbf{x}_w, \dot{\mathbf{x}}_w, \dot{\mathbf{x}}_{wr}, \ddot{\mathbf{x}}_{wr})\hat{\Theta}, \tag{39b}$$

where $\mathbf{R}_r \in \Re^{n\times s_2}$ is a known regressor matrix and $\Theta \in \Re^{s_2}$ is assumed to be unknown but constant. Note that $\mathbf{R}_r$ in (39a,b) is no longer a function of $\ddot{\mathbf{x}}_t (or\ \ddot{\mathbf{x}}_w)$. For robustness and stability analysis, the unstructured uncertainties (or external disturbances) $\mathbf{T}_u$ in Eq. (9a) are assumed to be bounded by

$$\|\mathbf{T}_u\| \le d_1, \tag{40}$$

where $d_1 (< \infty)$ is a positive constant. Since $\mathbf{J}_w^{-T}$ can be uniformly bounded by $\|\mathbf{J}_w^{-T}\| \le d_2 (< \infty)$ in the non-singular region of the manipulator (i.e., $\det(\mathbf{J}_w^{-T}) \ne 0$), there exists a positive constant d such that

$$\|\mathbf{F}_u\| \le \|\mathbf{J}_w^{-T}\|\|\mathbf{T}_u\| \le d,$$

where $d = d_1 d_2 (< \infty)$.

Now, the hybrid control law, which determines the position/force control inputs, is given by

$$\mathbf{F} = \mathbf{R}_r(\mathbf{x}_w, \dot{\mathbf{x}}_w, \dot{\mathbf{x}}_{wr}, \ddot{\mathbf{x}}_{wr})\hat{\Theta} - \mathbf{k}\mathbf{x}_{ws} + \mathbf{E}_f(\lambda - \mathbf{k}_f \mathbf{e}_\lambda), \tag{41}$$

where $\mathbf{k}$ and $\mathbf{k}_f$ are positive-definite gain matrices with appropriate dimensions. The parameter adaptation law is chosen as

$$\dot{\hat{\Theta}} = -\Gamma^{-1}(\mathbf{R}_r^T \mathbf{x}_{ws} + \sigma\hat{\Theta}), \tag{42}$$

where $\Gamma = \Gamma^T (> \mathbf{0})$ is an adaptation gain matrix and $\sigma \ge 0$. The term $\sigma(\bullet): \Re^{n_2} \to \Re^+$ referred to as the leakage, is introduced to achieve the robustness of adaptive law in the presence of uncertainties [3-4, 18].

$$\sigma(\hat{\Theta}) = \begin{cases} 0 & , \|\hat{\Theta}\| \le \overline{\Theta}_0 \\ \sigma_0[\dfrac{\|\hat{\Theta}\|}{\overline{\Theta}_0} - 1] & , \overline{\Theta}_0 \le \|\hat{\Theta}\| \le 2\overline{\Theta}_0 \\ \sigma_0 & , \|\hat{\Theta}\| \ge 2\overline{\Theta}_0 \end{cases} \tag{43}$$

where $\sigma_0 (> 0)$ and $\overline{\Theta}_0 (> \|\Theta\| > 0)$ are some design parameters. Note that $\sigma(\bullet)$ is a continuous function. In practice, it is considered that a large amount of leakage is needed as the uncertainties are significant, while small leakage is designed as the uncertainties are less significant. A block diagram of the proposed controller is given in Fig. 4.

Substituting the control law (41) with adaptation law (42) into Eq. (28a) and subtracting (39a) on both sides of the resulting equation leads to the following closed-loop error dynamics

$$\mathbf{M}_w \dot{\mathbf{x}}_{ws} = -\mathbf{C}_w \mathbf{x}_{ws} + \mathbf{R}_r \tilde{\Theta} - \mathbf{k}\mathbf{x}_{ws} - \mathbf{E}_f \mathbf{k}_f \mathbf{e}_\lambda - \mathbf{F}_u. \tag{44}$$

Now, the stability and robustness issues of the closed-loop system are analyzed in the following.

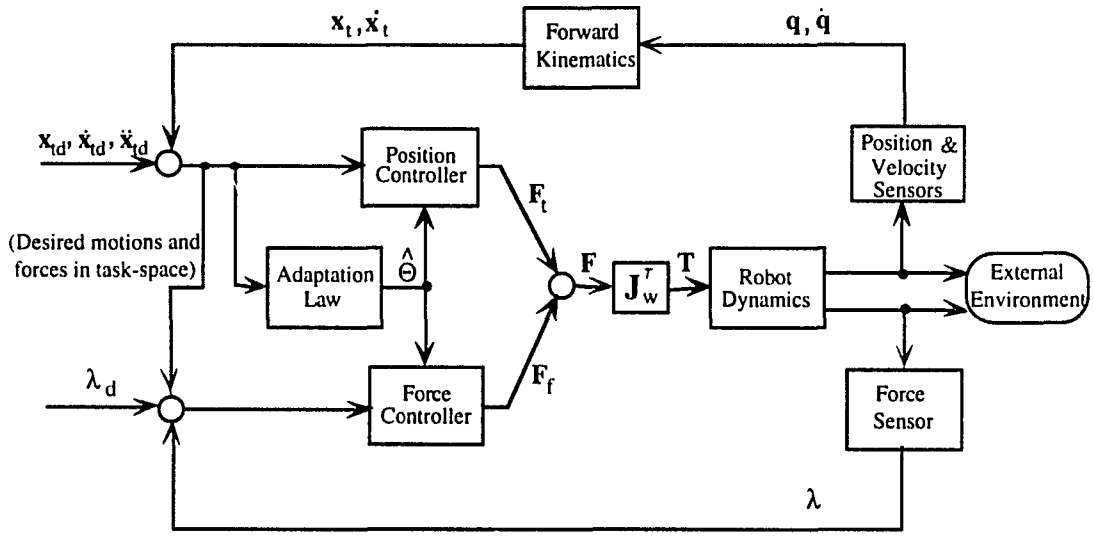

Figure 4. Block diagram of robust hybrid adaptive controller.

Theorem 2: Consider the control law (41) with the adaptation law (42) for the constrained robot system (28a,b) provided that all or some dynamic parameters are unknown. Then the solutions of the closed-loop system (44) are globally stable in the sense that the system state variables of interest $(\mathbf{x}_t, \dot{\mathbf{x}}_t, \lambda, \Theta)$ are uniformly ultimately bounded after a finite time. That is, the corresponding tracking errors converge to the compact set

$$\Delta_f = \{ \mathbf{x}_{ts} \in \Re^{(n-m)}: \|\mathbf{x}_{ts}\| \le \frac{d}{\rho_{\min}(\mathbf{k})} \}.$$

Proof: Consider a Lyapunov-like function candidate, $V:(t,\tilde{\mathbf{x}}) \in \Re^{+} \times \Re^{(n+s_2)} \rightarrow \Re^{+}$, as

$$V = \frac{1}{2}\tilde{\mathbf{x}}^T Q \tilde{\mathbf{x}}, \tag{45}$$

where $\tilde{\mathbf{x}}^T = [\mathbf{x}_{ws}{}^T, \ \tilde{\Theta}^T]$ and $Q = Block\ diag[\mathbf{M}_w, \Gamma]$. By Rayleigh's principle, an upper and lower bound on V can be estimated as

$$\frac{1}{2}\rho_{\min}(Q)\|\tilde{\mathbf{x}}\|^2 \le V \le \frac{1}{2}\rho_{\max}(Q)\|\tilde{\mathbf{x}}\|^2,$$

where $\rho_{\min}$ and $\rho_{\max}$ were previously defined. Since $\rho_{\min}(Q) > 0$, V is clearly positive-definite function. Differentiation of V with respect to time along Eq. (44) leads to

$$\dot{V} = \mathbf{x}_{ws}^T[-\mathbf{C}_w\mathbf{x}_{ws} + \mathbf{R}_r\tilde{\Theta} - \mathbf{k}\mathbf{x}_{ws} - \mathbf{E}_f\mathbf{k}_f\mathbf{e}_\lambda - \mathbf{F}_u] + \frac{1}{2}\mathbf{x}_{ws}^T\dot{\mathbf{M}}_w\mathbf{x}_{ws} + \tilde{\Theta}^T\Gamma\dot{\tilde{\Theta}} \tag{46}$$

which, by recalling that Property 2 in Eqs (26a,b) and $\dot{\tilde{\Theta}} = \dot{\hat{\Theta}}$ (assuming $\dot{\Theta} = \mathbf{0}$), can be rewritten as

$$\dot{V} = -\mathbf{x}_{ws}^T\mathbf{k}\mathbf{x}_{ws} - \mathbf{x}_{ws}^T\mathbf{E}_f\mathbf{k}_f\mathbf{e}_\lambda - \mathbf{x}_{ws}^T\mathbf{F}_u - \sigma\tilde{\Theta}^T\hat{\Theta}, \tag{47}$$

where $\sigma\tilde{\Theta}^T\hat{\Theta} \geq 0$ and the proof of this inequality is given in Appendix C. By exploiting $\mathbf{x}_{ws}^T\mathbf{E}_f = \mathbf{0}$ and $\sigma\tilde{\Theta}^T\hat{\Theta} \geq 0$, we have

$$\dot{V} \leq -\mathbf{x}_{ws}^T\mathbf{k}\mathbf{x}_{ws} - \mathbf{x}_{ws}^T\mathbf{F}_u. \tag{48}$$

Hence, $\dot{V}$ can be shown to be bounded as

$$\begin{aligned}\dot{V} &\leq -\rho_{\min}(\mathbf{k})\|\mathbf{x}_{ws}\|^2 + \|\mathbf{x}_{ws}\|d \\ &\leq -\frac{\rho_{\min}(\mathbf{k})}{2}\|\mathbf{x}_{ws}\|^2 - \frac{\rho_{\min}(\mathbf{k})}{2}[\|\mathbf{x}_{ws}\| - \frac{d}{\rho_{\min}(\mathbf{k})}]^2 + \frac{d^2}{2\rho_{\min}(\mathbf{k})} \\ &\leq -\frac{\rho_{\min}(\mathbf{k})}{2}\|\mathbf{x}_{ws}\|^2 + \frac{d^2}{2\rho_{\min}(\mathbf{k})}.\end{aligned} \tag{49}$$

It follows that $\dot{V} < 0$, $\forall (t, \mathbf{x}_{ws}) \in \Delta_f{}^c$, where $\Delta_f{}^c$ denotes the complement of Δ_f. Utilizing equation (45) and differential inequality (49) show that $\mathbf{x}_{ws}$ and $\tilde{\Theta}$ are globally bounded, which in turn implies that $\mathbf{R}_r\tilde{\Theta}$ is bounded. Premultiplying $\mathbf{E}_t^T$ on both sides of Eq. (44) and using $\mathbf{E}_t^T\mathbf{E}_f = \mathbf{0}$ yields

$$\mathbf{E}_t^T\mathbf{M}_w\mathbf{E}_t\dot{\mathbf{x}}_{ts} = -\mathbf{E}_t^T\mathbf{C}_w\mathbf{E}_t\mathbf{x}_{ts} + \mathbf{E}_t^T\mathbf{R}_r\tilde{\Theta} - \bar{\mathbf{k}}\mathbf{x}_{ts} - \mathbf{E}_t^T\mathbf{F}_u. \tag{50}$$

In light of the above results, all terms in the right hand side of (50) are bounded, which implies that $\dot{\mathbf{x}}_{ts}$ (or $\dot{\mathbf{x}}_{ws}$) is also bounded ($\in L_\infty$). Now, directly from Lemma 1, the tracking errors ($\dot{\mathbf{e}}_t$ and $\mathbf{e}_t$) remain bounded ($\in L_\infty$). To establish the global boundedness of the contact forces, once again from (44),

$$\mathbf{k}_f\mathbf{e}_\lambda = -\mathbf{E}_f{}^T\mathbf{M}_w\mathbf{E}_t\dot{\mathbf{x}}_{ts} - \mathbf{E}_f{}^T\mathbf{C}_w\mathbf{E}_t\mathbf{x}_{ts} + \mathbf{E}_f{}^T\mathbf{R}_r\tilde{\Theta} - \mathbf{E}_f{}^T\mathbf{F}_u. \tag{51}$$

Hence, it can be concluded that $\mathbf{e}_\lambda$ is globally bounded ($\in L_\infty$), but does not tend to zero asymptotically. Therefore, the uniform ultimate boundedness of all tracking errors follow immediately. Summarizing the above results, all signals of the closed-loop system remain

bounded with respect to the closed ball Δ_f. Furthermore, the tracking error bound (or the size of residual set) for global stability can be made arbitrary small by choosing larger control gains. However, from a practical point of view, the system designer should determine the trade-off between system performance and control energy. Therefore, it is shown that the adaptive control algorithm is robust with respect to parametric uncertainties and given external disturbances.

3.2 Adaptive Hybrid Impedance Control

In this subsection, assuming that an elastic environment is imposed on the system, a hybrid impedance approach will be introduced. Then the system dynamics under consideration can be expressed as

$$\mathbf{M}_w(\mathbf{x}_w;\Theta)\ddot{\mathbf{x}}_w + \mathbf{C}_w(\mathbf{x}_w,\dot{\mathbf{x}}_w;\Theta)\dot{\mathbf{x}}_w + \mathbf{G}_w(\mathbf{x}_w;\Theta) = \mathbf{F} - \mathbf{E}_f\mathbf{f}, \tag{52a}$$

$$\mathbf{x}_f = \mathbf{0}. \tag{52b}$$

The design procedures are similar to those in the previous subsection. Before controller design, a number of new tracking error vectors are defined as follows. The force tracking errors are defined as

$$\mathbf{e}_f = \mathbf{f}_d - \mathbf{f}, \tag{53a}$$

$$\bar{\mathbf{e}}_f = \int_0^t \mathbf{e}_f(\tau)d\tau, \tag{53b}$$

where $\mathbf{f}_d \in \Re^m$ is the desired force vector and $\bar{\mathbf{e}}_f$ is the vector of the accumulated force errors. The reference tracking error, $\dot{\bar{\mathbf{x}}}_{wr}$, is defined as

$$\dot{\bar{\mathbf{x}}}_{wr} = [\dot{\bar{\mathbf{x}}}_{fr}^T,\ \dot{\mathbf{x}}_{tr}^T]^T, \tag{54}$$

with $\dot{\bar{\mathbf{x}}}_{fr} = \mathbf{k}_b\bar{\mathbf{e}}_f$ and $\dot{\mathbf{x}}_{tr} = \dot{\mathbf{x}}_{td} - \mathbf{k}_a\mathbf{e}_t$, where the gain matrices are selected as positive-definite, i.e., $\mathbf{k}_a = k_a\mathbf{E}$ and $\mathbf{k}_b = k_b\mathbf{E}$, with $k_a, k_b > 0$. The sliding variable vector, $\bar{\mathbf{x}}_{ws}$, is defined as

$$\bar{\mathbf{x}}_{ws} = \dot{\mathbf{x}}_w - \dot{\bar{\mathbf{x}}}_{wr} = [\bar{\mathbf{x}}_{fs}^T,\ \mathbf{x}_{ts}^T]^T, \tag{55}$$

where $\bar{\mathbf{x}}_{fs} = -\mathbf{k}_b \bar{\mathbf{e}}_f$ and $\mathbf{x}_{ts} = \dot{\mathbf{e}}_t + \mathbf{k}_a \mathbf{e}_t$. It is worth noting that the contact force vector is always orthogonal to the position (or motion) vector on the constraint surfaces at contact point, then $\dot{\bar{\mathbf{x}}}_{fr} (or\ \bar{\mathbf{x}}_{fs})$ is orthogonal to $\mathbf{x}_{tr} (or\ \mathbf{x}_{ts})$. Let $\tilde{\Theta}(t) = \hat{\Theta}(t) - \Theta$ be the parameter error vector, where $\hat{\Theta}(t)$ denotes the current estimate of Θ. Using Property 3 in (26a,b), we can define the following functions:

$$\mathbf{M}_w(\mathbf{x}_w;\Theta)\ddot{\bar{\mathbf{x}}}_{wr} + \mathbf{C}_w(\mathbf{x}_w,\dot{\mathbf{x}}_w;\Theta)\dot{\bar{\mathbf{x}}}_{wr} + \mathbf{G}_w(\mathbf{x}_w;\Theta) = \bar{\mathbf{R}}_r(\mathbf{x}_w,\dot{\mathbf{x}}_w,\dot{\bar{\mathbf{x}}}_{wr},\ddot{\bar{\mathbf{x}}}_{wr})\Theta, \tag{56a}$$

$$\hat{\mathbf{M}}_w(\mathbf{x}_w;\hat{\Theta})\ddot{\bar{\mathbf{x}}}_{wr} + \hat{\mathbf{C}}_w(\mathbf{x}_w,\dot{\mathbf{x}}_w;\hat{\Theta})\dot{\bar{\mathbf{x}}}_{wr} + \hat{\mathbf{G}}_w(\mathbf{x}_w;\hat{\Theta}) = \bar{\mathbf{R}}_r(\mathbf{x}_w,\dot{\mathbf{x}}_w,\dot{\bar{\mathbf{x}}}_{wr},\ddot{\bar{\mathbf{x}}}_{wr})\hat{\Theta}, \tag{56b}$$

where $\bar{\mathbf{R}}_r \in \Re^{n\times s_3}$ is a known regressor matrix, and $\Theta \in \Re^{s_3}$ is assumed to be unknown but constant.

Consider the following hybrid control algorithm

$$\mathbf{F} = \bar{\mathbf{R}}_r(\mathbf{x}_w,\dot{\mathbf{x}}_w,\dot{\bar{\mathbf{x}}}_{wr},\ddot{\bar{\mathbf{x}}}_{wr})\hat{\Theta} - \mathbf{k}\bar{\mathbf{x}}_{ws} + \mathbf{E}_f(\mathbf{f}_d + \mathbf{k}_f\bar{\mathbf{e}}_f), \tag{57}$$

where $\mathbf{k}$ and $\mathbf{k}_f$ are positive-definite gain matrices with appropriate dimensions, i.e., $\mathbf{k}_f = k_f\mathbf{E}, k_f > 0$. The adaptation mechanism (σ-modification law) is chosen as

$$\dot{\hat{\Theta}} = -\Gamma^{-1}(\bar{\mathbf{R}}_r^T\bar{\mathbf{x}}_{ws} + \sigma\hat{\Theta}), \tag{58}$$

where $\Gamma = \Gamma^T > \mathbf{0}$ is an adaptive gain matrix, and the term $\sigma(\bullet):\Re^{s_3} \to \Re^+$ is selected as

$$\sigma(\Theta) = \begin{cases} 0, & \|\hat{\Theta}\| \le \Theta_0 \\ \sigma_0, & \|\hat{\Theta}\| \ge \Theta_0 \end{cases} \tag{59}$$

where $\sigma_0 (> 0)$ and $\Theta_0 (> \|\Theta\| > 0)$ are some design parameters. Note that $\sigma(\bullet)$ is a discontinuous function. Such an overall control scheme is shown in Fig. 5.

After substituting the control law (57) with adaptation law (58) into Eq. (52a) and subtracting (56a) on the both sides of the resulting equation, one can obtain the closed-loop error dynamics as

$$\mathbf{M}_w\dot{\bar{\mathbf{x}}}_{ws} = -\mathbf{C}_w\bar{\mathbf{x}}_{ws} + \bar{\mathbf{R}}_r\tilde{\Theta} - \mathbf{k}\bar{\mathbf{x}}_{ws} + \mathbf{E}_f(\mathbf{e}_f + \mathbf{k}_f\bar{\mathbf{e}}_f). \tag{60}$$

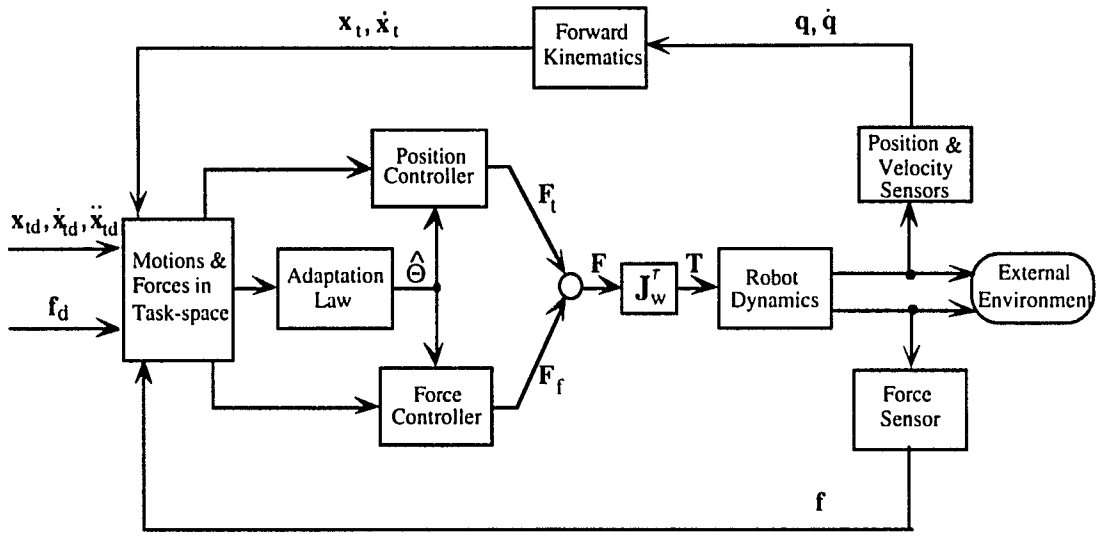

Figure 5. Block diagram of adaptive hybrid impedance controller.

Now, the stability of the closed-loop system is analyzed in the sense of Lyapunov approach.

Theorem 3: Consider the control law (57) with (58) for the constrained multiple robot system (52a,b) provided that some or all robot parameters are unknown. Then, the closed-loop system (60) is globally stable in the sense that some state variables of interest will be zero, namely,

$\mathbf{x}_t \to \mathbf{x}_{td}$ and $\mathbf{f} \to \mathbf{f}_d$ as $t \to \infty$,

and the vector of parameter estimation errors $\tilde{\Theta}$ remains bounded.

Proof: Define a Lyapunov function candidate, $V:(t,\tilde{\mathbf{x}}) \in \Re^+ \times \Re^{(n+m+s_3)} \to \Re^+$, by

$$V = \frac{1}{2}\tilde{\mathbf{x}}^T Q \tilde{\mathbf{x}}, \tag{61}$$

where $\tilde{\mathbf{x}} = [\bar{\mathbf{x}}_{ws}^T, \bar{\mathbf{e}}_f^T, \tilde{\Theta}^T]^T$ denotes the augmented state error vector and $Q = Block\ diag[\mathbf{M}_w, \mathbf{k}_b, \Gamma]$. By Rayleigh's principle, we can obtain

$$\frac{1}{2}\rho_{\min}(Q)\|\tilde{\mathbf{x}}\|^2 \le V \le \frac{1}{2}\rho_{\max}(Q)\|\tilde{\mathbf{x}}\|^2,$$

Since $\rho_{\min}(Q) > 0$, V is a positive definite function. Computing the time derivative of V along Eq. (60) leads to

$$\dot{V} = \bar{\mathbf{x}}_{ws}{}^T[-\mathbf{C}_w\bar{\mathbf{x}}_{ws} + \bar{\mathbf{R}}_r\tilde{\Theta} - \mathbf{k}\bar{\mathbf{x}}_{ws} + \mathbf{E}_f(\mathbf{e}_f + \mathbf{k}_f\bar{\mathbf{e}}_f)] + \frac{1}{2}\bar{\mathbf{x}}_{ws}{}^T\dot{\mathbf{M}}_w\bar{\mathbf{x}}_{ws} + k_b\bar{\mathbf{e}}_f{}^T\mathbf{e}_f + \tilde{\Theta}^T\Gamma\dot{\tilde{\Theta}} \tag{62}$$

which can be rewritten as

$$\dot{V} = -\bar{\mathbf{x}}_{ws}{}^T\mathbf{k}\bar{\mathbf{x}}_{ws} + \bar{\mathbf{x}}_{ws}{}^T\mathbf{E}_f(\mathbf{e}_f + \mathbf{k}_f\bar{\mathbf{e}}_f) + k_b\bar{\mathbf{e}}_f{}^T\mathbf{e}_f - \sigma\tilde{\Theta}^T\hat{\Theta}, \tag{63}$$

in which Property 2 in Eqs (26a,b) and $\dot{\tilde{\Theta}} = \dot{\hat{\Theta}}$ (assuming $\dot{\Theta} = \mathbf{0}$) have been conveniently exploited. By noting that $\bar{\mathbf{x}}_{ws}{}^T\mathbf{E}_f = \bar{\mathbf{x}}_{fs}{}^T$ and $\sigma\tilde{\Theta}^T\hat{\Theta} \geq 0$ (see Appendix C), it can be recognized that the following chains of inequalities hold

$$\begin{aligned}
\dot{V} &\leq -\bar{\mathbf{x}}_{ws}{}^T\mathbf{k}\bar{\mathbf{x}}_{ws} - k_b\bar{\mathbf{e}}_f{}^T(\mathbf{e}_f + \mathbf{k}_f\bar{\mathbf{e}}_f) + k_b\bar{\mathbf{e}}_f{}^T\mathbf{e}_f, \\
&\leq -\bar{\mathbf{x}}_{ws}{}^T\mathbf{k}\bar{\mathbf{x}}_{ws} - k_bk_f\bar{\mathbf{e}}_f{}^T\bar{\mathbf{e}}_f, \\
&\leq -\rho_{\min}(\mathbf{k})\|\bar{\mathbf{x}}_{ws}\|^2 - k_bk_f\|\bar{\mathbf{e}}_f\|^2 \leq 0.
\end{aligned} \tag{64}$$

Since $\dot{V}$ is negative semidefinite and $V(t,\tilde{\mathbf{x}})\,(\leq V_0(\bullet))$, $\forall t \geq 0$, is lower bounded by zero. From (61) and (64), it can be seen that $V \in L_\infty$ and accordingly $\bar{\mathbf{x}}_{ws} \in L_\infty$, $\bar{\mathbf{e}}_f \in L_\infty$, and $\tilde{\Theta} \in L_\infty$. In addition, from (64),

$$\rho_{\min}(\mathbf{k})\int_0^\infty \|\bar{\mathbf{x}}_{ws}\|^2 dt + k_bk_f\int_0^\infty \|\bar{\mathbf{e}}_t\|^2 dt \leq V_0 - \lim_{t\to\infty} V \leq V_0 < \infty,$$

which implies that $\bar{\mathbf{x}}_{ws} \in L_2$ and $\bar{\mathbf{e}}_f \in L_2$. On the other hand, due to fact that $\|\mathbf{e}_f\| \leq \|\mathbf{e}_t\|$, the force tracking error ($\mathbf{e}_f$) is bounded too. The detailed proof of $\|\mathbf{e}_f\| \leq \|\mathbf{e}_t\|$ can be found in Ref. [14]. In this case, the external environment can be actually regarded as a passive mechanism, thus it only provides a finite amount of energy due to physical limitations. Based on these approaches, $\mathbf{f}$ is reasonably assumed to be bounded. Consequently, the matrix $\bar{\mathbf{R}}_r$ can be readily shown to be bounded. And from (60), one obtain $\dot{\bar{\mathbf{x}}}_{ws} \in L_\infty$. Hence, $\bar{\mathbf{x}}_{ws} \in L_\infty \cap L_2$ and $\dot{\bar{\mathbf{x}}}_{ws} \in L_\infty$. By using Barbalst's Lemma ([19] or Lemma 1 in Part I of this thesis), we get $\lim_{t\to\infty}\bar{\mathbf{x}}_{ws} \to \mathbf{0}$. Evidently, this result shows that $\bar{\mathbf{e}}_f \to \mathbf{0}$ and $(\dot{\mathbf{e}}_t + \mathbf{k}_a\mathbf{e}_t) \to \mathbf{0}$ as $t \to \infty$, which in turns implies that

$\mathbf{e}_t(t) = \mathbf{e}_t(t_0)\exp[-k_a(t-t_0)]$ with $\|\mathbf{e}_t(t_0)\| < \infty$ and $\int \mathbf{e}_f(\tau)d\tau \to \mathbf{0}$,

that is, $\mathbf{e}_t \to \mathbf{0}$ and $\mathbf{e}_f \to \mathbf{0}$ (by Lemma 2) as $t \to \infty$.

Finally, it can be concluded from the above observations that the tracking errors of interest converge to zero, namely, $(\mathbf{e}_t, \mathbf{e}_f) \to \mathbf{0}$ as $t \to \infty$, and all other signals in the closed-loop system (i.e., the robot parameter vector) are shown to be bounded. Thus, the proof is completed according to the Lyapunov stability theory.

4. AN ILLUSTRATIVE EXAMPLE

An illustrative example is introduced to demonstrate the design procedures given in the previous sections. The scope of this example is to present brief design procedures without specific numerical values. Fig. 6 depicts the two-link planer manipulator and its task geometry in which the endpoint of the manipulator is required to trace the constraint surface.

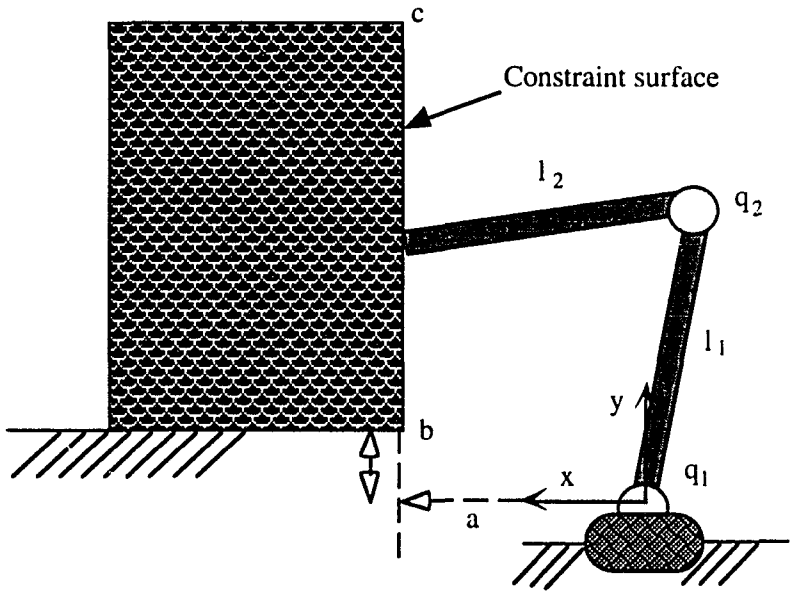

Figure 6. The two-link robot manipulator and its workspace.

The joint-space and end-effector variables are defined by $\mathbf{q} = [q_1,\ q_2]^T$ and $\mathbf{p} = [x,\ y]^T$, respectively. The natural constraint surface (at $x = a$) is assumed to be frictionless and the corresponding constraint equation is simply expressed as

$\phi_f(\mathbf{p}) = x - a = 0$ (i.e., $x = a = const.$),

where $\phi_f : \Re^2 \rightarrow \Re^1$, i.e., $n = 2$ and $m = 1$. And the corresponding artificial constraint is defined along the constraint surface (i.e., y direction, with $b \le y \le c$), as shown in Fig. 6.

The dynamic model interacting with the external environment can be written in a compact vector and matrix form as

$$\mathbf{M}(\mathbf{q};\Theta)\ddot{\mathbf{q}} + \mathbf{C}(\mathbf{q},\dot{\mathbf{q}};\Theta)\dot{\mathbf{q}} + \mathbf{G}(\mathbf{q};\Theta) + \mathbf{T}_u = \mathbf{T} - \mathbf{T}_c,$$

$$\phi_f(\mathbf{p}) = 0,$$

where all terms are defined as

$$\mathbf{M}(\mathbf{q};\Theta) = \begin{bmatrix} m_2 l_2^2 + 2m_2 l_1 l_2 c_2 + (m_1 + m_2) l_1^2 & m_2 l_2^2 + m_2 l_1 l_2 c_2 \\ m_2 l_2^2 + m_2 l_1 l_2 c_2 & m_2 l_2^2 \end{bmatrix},$$

$$\mathbf{C}(\mathbf{q},\dot{\mathbf{q}};\Theta) = \begin{bmatrix} -2m_2 l_1 l_2 s_2 \dot{q}_2 & -m_2 l_1 l_2 s_2 \dot{q}_2 \\ m_2 l_1 l_2 s_2 \dot{q}_1 & 0 \end{bmatrix},$$

$$\mathbf{G}(\mathbf{q};\Theta) = \begin{bmatrix} m_2 l_2 g c_{12} + (m_1 + m_2) l_1 g c_1 \\ m_2 l_2 g c_{12} \end{bmatrix},$$

$$\mathbf{T}_u = \begin{bmatrix} \mathrm{T}_{u1} \\ \mathrm{T}_{u2} \end{bmatrix}, \text{ and } \mathbf{T}_c = \begin{bmatrix} \mathrm{T}_{c1} \\ \mathrm{T}_{c2} \end{bmatrix},$$

where $c_i = \cos(q_i)$, $s_i = \sin(q_i)$, $c_{ij} = \cos(q_i + q_j)$, $s_{ij} = \sin(q_i + q_j)$, for i=1, 2; j=1, 2.

In the following, the joint-space dynamics will be transformed into the task-space form through appropriate transformations. First, the forward kinematics, $\mathbf{p} = \mathbf{h}(\mathbf{q})$, can be written as

$$x = l_1 c_1 + l_2 c_{12},$$

$$y = l_1 s_1 + l_2 s_{12}.$$

Taking time derivative of the above equation leads to $\mathbf{v}(=\dot{\mathbf{p}}) = \mathbf{J}\dot{\mathbf{q}}$, where the standard Jacobian matrix and its elements are defined as

$$\mathbf{J} = \begin{bmatrix} J_{11} & J_{12} \\ J_{21} & J_{22} \end{bmatrix} = \begin{bmatrix} -l_1 s_1 - l_2 s_{12} & -l_2 s_{12} \\ l_1 c_{11} + l_2 c_{12} & l_2 c_{12} \end{bmatrix}.$$

Now, the position and velocity vectors are given in the constraint-space formulation as

$$\mathbf{x}_w = [x_f,\ x_t]^T = \begin{bmatrix} x - a \\ y \end{bmatrix},$$

$$\dot{\mathbf{x}}_w = \mathbf{J}_\phi \dot{\mathbf{p}} = \begin{bmatrix} 1 & 0 \\ 0 & 1 \end{bmatrix} \dot{\mathbf{p}}.$$

Based on the above results, some matrices are now given as follows:

$$\mathbf{J}_\phi = \mathbf{E}_{2\times 2},\quad \mathbf{J}_f = [1,\ 0],\quad \mathbf{J}_t = [0,\ 1],$$

$$\mathbf{J}_w = \mathbf{J}_\phi \mathbf{J} = \mathbf{J},\quad \mathbf{J}_\Omega = \mathbf{J}_f \mathbf{J} = [J_{11},\ J_{12}].$$

Additionally, we have $\mathbf{E}_{2\times 2} = [\mathbf{E}_f \vdots \mathbf{E}_f]$, with $\mathbf{E}_f = [1,\ 0]^T$ and $\mathbf{E}_t = [0,\ 1]^T$. Then the contact force vector due to external constraint is found to be

$$\mathbf{T}_c = \mathbf{J}_\Omega{}^T \bar{f}$$

with $\mathrm{T}_{c1} = J_{11}\bar{f}$ and $\mathrm{T}_{c2} = J_{12}\bar{f}$, where $\bar{f}(=\lambda \text{ or } f) \in \Re^1$.

Now, following the approach described in the previous sections and using the definitions given above, one can obtain the constraint-space dynamics as

$$\mathbf{M}_w(\mathbf{x}_w;\Theta)\ddot{\mathbf{x}}_w + \mathbf{C}_w(\mathbf{x}_w,\dot{\mathbf{x}}_w;\Theta)\dot{\mathbf{x}}_w + \mathbf{G}_w(\mathbf{x}_w;\Theta) + \mathbf{F}_u = \mathbf{F} - \mathbf{E}_f\bar{f}$$

$$x_f = 0 \quad (\text{or } x = a)$$

with $\mathbf{x}_w = \mathbf{E}_t x_t = [0,\ y]^T$. Based on the above transformed dynamics, a class of hybrid control laws can be defined. In this formulation, the x coordinate is force-controlled direction (or normal direction), while y is position controlled direction (or tangential direction).

As a result, the computed torque controller (with $\mathbf{F}_u = \mathbf{0}$ in the system dynamics) is given by

$$\mathbf{F} = \mathbf{M}_w(\mathbf{x}_w)[\ddot{\mathbf{x}}_{wd} - \mathbf{k}_v\dot{\mathbf{e}}_w - \mathbf{k}_p\mathbf{e}_w] + \mathbf{C}_w(\mathbf{x}_w,\dot{\mathbf{x}}_w)\dot{\mathbf{x}}_w + \mathbf{G}_w(\mathbf{x}_w) + \mathbf{E}_f(\lambda_d - k_f e_\lambda).$$

For the adaptive controls, the regressor matrix $\mathbf{R}_r(or\ \overline{\mathbf{R}}_r)$ and the parameter vector Θ to be identified should be appropriately defined. In this case, the parameter vector (Θ) may be selected as $\Theta = [\theta_1 \quad \theta_2 \quad \theta_2 \quad \theta_4]^T = [l_1 \quad l_2 \quad m_1 \quad m_2]^T$.

Then, the robust adaptive controller is given by

$$\mathbf{F} = \mathbf{R}_r(\mathbf{x}_w,\dot{\mathbf{x}}_w,\dot{\mathbf{x}}_{wr},\ddot{\mathbf{x}}_{wr})\hat{\Theta} - \mathbf{k}\mathbf{x}_{ws} + \mathbf{E}_f(\lambda - k_f e_\lambda).$$

In case of impedance control (with $\mathbf{F}_u = \mathbf{0}$ in the system dynamics), the control equation is given by

$$\mathbf{F} = \overline{\mathbf{R}}_r(\mathbf{x}_w, \dot{\mathbf{x}}_w, \dot{\overline{\mathbf{x}}}_{wr}, \ddot{\overline{\mathbf{x}}}_{wr})\hat{\Theta} - \mathbf{k}\overline{\mathbf{x}}_{ws} + \mathbf{E}_f(f_d + k_f\overline{e}_f).$$

Once the hypothetical force vector $\mathbf{F}$ is computed, the corresponding joint torque vector is given by

$$\mathbf{T} = \mathbf{J}_w{}^T\mathbf{F}.$$

If the system and design parameters are chosen appropriately, then the design objectives can be accomplished by utilizing the proposed control laws. The remaining procedures are omitted.

5. CONCLUSIONS

This research has presented systematic approach to the dynamic formulation and the hybrid position/force controls for the constrained robotic manipulator over known contact surfaces. The compact mathematical model has been derived in terms of the constraint-surface variables. The constraint frame is set up as a direct sum of force-controlled subspace and (purely kinetic) position-controlled subspace in which position and force DOF are specified on the tangential and normal directions of the external surfaces, respectively. For the dynamic behavior of external environments, both elastic and rigid surfaces are considered. Based on a new reduced dynamic model, a class of hybrid control algorithms are synthesized to address the control issues of constrained robot system, that is, the generalized positions and the contact forces are simultaneously regulated in two orthogonal directions during the contact task. In the ideal case, the modified computed torque has been adopted. Without exact knowledge of the robot dynamics, the robust adaptive hybrid controls are formulated. In case of elastic environment, the adaptive impedance control has been synthesized in the presence of parametric uncertainties. The global stability and convergence issues of the corresponding closed-loop systems were widely discussed, as shown in Theorem 1-3.

Finally, it is shown that the proposed control laws guarantee global stability (boundedness and convergence) of the position (or motion) tracking as well as the contact-force tracking errors.

REFERENCES

[1] J.J.E. Soltine and W. Li, "On the adaptive control of robot manipulators," Int. J. Robotics Research, no. 6, pp. 49-59, 1897.

[2] R. Ortega and M.W. Spong, "Adaptive motion control of rigid robots: a tutorial," Automatica, vol. 25, no. 6, pp. 877-888, 1989.

[3] J.S. Reed and P. Ioannou, "Instability analysis and robust adaptive control of robotic manipulators," IEEE J. Robotics and Automat., vol. RA-5, no. 3, pp. 381-386, 1989.

[4] S.S. You and J.L. Hall, "Model-based approach with adaptive bounds of robust controllers for robot manipulators," in Proc. IEEE Int. SMC (2), pp. 1279-1284, 1994.

[5] M.T. Mason, "Compliance and force control for computer controlled manipulators," IEEE Trans. Syst. Man Cybern., vol. 11, no. 6, pp. 418-432, 1981

[6] M.H. Raibert and J.J. Craig, "Hybrid position/force control of manipulators," ASME, J. Dyn. Syst. Meas. Contr., vol. 102, no.(6), pp. 126-133, 1981.

[7] V. Potkonjak and M. Vukobratovic, "Dynamics of manipulation mechanism with constrained gripper motion: Part I-II," J. Robotic Systems 3(3), pp. 321-334, 1986.

[8] O. Khatib, "A unified approach for motion and force control of robot manipulators: The operational space formulation," IEEE J. Robotics and Automat., RA-3, pp. 43-53, 1987.

[9] N. Hogan, "Impedance control: an a approach to manipulation (part 1-3)," ASME J. Dyn. Syst. Meas. Contr., vol. 107, pp. 1-24, 1985.

[10] H. Kazerooni, P.K. Houpt, and T.B. Sheridan, "Robust compliant motion for manipulators," IEEE J. Robot. Automat. vol. RA-2, pp. 83-105, 1986.

[11] J.T. Wen and S. Murphy, "Stability analysis of position and force control for robot arms," IEEE Trans. Automat. Contr., vol. 36, no 3, pp. 365-371, 1991.

[12] T. Yoshikawa, "Dynamic hybrid position/force control of robot manipulators-Description of hand constraints and calculation of joint driving force," IEEE J. Robotics Automat., vol. RA-3 (5), pp. 386-392,1987.

[13] N.H. McClamroch and D. Wang, "Feedback stabilization and tracking of constrained robots," IEEE Trans. Automat. Contr., vol. 33, pp. 419-426, 1988.

[14] L. Lui, Y. Han, R. Lingarkar, N.K. Sinha, and M.A. Elbestawi, "Adaptive control of constrained robotic manipulators," Int. J. Robot. Automat., vol. 7, no 8, pp. 50-56, 1990.

[15] R. Carelli, R. Kelly, and R. Ortega, "Adaptive force control of robot manipulators," Int. J. Contr., vol. 52(1), pp. 37-54, 1990.

[16] T. Fossen and S. Sagatun, "Adaptive control of nonlinear systems: A case study of underwater robotic systems," J. Robotic Systems 8(3), pp. 393-412, 1991.

[17] B. Yao, S.P. Chan, and D. Wang, "A unified approach to variable structure control of robot manipulators," in Proc. American Contr. Conf., pp. 1282-1286, 1992.

[18] Y.H. Chen, "Robust control design: non-adaptive versus adaptive," Int. J. Contr., vol. 51, no. 6, pp. 1457-1477, 1990.

[19] S.S. Sastry and M. Bodson, "Adaptive control: stability, convergence and robustness," Prentice-Hall, Englewood Cliffs, NJ, 1989.

[20] N. Sadegh and R. Horowitz, "Stability and robustness analysis of a class of adaptive controllers for robotic manipulators," Int. J. Robotics Res., 9(3), pp. 74-92, 1990.

APPENDIX

Appendix A

Proof of $\dot{\mathbf{J}}_w^{-1} = -\mathbf{J}_w^{-1}\dot{\mathbf{J}}_w\mathbf{J}_w^{-1}$:

Since $\mathbf{J}_w\mathbf{J}_w^{-1} = \mathbf{E}$, then $\dot{\mathbf{J}}_w\mathbf{J}_w^{-1} + \mathbf{J}_w\dot{\mathbf{J}}_w^{-1} = \mathbf{0}$. Therefore, $\dot{\mathbf{J}}_w^{-1} = -\mathbf{J}_w^{-1}\dot{\mathbf{J}}_w\mathbf{J}_w^{-1}$

Appendix B

Proof of Property 2 in Eqs (26a,b):

If $\mathbf{N}_w$ is skew-symmetric matrix, then $\mathbf{x}^T\mathbf{N}_w\mathbf{x} = 0$, $\forall\ \mathbf{x} \in \Re^n$. To show this,

$$\begin{aligned}
&\mathbf{x}^T\mathbf{N}_w\mathbf{x} \\
&= \mathbf{x}^T\{\frac{d}{dt}[\mathbf{J}_w^{-T}\mathbf{M}\mathbf{J}_w^{-1}] - 2[\mathbf{J}_w^{-T}\mathbf{C}\mathbf{J}_w^{-1} - \mathbf{J}_w^{-T}\mathbf{M}\mathbf{J}_w^{-1}\dot{\mathbf{J}}_w\mathbf{J}_w^{-1}]\}\mathbf{x} \\
&= \mathbf{x}^T\{2\mathbf{J}_w^{-T}\mathbf{M}\dot{\mathbf{J}}_w^{-1} + \mathbf{J}_w^{-T}\dot{\mathbf{M}}\mathbf{J}_w^{-1} - 2\mathbf{J}_w^{-T}\mathbf{C}\mathbf{J}_w^{-1} + 2\mathbf{J}_w^{-T}\mathbf{M}\mathbf{J}_w^{-1}\dot{\mathbf{J}}_w\mathbf{J}_w^{-1}\}\mathbf{x} \\
&= \mathbf{x}^T\mathbf{J}_w^{-T}[\dot{\mathbf{M}} - 2\mathbf{C}]\mathbf{J}_w^{-1}\mathbf{x} \text{ (where } \dot{\mathbf{J}}_w^{-1} = -\mathbf{J}_w^{-1}\dot{\mathbf{J}}_w\mathbf{J}_w^{-1})
\end{aligned}$$

Since the matrix $(\dot{\mathbf{M}} - 2\mathbf{C})$ is skew-symmetric [1-3], thus,

$\mathbf{Y}^T[\dot{\mathbf{M}} - 2\mathbf{C}]\mathbf{Y} = \mathbf{0}$ (where $\mathbf{Y} = J_w^{-1}\mathbf{x}$)

Therefore, the matrix $(\dot{\mathbf{M}}_w - 2\mathbf{C}_w)$ is also skew-symmetric. Note that the change of coordinates do not affect the property. Actually, this physical property is inherent to robot manipulator regardless of any chosen coordinates. This completes the proof.

Appendix C

Proof of $\sigma\tilde{\Theta}^T\tilde{\Theta} \geq 0$:

$$\begin{aligned}
\sigma\tilde{\Theta}^T\hat{\Theta} &= \sigma(\hat{\Theta}^T - \Theta^T)\hat{\Theta} = -\sigma(\|\hat{\Theta}\|^2 - \Theta^T\hat{\Theta}) \\
&\leq \sigma\|\hat{\Theta}\|(\|\hat{\Theta}\| - \Theta_0 + \Theta_0 - \|\Theta\|)
\end{aligned}$$

Note that $\sigma\|\hat{\Theta}\|(\|\hat{\Theta}\| - \Theta_0) \geq 0$ and $\Theta_0 \geq \|\Theta\|$, it follows that $\sigma\tilde{\Theta}^T\hat{\Theta} \geq 0$. Therefore, the proof is completed. $\Delta\Delta$

PART III

DYNAMICS AND CONTROLS OF MULTIPLE ROBOT SYSTEMS WITH CONSTRAINED MOTION TASKS

OVERVIEW

This part of the dissertation deals with a mathematical model and coordinated control of multiple robot manipulators (or equivalently multifingered robot hands) holding and transporting a rigid common object on the constraint surfaces, subject to a set of holonomic (integrable) constraints. First, the kinematics and dynamics of multiple robot systems containing the closed-chain mechanisms are formulated from a unified viewpoint. After a series of model transformations, a new combined dynamic model is derived for dynamic analysis and control synthesis in which the system dynamics can be decomposed into two orthogonal subsystems: the (reduced-order) motion-controlled subsystem, and the force-controlled subsystem. Next, a class of hybrid position/force controllers are developed. The control laws can be used to simultaneously control the motion (or position) of the object along the constraint surfaces and the contact forces (the internal forces exerted on the object by the multiple arms and the constraint forces due to the rigid contacts between the common object and the constraint surfaces). It is shown that the presented control algorithms guarantee the global boundedness (stability) of the object position tracking as well as the contact forces.

1. INTRODUCTION

During the last decade, a single robot system has been extensively used in many modern industries. However, practical applications of such a system to higher level tasks are severely limited due to its capability (or capacity) and performance. To overcome the above limitations as well as greatly enhance system performance, multiple robot systems have been recently adopted. For example, in the execution of the advanced tasks involved in flexible manufacturing systems, such as grasping big and heavy objects, various material handling, and fine assembly operations, the cooperation among two or more robots is essential to accomplish such tasks. Additionally, like human arms, the multi-manipulator systems provide higher flexibility (or versatility) and dexterity in performing complex (or sophisticated) tasks. Unfortunately, the multiple robot systems form closed kinematic chains which impose additional kinematic and dynamic constraints (or couplings) on the systems. Thus the control of such systems is generally very complicated. An important prerequisite to the control of multiple robot systems is to derive a proper mathematical model of such systems. The kinematics and dynamics of multiple robot systems are discussed in Refs. [1-3]. Several control schemes for the multiple robots have been suggested by researchers. Some of these works utilize the so-called master/slave method (see [4-5], for example). Recently, the hybrid (position/force) control has been proposed for a constrained single robot system [6-9]. However, only a few articles consider the constrained multiple robot systems carrying a common object in which the motion of the object is constrained in some direction due to the rigid contacts between the object and the constraint surfaces (or its environments). In general, it is necessary to simultaneously control the motion of the object and the contact forces (the internal grasping forces and the constraint forces). Based on exact knowledge of system dynamics, a number of researchers proposed the computed torque method (see [10-12], for example).

Unfortunately, a precise knowledge of the system dynamics is typically unavailable. To remedy this problem, the adaptive control strategies based on imprecise knowledge of the system dynamics have been proposed to cope with system uncertainties [13-15]. And Yao *et al.* [17] used a variable structure control (VSC) method to handle the system uncertainties. In this study, the uncertainties include the parametric uncertainties, the external disturbances, and the unmodelled dynamics (perhaps from sensors and actuators). Even if the aforementioned methods have their own characteristics, the research on the robust adaptive coordinated control of constrained multiple robot systems is still in its early stage of development and an open problem. This study provides a unified framework for characterizing the features of the constrained multiple robot systems.

The main objective of this work is to develop the dynamic model and coordinated control for multi-fingered robot hands cooperatively manipulating a rigid object along the constraint surfaces. In this applications, the multiple robot manipulators are constrained with each other as well as constrained by the external environment through the common object in their workspaces. We first discuss the overall dynamic model obtained by combining the kinematic and dynamic constraints of the closed-chain mechanisms with the milti-manipulator dynamics. After a series of model transformations, a reduced-order (decoupled) dynamic model is derived. Next, a class of coordinated controllers are designed to simultaneously manipulate the motion of the object in the unconstrained directions (i.e., in the tangent to the constraint surfaces), and the contact forces (the internal grasping forces and the constraint forces) in the constrained directions (i.e., in the normal to the constraint surfaces). Since the position- and force-controlled subsystems are decoupled, each subsystem can be controlled independently and simultaneously. In the absence of uncertainties (i.e., ideal case), the modified computed torque controller is synthesized while guaranteeing the asymptotic stability of the corresponding closed-loop system. In addition, the robust adaptive controller will be presented to overcome the system

uncertainties. It will be shown that the adaptive control guarantees the global stability of the position of the object as well as the contact forces (the internal forces and the constraint forces) by a Lyapunov stability method.

This chapter is organized as follows: In Section 2, through appropriate model transformations, we formulate a unified dynamic model of constrained multiple robots. A class of hybrid controllers are proposed in Section 3. Finally, Section 4 presents the conclusions of this work.

The work presented in this part is a direct extension of the works (constrained single robot system) presented in Part II of this thesis.

2. KINEMATICS AND DYNAMICS OF CONSTRAINED MULTIPLE ROBOTIC SYSTEMS

This section provides a unified formulation for the kinematics and dynamics of physically constrained multiple robot systems so that a class of hybrid control algorithms can be conveniently formulated in the section that follows. Consider multiple robots for cooperative tasks, as shown in Fig. 1, which is constituted by multifingered robot hands manipulating a common object along rigid constraint surfaces with appropriate contact forces. Note that the overall system under consideration comprises three main components: ν (≥ 2) robotic manipulators, the common object (or equivalently the payload) being manipulated, and the (rigid) external constraint surfaces.

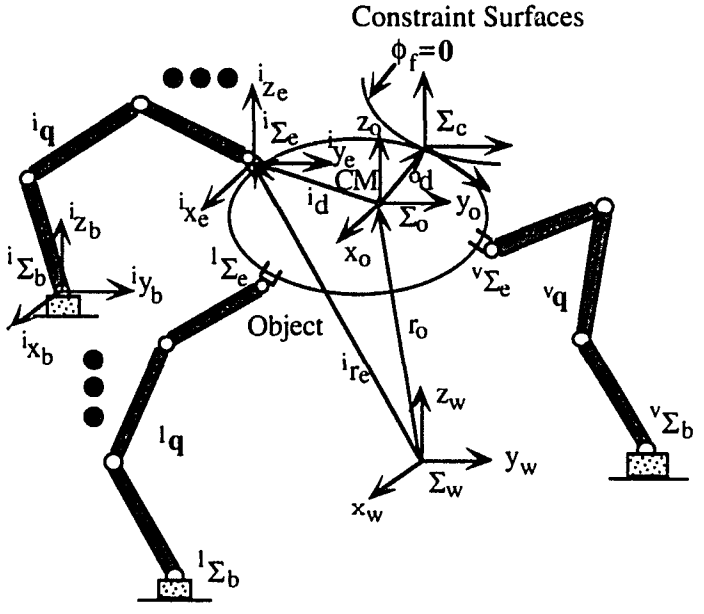

Figure 1. Multiple robot manipulators carrying a common object on the constraint surfaces.

To facilitate further development, the following assumptions are made throughout the study:

Assumption 1: Each robotic manipulator with an n-link (revolute) joints contacts the common object with a point (imposing the internal constraints). Also, the constrained motion between the object and the external constraint surfaces (imposing the external constraints) is achieved through a frictionless point contact. Thus multiple closed kinematic chains are always formed through the contact points during the motion.

Assumption 2: Each manipulator grasps the object firmly at initial time at a specified point, and their mutual positions and orientations are invariant throughout the system motions, i.e., a rigid grasping. $\nabla\nabla$

The following notation will be utilized throughout this research for system modeling and control synthesis. The vector norm $\|\mathbf{x}\|$ is the Euclidean one of vector $\mathbf{x} \in \Re^n$ (the set of all n-dimensional Euclidean space), i.e., $\|\mathbf{x}\| = (\mathbf{x}^T\mathbf{x})^{1/2}$, and the matrix norm is the corresponding induced one of matrix $\mathbf{A} \in \Re^{m\times n}$ (the set of all $m \times n$ real matrices), i.e., $\|\mathbf{A}\| = [\rho_{\max}(\mathbf{A}^T\mathbf{A})]^{1/2}$, where $\rho_{\max}(\bullet)[\rho_{\min}(\bullet)]$ denotes the maximum (minimum) eigenvalue of the designated matrix, and the superscript T represents a transpose operation. In addition, $RS(\mathbf{A})$ (or $\mathrm{Im}(\mathbf{A})$) and $rk(\mathbf{A})$ denote the range (or image) space and the rank of matrix $\mathbf{A}$, respectively, while $NS(\mathbf{A})$ (or $Ker(\mathbf{A})$) represents the null space (or kernel) of $\mathbf{A}$.

In this section, the kinematic and dynamic constraints among the components of the closed-chain structures are first discussed. Then, these constraints are combined with the dynamic equations of multifingered robot hands through common object to obtain the complete dynamic model of the system.

2.1 System Parameters and Kinematic Formulations

This subsection is devoted to introducing the system variables and to formulating the kinematic constraints, which are originated from the closed-chain mechanisms.

In order to fully describe the kinematic and dynamic relationships among the components of the overall system in a three-dimensional workspace, a set of coordinate systems are defined as follows (also see Fig. 1):

A frame $\Sigma_w\{o_w - x_w y_w z_w\}$ is the world (or absolute) coordinate system, which is fixed to the ground as the reference frame; ${}^i\Sigma_b\{{}^i o_b - {}^i x_b\, {}^i y_b\, {}^i z_b\}$ is the ith base frame ($i = 1, \cdots, v$), which is fixed at the base of the ith robot; ${}^i\Sigma_e\{{}^i o_e - {}^i x_e\, {}^i y_e\, {}^i z_e\}$ is the ith end-effector coordinate system, and the origin ${}^i o_e$ is assigned to the ith contact point between the end-effector and the common object; $\Sigma_o\{o_o - x_o y_o z_o\}$ is the common object frame, and its origin o_o is fixed to the mass center (CM) of the object; $\Sigma_c\{o_c - x_c y_c z_c\}$ is the constraint coordinate system, and the origin o_c is located at the contact point between the object and the constraint surface. Unless mentioned otherwise, all Cartesian quantities are to be expressed in frame Σ_w. In addition, it is supposed that index i takes all values from the integer set [1, v] and indicates the quantity corresponding to the ith manipulator.

Now, some system variables are defined. $\mathbf{p}_o = [\mathbf{r}_o^T, \Psi_o^T]^T \in \Re^6$ (the dimension of the operational space) is the generalized Cartesian position vector representing the configuration of the common object, with $\mathbf{r}_o \in \Re^3$ (the Cartesian position vector) and $\Psi_o = [\alpha_o, \beta_o, \gamma_o]^T$ (the orientation vector). ${}^i\mathbf{p}_e = [{}^i\mathbf{r}_e^T, {}^i\Psi_e^T]^T$ denotes the generalized position vector of ith end-effector frame ${}^i\Sigma_e$, with ${}^i\mathbf{r}_e \in \Re^3$ and ${}^i\Psi_e = [{}^i\alpha_e, {}^i\beta_e, {}^i\gamma_e]^T$. The generalized position vector of o_c relative to Σ_w is given by $\mathbf{p}_c = [\mathbf{r}_c^T, \Psi_c^T]^T$, with $\mathbf{r}_c \in \Re^3$ and $\Psi_c = [\alpha_c, \beta_c, \gamma_c]^T$. And ${}^i\mathbf{d} \in \Re^3$ denotes the distance vector from the mass center o_o to each contact point ${}^i o_e$ measured in Σ_o, while the distance between o_o and o_c in terms of Σ_o is specified by ${}^o\mathbf{d} \in \Re^3$. In addition to the generalized position variables,

${}^{i}\mathbf{F}_{e} = [{}^{i}\mathbf{f}_{e}{}^{T}, {}^{i}\mathbf{n}_{e}{}^{T}]^{T} \in \Re^{6}$ denotes the vector of generalized end-effector forces (or wrenches) acting through contact point ${}^{i}o_{e}$ to the common object, where ${}^{i}\mathbf{f}_{e} \in \Re^{3}$ and ${}^{i}\mathbf{n}_{e} \in \Re^{3}$ are the vectors of the Cartesian linear forces and the torques, respectively. $\mathbf{F}_{o} = [\mathbf{f}_{o}{}^{T}, \mathbf{n}_{o}{}^{T}]^{T} \in \Re^{6}$ denotes the generalized equivalent forces acting on the mass center of the object by ${}^{i}\mathbf{F}_{e}$. In this study, the term generalized position includes both position and orientation, and the term generalized force includes both force and moment.

Even if there exist several methods of defining a set of independent parameters to represent an arbitrary orientation of a rigid body in the space $\Re^{3}$, the rotational motion ${}^{(\bullet)}\Psi_{(\bullet)}$ can be described by Euler angles in this study [3, 21], as shown pictorially in Fig. 2. More specifically, the Euler angles are specified in terms of the image of the three parameters $\{({}^{(\bullet)}\alpha_{(\bullet)}), ({}^{(\bullet)}\beta_{(\bullet)}),$ and $({}^{(\bullet)}\gamma_{(\bullet)})\}$ obtained by performing three elementary rotations of body-attached frame (or rotating frame) ${}^{(\bullet)}\Sigma_{(\bullet)}$ with respect to the principle axes of world frame Σ_{w} (or fixed frame) in a right-handed sense, i.e., rotating ${}^{(\bullet)}\alpha_{(\bullet)}$ (yaw angle) about the z axis, then ${}^{(\bullet)}\beta_{(\bullet)}$ (pitch angle) about the new y axis, and finally ${}^{(\bullet)}\gamma_{(\bullet)}$ (roll angle) about the new x axis.

Then the resulting overall transformation with Euler angles is given in a 3×3 matrix as

$$
\begin{aligned}
{}^{w}_{(\bullet)}R &= {}^{w}_{(\bullet)}YPR({}^{(\bullet)}\alpha_{(\bullet)}, {}^{(\bullet)}\beta_{(\bullet)}, {}^{(\bullet)}\gamma_{(\bullet)}) = [{}^{w}_{(\bullet)}\mathbf{i} \quad {}^{w}_{(\bullet)}\mathbf{j} \quad {}^{w}_{(\bullet)}\mathbf{k}] \\
&= \begin{bmatrix} C\alpha C\beta & C\alpha S\beta S\gamma - S\alpha C\gamma & C\alpha S\beta C\gamma + S\alpha S\gamma \\ S\alpha C\beta & S\alpha S\beta S\gamma + C\alpha C\gamma & S\alpha S\beta C\gamma - C\alpha S\gamma \\ -S\beta & C\beta S\gamma & C\beta C\gamma \end{bmatrix},
\end{aligned} \tag{1}
$$

where ${}^{w}_{(\bullet)}\mathbf{i}$, ${}^{w}_{(\bullet)}\mathbf{j}$, and ${}^{w}_{(\bullet)}\mathbf{k} \in \Re^{3}$ denote the mutually orthogonal unit (or orthonormal) vectors of body frame ${}^{(\bullet)}\Sigma_{(\bullet)}$ relative to frame Σ_{w}; For the notational convenience, we have introduced the following, $C\alpha = \cos({}^{(\bullet)}\alpha_{(\bullet)})$, $S\beta = \sin({}^{(\bullet)}\beta_{(\bullet)})$, and $C\gamma = \cos({}^{(\bullet)}\gamma_{(\bullet)})$, and so on. Thus, the orthogonal rotation matrix ${}^{w}_{(\bullet)}R$: $\Re^{3} \rightarrow \Re^{3}$ (with ${}^{w}_{(\bullet)}R^{-1} = {}^{w}_{(\bullet)}R^{T}$) maps (or transforms) the vectors from coordinate system ${}^{(\bullet)}\Sigma_{(\bullet)}$ into frame Σ_{w}.

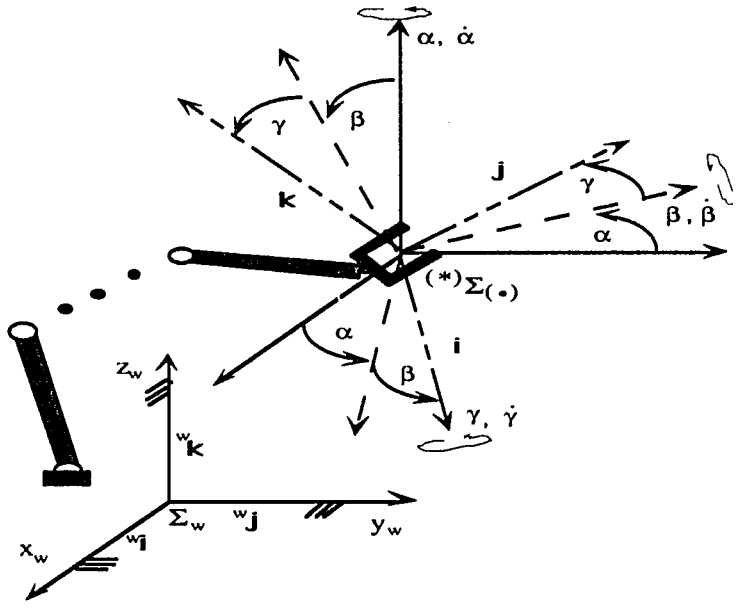

Figure 2. Geometrical representation of Euler angles (yaw, pitch, and roll).

In addition, ${}^{(*)}\omega_{(*)} \in \Re^3$ is the vector of the angular velocity of the frame ${}^{(*)}\Sigma_{(*)}$ as viewed in Σ_w. For the purpose of the present study, the exact representation of a rigid body (or frame) motions in a three-dimensional workspace is specified by $({}^{(*)}\mathbf{r}_{(*)}, {}^{w}_{(*)}R) \in \Re^3 \times SO(3) = SE(3)$, where $SO(3)$ denotes a set (or group) of all proper 3×3 rotation matrices on $\Re^3$ (i.e., a three-dimensional submanifold of $\Re^9$). More specifically, $SO(3) = \{R \in \Re^{3\times3}; \det(R) = +1, R^T R = \mathbf{E}\}$, where $\mathbf{E}$ is an identity matrix with an appropriate dimension. Consequently, the motions (position and orientation) of rigid body belong to 6-dimensional manifold. Here, it is worth nothing that the configuration space $SE(3)$ which consists of the translations and proper rotations can also be expressed in 4×4 matrices, which is often referred to as the homogeneous transformation matrices in the robotics literature.

Now, the time derivatives of orientation vector (or Euler angles) are called Euler rates (or Euler frequencies) and related as (see, Fig. 2)

$$^{(\bullet)}\omega_{(\bullet)} = (-\dot{\beta}S\alpha + \dot{\gamma}C\beta C\alpha)\,{}^{w}\mathbf{i} + (\dot{\beta}C\alpha + \dot{\gamma}C\beta S\alpha)\,{}^{w}\mathbf{j} + (\dot{\alpha} - \dot{\gamma}S\beta)\,{}^{w}\mathbf{k},$$

where ${}^{w}\mathbf{i}$, ${}^{w}\mathbf{j}$, and ${}^{w}\mathbf{k}$ represent mutually orthogonal unit vectors of the principle axes of Σ_w. As a consequence, the rotational velocity (along with relationship between the angular velocity, $^{(\bullet)}\omega_{(\bullet)} \in \Re^3$, and the rates of Euler angles, $^{(\bullet)}\dot{\Psi}_{(\bullet)} = [\dot{\alpha}, \dot{\beta}, \dot{\gamma}]^T$) is given by

$$^{(\bullet)}\omega_{(\bullet)} = \Delta_{(\bullet)}(^{(\bullet)}\Psi_{(\bullet)})^{(\bullet)}\dot{\Psi}_{(\bullet)}, \tag{2}$$

where the transformation matrix $\Delta_{(\bullet)} \in \Re^{3\times 3}$ is readily defined as

$$\Delta_{(\bullet)} = \begin{bmatrix} 0 & -S\alpha & C\beta C\alpha \\ 0 & C\alpha & C\beta S\alpha \\ 1 & 0 & -S\beta \end{bmatrix}.$$

Since $\det(\Delta_{(\bullet)}) = C\beta$, the singularity (or degeneracy) is likely to occur at $\det(\Delta_{(\bullet)}) = 0$ in which the Jacobian $\Delta_{(\bullet)}$ is rank deficient. Thus the Euler angles are not uniquely defined when the robot operates near a singular point. Without loss of generality, $\Delta_{(\bullet)}$ is assumed a nonsingular matrix so that any singular point is eliminated, although the singularity is not avoided in any Euler angles representations with three independent parameters.

With the notations defined above, the two representations of the generalized velocities (or twists) of a rigid body are related as

$$^{(\bullet)}\mathbf{v}_{(\bullet)} = \mathbf{N}_{(\bullet)}\,{}^{(\bullet)}\dot{\mathbf{p}}_{(\bullet)}, \tag{3}$$

where the vectors $^{(\bullet)}\mathbf{v}_{(\bullet)} = [^{(\bullet)}\dot{\mathbf{r}}_{(\bullet)}{}^{T}, {}^{(\bullet)}\omega_{(\bullet)}{}^{T}]^T \in \Re^6$ and $^{(\bullet)}\dot{\mathbf{p}}_{(\bullet)} = [^{(\bullet)}\dot{\mathbf{r}}_{(\bullet)}{}^{T}, {}^{(\bullet)}\dot{\Psi}_{(\bullet)}{}^{T}]^T \in \Re^6$, with $\mathbf{N}_{(\bullet)} = \begin{bmatrix} \mathbf{E}_{3\times 3} & \mathbf{0}_{3\times 3} \\ \mathbf{0}_{3\times 3} & \Delta_{(\bullet)} \end{bmatrix} \in \Re^{6\times 6}$, and $\mathbf{E}_{n\times n}$ and $\mathbf{0}_{n\times n}$ represent $(n\times n)$ identity and null matrices, respectively. Of course, $\mathbf{N}_{(\bullet)}$ is a nonsingular Jacobian matrix. More kinematic constraints imposed on the system are discussed in the following. Let ${}^{i}\mathbf{q} = [{}^{i}q_1, \cdots, {}^{i}q_n]^T$ be the vector of joint position for the ith manipulator, and these joint-space vectors can be suitably arranged to form the vector of the extended (or augmented) joint-space variables, $\mathbf{q}_x \in \Re^{nv}$, with $\mathbf{q}_x = [{}^{1}\mathbf{q}^T, \cdots, {}^{v}\mathbf{q}^T]^T \in \Re^n \times \cdots \times \Re^n$. And each robotic manipulator has a

direct (or forward) kinematics to define the relationships between the joint-space variables and the Cartesian (or operational) space variables in a unique manner as

$$ {}^{i}\mathbf{p}_{e}={}^{i}\mathbf{h}({}^{i}\mathbf{q}),\ i=1,\cdots,v \tag{4} $$

where ${}^{i}\mathbf{h}(\bullet)$: $C^2(\Re^n \rightarrow \Re^6)$ is a twice differentiable (i.e., a C^2 function) and nonlinear vector-valued function whose structures are known for given manipulators. By virtue of equation (3), the corresponding twist vector of the end-effector is analogously given as

$$ {}^{i}\mathbf{v}_{e} = \mathbf{N}_{i}\,{}^{i}\dot{\mathbf{p}}_{e}={}^{i}\mathbf{J}({}^{i}\mathbf{q})\,{}^{i}\dot{\mathbf{q}}, \tag{5} $$

where ${}^{i}\mathbf{v}_{e}=[{}^{i}\dot{\mathbf{r}}_{e}^{T}, {}^{i}\omega_{e}^{T}]^{T}$ and ${}^{i}\mathbf{p}_{e}=[{}^{i}\dot{\mathbf{r}}_{e}^{T}, {}^{i}\dot{\Psi}_{e}^{T}]^{T}$, with $\mathbf{N}_{i}=\begin{bmatrix}\mathbf{E}_3 & \mathbf{0}_3\\ \mathbf{0}_3 & \Delta_i\end{bmatrix}\in\Re^{6\times 6}$; ${}^{i}\mathbf{J}=\mathbf{N}_{i}\dfrac{\partial({}^{i}\mathbf{h})}{\partial({}^{i}\mathbf{q})}\in\Re^{6\times n}$ is the standard Jacobian matrix of the ith manipulator with a full rank and transforms the vector of joint-space velocity to that of the end-effector velocity. Assume also that all manipulators are in nonsingular regions, i.e., $\det({}^{i}\mathbf{J})\neq 0$. Since there are no relative motions (position and orientation) among the object and the arm's end-effectors due to rigid grasping, the following kinematic relation can be established, at each grasping or contact point ${}^{i}o_{e}$, as

$$ {}^{i}\mathbf{r}_{e} = \mathbf{r}_{o}+{}^{w}_{o}R\,{}^{i}\mathbf{d}, \tag{6a} $$

$$ {}^{i}\omega_{e} = \omega_{o}, \tag{6b} $$

where ${}^{w}_{o}R\in\Re^{3\times 3}$ (namely, $SO(3)$) is an orthogonal rotation matrix that transforms the local vectors measured in frame Σ_o to the vector representations in frame Σ_w. And the following properties can be utilized for the further development:

$$ \frac{d}{dt}\,{}^{w}_{(\bullet)}R={}^{(\bullet)}\omega_{(\bullet)}\otimes{}^{w}_{(\bullet)}R \text{ and } {}^{(\bullet)}\omega_{(\bullet)}\otimes\mathbf{x}=-\mathbf{x}\otimes{}^{(\bullet)}\omega_{(\bullet)},\ \forall\,\mathbf{x}\in\Re^3 $$

where the symbol $\otimes$ denotes the cross-product operation. Under these setting, the following equations can relate the generalized velocity of the end-effector to that of the object's center of mass

$$ {}^{i}\mathbf{v}_{e} = \mathbf{Q}_{i}^{T}\mathbf{N}_{o}\dot{\mathbf{p}}_{o} = \mathbf{Q}_{i}^{T}\mathbf{v}_{o}, \tag{7} $$

where $\mathbf{v}_o = [\dot{\mathbf{r}}_o^T, \omega_o^T]^T \in \Re^6$ and $\dot{\mathbf{p}}_o = [\dot{\mathbf{r}}_o^T, \dot{\Psi}_o^T]^T \in \Re^6$, with $\mathbf{N}_o = \begin{bmatrix} \mathbf{E}_{3\times3} & \mathbf{0} \\ \mathbf{0} & \Delta_o \end{bmatrix} \in \Re^{6\times6}$,

and the mapping (or transformation) $\mathbf{Q}_i \in \Re^{6\times6}$ is compactly defined as

$$\mathbf{Q}_i = \begin{bmatrix} \mathbf{E}_{3\times3} & \mathbf{0}_{3\times3} \\ -\mathbf{D}_i({}_o^w R\, {}^i\mathbf{d}) & \mathbf{E}_{3\times3} \end{bmatrix}. \tag{8}$$

In this formulation, $\mathbf{Q}_i$ is positive-definite and nonsingular matrix, and the operator $\mathbf{D}_i(\bullet) \in \Re^{3\times3}$ is introduced as

$$\mathbf{D}_i(\mathbf{b}_i) = (\mathbf{b}_i)\otimes, \text{ with } \mathbf{b}_i \in \Re^3$$

In which

$$\mathbf{D}_i(\bullet): \Re^3 \to so(3) \left\| \begin{bmatrix} b_{i1} \\ b_{i2} \\ b_{i3} \end{bmatrix} \mapsto \begin{bmatrix} 0 & -b_{i3} & b_{i2} \\ b_{i3} & 0 & -b_{i1} \\ -b_{i2} & b_{i1} & 0 \end{bmatrix}, \right.$$

which identifies a one-to-one correspondence between a three-dimensional vector, $\mathbf{b}_i = [b_{i1}, b_{i2}, b_{i3}]^T$, with $so(3)$, i.e., the associated vector space of 3×3 skew-symmetric (or antisymmetric) matrix, more formally, $so(3) = \{\mathbf{A} \in \Re^{3\times3}; \mathbf{A}^T = -\mathbf{A}\}$.

Aggregating all robots acting on the common object gives the extended velocity constraints as

$$\mathbf{v}_e = \mathbf{N}\dot{\mathbf{p}}_e = \mathbf{J}_s\dot{\mathbf{q}}_s = \mathbf{Q}_s^T\mathbf{v}_o, \tag{9}$$

where all terms can be augmented as

$$\mathbf{v}_e = [{}^1\mathbf{v}_e^T, \cdots, {}^v\mathbf{v}_e^T]^T, \quad \mathbf{v}_e \in \Re^{6v}$$
$$\dot{\mathbf{p}}_e = [{}^1\dot{\mathbf{p}}_e^T, \cdots, {}^v\dot{\mathbf{p}}_e^T]^T, \quad \dot{\mathbf{p}}_e \in \Re^{6v}$$
$$\dot{\mathbf{q}}_s = [{}^1\dot{\mathbf{q}}^T, \cdots, {}^v\dot{\mathbf{q}}^T]^T, \quad \dot{\mathbf{q}}_s \in \Re^{vn}$$
$$\mathbf{N} = Block\ diag[\mathbf{N}_1, \cdots, \mathbf{N}_v], \quad \mathbf{N} \in \Re^{6v\times6v}$$
$$\mathbf{J}_s = Block\ diag\,[{}^1\mathbf{J}, \cdots, {}^v\mathbf{J}], \quad \mathbf{J}_s \in \Re^{6v\times vn}$$
$$\mathbf{Q}_s = [\mathbf{Q}_1, \cdots, \mathbf{Q}_v], \quad \mathbf{Q}_s \in \Re^{6\times6v}$$

In this formulation, $\mathbf{Q}_s$ has a full row rank, i.e., $rk(\mathbf{Q}_s) = 6$, and is called the "grasp" matrix [2, 15-17] that maps the vectors from the contact spaces into the common object space (CM). A more detailed discussion of the grasp matrix is given later.

Similarly, the generalized position vector of o_c relative to Σ_w is given by

$$\mathbf{r}_c = \mathbf{r}_o + {}^w_o R\, {}^o\mathbf{d}, \tag{10a}$$

$$\omega_c = \omega_o. \tag{10b}$$

Then the corresponding velocity constraint on the rigid surface is obtained as

$$\mathbf{v}_c = \mathbf{Q}_o^T \mathbf{v}_o, \tag{11}$$

where, by the virtue of (8), $\mathbf{Q}_o$ is similarly defined as

$$\mathbf{Q}_o = \begin{bmatrix} \mathbf{E}_{3\times3} & \mathbf{0} \\ -\mathbf{D}_o({}^w_o R\, {}^o\mathbf{d}) & \mathbf{E}_{3\times3} \end{bmatrix}, \quad \mathbf{Q}_o \in \Re^{6\times6}.$$

2.2 Dynamics of Manipulated Object System

We begin by considering the object system in which the common object is rigidly grasped by v robotic arms without environmental (or external) constraints. Under this assumption, the dynamics of manipulated object in frame Σ_w are described as follows:

$$\overline{m}\ddot{\mathbf{r}}_o + \overline{m}\mathbf{g} = \mathbf{f}_o, \tag{12a}$$

$${}^w_o R I_o {}^w_o R^T \dot{\omega}_o + \omega_o \otimes [{}^w_o R I_o {}^w_o R^T \omega_o] = \mathbf{n}_o, \tag{12b}$$

where $\overline{m} \in \Re^+$ and $I_o \in \Re^{3\times3}$ represent the object's mass and inertia matrix, respectively. Note that I_o is constant in Σ_o, regardless of the orientation of the object. However, I_o can be expressed in frame Σ_w by ${}^w_o R$, for overall convenience. $\mathbf{g} = [0 \quad 0 \quad -9.8]^T$ denotes the vector of gravitational acceleration. And the wrenches ($\mathbf{f}_o \in \Re^3$ and $\mathbf{n}_o \in \Re^3$) represent the vectors of the resultant (external) forces applied to the mass center of the object by v manipulators through the contact points, namely,

$$\mathbf{f}_o = \sum_{i=1}^{v} {}^i\mathbf{f}_c, \tag{13a}$$

$$\mathbf{n}_o = \sum_{i=1}^{v} ({}^i\mathbf{n}_c - {}^w_o R\, {}^i\mathbf{d} \otimes {}^i\mathbf{f}_c). \tag{13b}$$

Now, the manipulated object dynamics (12a,b) can be put into compact matrix-vector form as

$$\mathbf{M}_o\dot{\mathbf{v}}_o + \mathbf{C}_o\mathbf{v}_o + \mathbf{G}_o = \mathbf{F}_o, \tag{14}$$

where

$$\dot{\mathbf{v}}_o = [\ddot{\mathbf{r}}_o^T, \dot{\omega}_o^T]^T,$$

$$\mathbf{M}_o = \begin{bmatrix} \overline{m}\mathbf{E}_{3\times3} & \mathbf{0} \\ \mathbf{0} & {}^w_oRI_{oo}{}^wR^T \end{bmatrix}, \quad \mathbf{M}_o \in \Re^{6\times6}$$

$$\mathbf{C}_o = \begin{bmatrix} \mathbf{0} & \mathbf{0} \\ \mathbf{0} & \mathbf{D}(\omega_o){}^w_oRI_{oo}{}^wR^T \end{bmatrix}, \quad \mathbf{C}_o \in \Re^{6\times6}$$

$$\mathbf{G}_o = \begin{bmatrix} \overline{m}\mathbf{g} \\ \mathbf{0} \end{bmatrix}, \quad \mathbf{G}_o \in \Re^6$$

$$\mathbf{F}_o = [\mathbf{f}_o^T, \mathbf{n}_o^T]^T, \quad \mathbf{F}_o \in \Re^6.$$

The dynamic model (14) satisfies the following fundamental properties (see Ammad and Zribi [15] for details).

Property 1: $\mathbf{M}_o$ is a symmetric and positive-definite inertia matrix.

Property 2: $\dot{\mathbf{M}}_o - 2\mathbf{C}_o$ is a skew-symmetric matrix. $\nabla\nabla$

From Eq. (13a,b), the equivalent forces on the object (CM) can be further characterized as

$$\mathbf{F}_o = \sum_{i=1}^{v} \mathbf{Q}_i{}^i\mathbf{F}_e = \mathbf{Q}_s\mathbf{F}_s, \tag{15}$$

with $\mathbf{F}_s = [{}^1\mathbf{F}_e{}^T, \cdots, {}^v\mathbf{F}_e{}^T]^T \in \Re^6 \times \cdots \times \Re^6$. By virtue of the duality between force (wrench) and velocity (twist) (based on the principles of virtual work), one may also determine the wrench (15) by just referring to (9). In this case, the grasp matrix $\mathbf{Q}_s$ is sometimes referred to as the force transmission matrix, which is to identify the contributions of the interaction forces of each manipulator to the external forces on the mass center of the object, and can be determined if the grasp geometry is assigned. In case of frictionless point contacts, the number of constraints imposed on the system by rigid grasping is equal to $m_c\,(= 6v - rk(\mathbf{Q}_s))$. However, other types of contacts may have different dimension of the contact space.

Next, consider the external constraints imposed on the common object by frictionless constraint surfaces (along with the internal constraints by v robotic arms). Let the

constraint surfaces have dimension m (<6), i.e., a set of m rigid hypersurfaces. Then the algebraic equations for the external constraints may be expressed as

$$\phi_f(\mathbf{p}_o) = [\phi_{f1}(\mathbf{p}_o), \cdots, \phi_{fm}(\mathbf{p}_o)]^T = \mathbf{0}_m, \text{ with } \mathbf{p}_o \in SE(3) \tag{16}$$

where $\phi_f(\bullet): C^2\ (\Re^6 \rightarrow \Re^m)$ is differentiable mapping with respect to $\mathbf{p}_o$ and mutually independent functions over any $\mathbf{p}_o$ of interest in a subset of $\Re^6$. The "natural" (or geometric) restrictions given by (16) are commonly called "holonomic" constraints in the literature [8-9]. The corresponding velocity constraints on the surfaces can be obtained by

$$\mathbf{J}_f \mathbf{v}_o = \mathbf{0}, \tag{17}$$

where

$$\mathbf{J}_f = \frac{\partial \phi_f}{\partial \mathbf{p}_o} = [\frac{\partial \phi_{f1}}{\partial \mathbf{p}_o}^T, \cdots, \frac{\partial \phi_{fm}}{\partial \mathbf{p}_o}^T]^T \in \Re^{m\times 6}, \text{ with } \frac{\partial \phi_{fi}}{\partial \mathbf{p}_o}^T \in \Re^6.$$

Since the geometric constraints are mutually independent, $\mathbf{J}_f$ has a full row rank, i.e., $rk(\mathbf{J}_f) = m$. Note that the row vectors of $\mathbf{J}_f$ span the normal space (or normal directions) of the constraint surfaces. If the common object is constrained to follow rigid physical surfaces, the system is also subject to a set of $(6-m)$ "artificial" constraints, namely,

$$\phi_t(\mathbf{p}_o) = [\phi_{t1}(\mathbf{p}_o), \cdots, \phi_{t(6-m)}(\mathbf{p}_o)]^T, \tag{18}$$

where $\phi_t(\bullet): C^2(\Re^6 \rightarrow \Re^{6-m})$ are also mutually independent functions. Evidently, a combined set $\{\phi_{fi}(\mathbf{p}_o), i = 1, \cdots, m; \phi_{tj}(\mathbf{p}_o), j = 1, \cdots, (6-m)\}$ are mutually independent and twice differentiable functions such that the constraint surfaces can be parametrized by

$$\mathbf{p}_c = [\phi_f(\mathbf{p}_o)^T, \phi_t(\mathbf{p}_o)^T]^T \in \Re^6. \tag{19}$$

Then the corresponding velocity relation can be obtained as

$$\mathbf{v}_c = \mathbf{J}_{tf} \mathbf{v}_o, \tag{20}$$

with $\mathbf{J}_{tf} = [\mathbf{J}_f^T, \mathbf{J}_t^T]^T \in \Re^{6\times 6}$. Here, we can define $\mathbf{J}_t \in \Re^{(6-m)\times 6}$, with $rk(J_t) = 6-m$, whose row vectors span the tangent space of the constraint surfaces as

$$\mathbf{J}_t = \frac{\partial \phi_t}{\partial \mathbf{p}_o} = [\frac{\partial \phi_{t1}}{\partial \mathbf{p}_o}^T, \cdots, \frac{\partial \phi_{t(6-m)}}{\partial \mathbf{p}_o}^T]^T, \text{ with } \frac{\partial \phi_{tj}}{\partial \mathbf{p}_o}^T \in \Re^6$$

such that the following relations hold:

$$\mathbf{J}_t \bullet \mathbf{J}_f^T = \mathbf{0} \text{ (or } \mathbf{J}_f \bullet \mathbf{J}_t^T = \mathbf{0}).$$

In this context, it is clear that the column vectors of $\mathbf{J}_f^T$ span the null space of $\mathbf{J}_t$ (i.e., $RS(\mathbf{J}_f^T) \subseteq NS(\mathbf{J}_t)$). As a consequence, the constraint surface frame has a set of vectors

$$\{\frac{\partial \phi_{fi}}{\partial \mathbf{p}_o}^T, i = 1,\cdots,m; \frac{\partial \phi_{tj}}{\partial \mathbf{p}_o}^T, j = 1,\cdots,(6-m)\}$$

as basis. Moreover, it is possible to decompose a given position vector, $\mathbf{p}_c \in \Re^6$, on the constraint frame into two orthogonal subspaces as

$$\Re^6 = RS(\mathbf{J}_f^T) \oplus RS(\mathbf{J}_t^T), \text{ with } RS(\mathbf{J}_f^T) \cap RS(\mathbf{J}_t^T) = \{\mathbf{0}\}.$$

In other words, the $RS(\mathbf{J}_t^T)$ (column space of $\mathbf{J}_t^T$) specifies the motion-controlled subspace, and the $RS(\mathbf{J}_f^T)$ spans the force-controlled subspace. Since the constraint surfaces are assumed to be frictionless, the resultant forces $\mathbf{F}_{oc} \in \Re^6$ at the object center of mass exerted by contact forces λ (normal to the constraint surfaces) can be obtained by

$$\mathbf{F}_{oc} = \mathbf{J}_f^T \lambda, \tag{21}$$

where $\lambda \in \Re^m$ is the vector of Lagrange multipliers (or the constraint forces) associated with m constraint surfaces, and $\mathbf{J}_f^T$ transforms the normal constraint forces λ in frame Σ_c to the mass center of the object. Now, the dynamic model of the manipulated object subject to internal and external constraints may be given as

$$\mathbf{M}_o \dot{\mathbf{v}}_o + \mathbf{C}_o \mathbf{v}_o + \mathbf{G}_o = \mathbf{Q}_s \mathbf{F}_s - \mathbf{J}_f^T \lambda. \tag{22}$$

Note that the vector of constraint forces appears in the dynamics (22). Later, the above equation can be combined with the dynamic model of multiple robot manipulators to formulate the entire system dynamics.

2.3 The Complete Dynamic Model of Constrained Multiple Robot Systems

As stated above, the overall dynamic model of the closed kinematic chains can be obtained by incorporating the kinematic and dynamic constraints (or couplings) into the dynamic equations of multi-manipulators through the common object system.

Using Lagrange's formulation, the dynamic model for ith rigid robot manipulator is described in the joint-space variables as

$$ {}^{i}\mathbf{M}({}^{i}\mathbf{q};\Theta){}^{i}\ddot{\mathbf{q}}+{}^{i}\mathbf{C}({}^{i}\mathbf{q},{}^{i}\dot{\mathbf{q}};\Theta){}^{i}\dot{\mathbf{q}}+{}^{i}\mathbf{G}({}^{i}\mathbf{q};\Theta)+{}^{i}\mathbf{T}_{u}={}^{i}\mathbf{T}-{}^{i}\mathbf{J}^{T}({}^{i}\mathbf{q}){}^{i}\mathbf{F}_{e}, \tag{23} $$

where ${}^{i}\mathbf{q}$, ${}^{i}\dot{\mathbf{q}}$, and ${}^{i}\ddot{\mathbf{q}} \in \Re^{n}$ are the vectors representing the joint position, velocity, and acceleration of the ith robot manipulator, respectively, ${}^{i}\mathbf{M} \in \Re^{n\times n}$ is a inertia matrix, ${}^{i}\mathbf{C} \in \Re^{n\times n}$ is a matrix function containing terms such as Coriolis and centripetal torques, ${}^{i}\mathbf{G} \in \Re^{n}$ is the vector of gravity torques, ${}^{i}\mathbf{T}_{u} \in \Re^{n}$ is the vector of disturbance torques which encompasses all exogenous inputs, i.e., the unstructured uncertainties, $\Theta \in \Re^{k}$ is the vector of system parameters (e.g., link masses, link lengths, moments of inertia), and ${}^{i}\mathbf{T} \in \Re^{n}$ is the joint torque vector. And all other terms have been defined previously.

It is well known that the dynamic equation of an individual manipulator (23) satisfies the following several fundamental properties, which are useful in constructing higher level controllers (see such as those in Ortega and Spong [18]):

Property 1: ${}^{i}\mathbf{M}$ is symmetric, and positive-definite inertia matrix. Furthermore, both ${}^{i}\mathbf{M}$ and ${}^{i}\mathbf{M}^{-1}$ are uniformly bounded above and below as a function of ${}^{i}\mathbf{q}$.

Property 2: ${}^{i}\dot{\mathbf{M}}-2{}^{i}\mathbf{C}$ is skew-symmetric matrix with a proper choice of ${}^{i}\mathbf{C}$. That is, $\mathbf{x}^{T}({}^{i}\dot{\mathbf{M}}-2{}^{i}\mathbf{C})\mathbf{x}=\mathbf{0}$, $\forall \mathbf{x} \in \Re^{n}$.

Property 3: A part of the dynamics (23) is linear in terms of suitably selected set of dynamic parameters, specifically,

$${}^{i}\mathbf{M}({}^{i}\mathbf{q};\Theta)\mathbf{y}+{}^{i}\mathbf{C}({}^{i}\mathbf{q},{}^{i}\dot{\mathbf{q}};\Theta)\mathbf{x}+{}^{i}\mathbf{G}({}^{i}\mathbf{q};\Theta)={}^{i}\mathbf{R}({}^{i}\mathbf{q},{}^{i}\dot{\mathbf{q}},\mathbf{x},\mathbf{y})\Theta,$$

where ${}^{i}\mathbf{R}\in\Re^{n\times k}$ is a regressor matrix which depends on known functions of $({}^{i}\mathbf{q},{}^{i}\dot{\mathbf{q}},\mathbf{x},\mathbf{y})\in\Re^{n}$, and $\Theta\in\Re^{k}$ is the vector of unknown (or known) system parameters. ∇∇

Note also that the choice of the vector of system parameters in the above formulation is not unique.

In a similar manner, the extended joint-space dynamics can be obtained by grouping v such equations and expressed in a concise form as

$$\mathbf{M}_{s}(\mathbf{q}_{s};\Theta)\ddot{\mathbf{q}}_{s}+\mathbf{C}_{s}(\mathbf{q}_{s},\dot{\mathbf{q}}_{s};\Theta)\dot{\mathbf{q}}_{s}+\mathbf{G}_{s}(\mathbf{q}_{s};\Theta)+\mathbf{T}_{us}=\mathbf{T}_{s}-\mathbf{J}_{s}^{T}(\mathbf{q}_{s})\mathbf{F}_{s}, \tag{24}$$

where all terms are compacted into

$$\mathbf{q}_{s}=[{}^{1}\mathbf{q}^{T},\cdots,{}^{v}\mathbf{q}^{T}]^{T},\quad \mathbf{q}_{s}\in\Re^{vn}$$

$$\mathbf{M}_{s}=\textit{Block diag}[{}^{1}\mathbf{M}({}^{1}\mathbf{q}),\cdots,{}^{v}\mathbf{M}({}^{v}\mathbf{q})],\quad \mathbf{M}_{s}\in\Re^{vn\times vn}$$

$$\mathbf{C}_{s}=\textit{Block diag}[{}^{1}\mathbf{C}({}^{1}\mathbf{q},{}^{1}\dot{\mathbf{q}}),\cdots,{}^{v}\mathbf{C}({}^{v}\mathbf{q},{}^{v}\dot{\mathbf{q}})],\quad \mathbf{C}_{s}\in\Re^{vn\times vn}$$

$$\mathbf{G}_{s}=[{}^{1}\mathbf{G}^{T}({}^{1}\mathbf{q}),\cdots,{}^{v}\mathbf{G}^{T}({}^{v}\mathbf{q})]^{T},\quad \mathbf{G}_{s}\in\Re^{vn}$$

$$\mathbf{J}_{s}=\textit{Block diag}[{}^{1}\mathbf{J}({}^{1}\mathbf{q}),\cdots,{}^{v}\mathbf{J}({}^{v}\mathbf{q})],\quad \mathbf{J}_{s}\in\Re^{6v\times vn}$$

$$\mathbf{F}_{s}=[{}^{1}\mathbf{F}_{e}{}^{T},\cdots,{}^{v}\mathbf{F}_{e}{}^{T}]^{T},\quad \mathbf{F}_{s}\in\Re^{6v}$$

$$\mathbf{T}_{us}=[{}^{1}\mathbf{T}_{u}{}^{T},\cdots,{}^{v}\mathbf{T}_{u}{}^{T}]^{T},\quad \mathbf{T}_{us}\in\Re^{vn}$$

$$\mathbf{T}_{s}=[{}^{1}\mathbf{T}^{T},\cdots,{}^{v}\mathbf{T}^{T}]^{T},\quad \mathbf{T}_{s}\in\Re^{vn}$$

In this equation, the physical meanings of all terms have been given previously. Notice that the extended joint-space dynamics (24) also satisfies the fundamental properties, as listed in an individual robot dynamics (23). In the present study, without loss of generality, we will focus our attention only on kinematically non-redundant arms (i.e., $n=6$), although the kinematic redundancies are important to the development of more dexterous robot systems. In what follows, the object dynamics can be transformed into the extended joint-space formulations for overall convenience. Since there are more equations than unknowns (i.e.,

$6 < 6v$, or overdetermined case) in the kinematic equation (9), one can choose six of $6v$ equations to solve $\mathbf{v}_o$ for given $\dot{\mathbf{q}}_s$. Thus the twist vector for the common object in the Cartesian space can be written as

$$\mathbf{v}_o = \mathbf{J}_{sL}\dot{\mathbf{q}}_s, \tag{25}$$

where $\mathbf{J}_{sL} = (\mathbf{Q}_s^T)^+ \mathbf{J}_s$, with $\mathbf{J}_{sL} \in \Re^{6\times 6v}$ and $(\mathbf{Q}_s^T)^+ \in \Re^{6\times 6v}$, and $(\mathbf{Q}_s^T)^+$ denotes pseudoinverse or Moore-Penrose inverse of matrix $\mathbf{Q}_s^T$ [3]. Note that $\mathbf{Q}_s$ has full rank, thus $(\mathbf{Q}_s)^+$ exists and is defined as

$$(\mathbf{Q}_s)^+ = \mathbf{Q}_s^T[\mathbf{Q}_s\mathbf{Q}_s^T]^{-1}, \text{ with } \mathbf{E} = \mathbf{Q}_s(\mathbf{Q}_s)^+$$

such that the matrix $(\mathbf{Q}_s)^+$ defined above satisfies the following four Penroes conditions:

$$\mathbf{Q}_s(\mathbf{Q}_s)^+\mathbf{Q}_s = \mathbf{Q}_s, \quad [(\mathbf{Q}_s)^+\mathbf{Q}_s]^T = (\mathbf{Q}_s)^+\mathbf{Q}_s,$$

$$(\mathbf{Q}_s)^+\mathbf{Q}_s(\mathbf{Q}_s)^+ = (\mathbf{Q}_s)^+, \text{ and } [\mathbf{Q}_s(\mathbf{Q}_s)^+]^T = \mathbf{Q}_s(\mathbf{Q}_s)^+.$$

Furthermore, differentiating (25) with respect to time yields

$$\dot{\mathbf{v}}_o = \dot{\mathbf{J}}_{sL}\dot{\mathbf{q}}_s + \mathbf{J}_{sL}\ddot{\mathbf{q}}_s. \tag{26}$$

Bearing in mind the general form (22), the object dynamics can be put into the following form

$$\mathbf{M}_o\dot{\mathbf{v}}_o + \mathbf{C}_o\mathbf{v}_o + \mathbf{G}_o + \mathbf{J}_f^T\lambda = \mathbf{Q}_s\mathbf{F}_s = \mathbf{F}_{os}, \tag{27}$$

where $\mathbf{F}_{os} \in \Re^6$ represents the vector of total resultant forces on the object system. Let us now illustrate the problem of decomposing the end-effector forces (i.e., dynamic load distribution). For the given resultant forces $\mathbf{F}_{os}$, the general solution of Eq. (27) can be obtained in the form

$$\mathbf{F}_s = (\mathbf{Q}_s)^+\mathbf{F}_{os} + \mathbf{S}\mathbf{f}_{cl}, \tag{28}$$

where $\mathbf{S} \in \Re^{6v\times m_c}$ and $\mathbf{f}_{cl} \in \Re^{m_c}$, with $rk(\mathbf{S}) = m_c$ and $RS(\mathbf{S}) \subset RS(\mathbf{E}_{6v} - (\mathbf{Q}_s)^+\mathbf{Q}_s)$. Since the matrix $\mathbf{S}$ is the orthogonal complement to $\mathbf{Q}_s$, i.e., $\mathbf{Q}_s \bullet \mathbf{S} = \mathbf{0}$, the operator $\mathbf{S}$ projects any arbitrary vector $\mathbf{f}_{cl}$ into the null space of $\mathbf{Q}_s$. Notice also that the choice for $\mathbf{f}_{cl}$ is not unique, however, $\mathbf{S}\mathbf{f}_{cl}$ lies in the null space of $\mathbf{Q}_s$, i.e., $RS(\mathbf{S}) \subset NS(\mathbf{Q}_s)$. Due to the kinematically redundant mapping between the end-effector contact space and the

object space (i.e., $\dim(\mathbf{F}_s) > \dim(\mathbf{F}_{os})$ or underdetermined case), there exist an infinite number of solutions for the end-effector forces to provide $\mathbf{F}_{os}$. In case of cooperative tasks by multiple manipulators, a choice is often made as to an optimal load sharing. In other words, how best the fingertip forces should be distributed to the common object in order to achieve the design objective. Based on this concept, the first term of (28), denoted by $(\mathbf{Q}_s)^+\mathbf{F}_{os}$, is called the minimum (Euclidean) norm solution (or the particular solution) and is an component of $\mathbf{F}_s$ that contributes the motion of object, $\mathbf{F}_{os}$. In other words, these forces are called the "manipulation" forces which cause the common object to physically move. The other term, denoted by $\mathbf{Sf}_{cl}$, is referred to as the null solution (or the homogeneous solution) and is the subspace of the forces $\mathbf{F}_s$ that cause the internal or grasping forces on the object. These internal forces do not affect any motion of object ($\mathbf{F}_{os}$), i.e., the zero net forces at the mass center of the object. As a matter of fact, the manipulation forces and internal forces can be determined by the column spaces and null spaces of $\mathbf{Q}_s$, respectively. Since the null solution does not affect the overall motion of the system, it can be frequently used to optimize some additional criteria of performance, such as dexterous manipulation, singularity and obstacle avoidance. In this study, it should be noted that the significance of the internal forces lies in the fact that it provides the load distribution (or load sharing) of a set of manipulators grasping the object (see, e.g., [2-3]).

To include all contact forces in the dynamic formulation, they should be clearly identified. In what follows, we consider the motion constraints resulting from physical contacts among the components of closed kinematic chains. To begin with, the external constraints between the common object and the rigid constraint surfaces are investigated. The corresponding constraint equation given in (17) now can be expressed in the extended joint-space variables as

$$\mathbf{J}_f\mathbf{J}_{sL}\dot{\mathbf{q}}_s = \mathbf{0}_m. \tag{29}$$

In addition to the above constraints, there exist contact constraints (or internal constraints) among the end-effectors and the common object. Suppose that the constraint equation in the end-effector variables is given by

$$\varphi_f(\mathbf{p}_e) = \mathbf{0}_{m_c}, \text{ with } \mathbf{p}_e \in SE(3) \tag{30}$$

where $\varphi_f(\bullet): C^2(\Re^{6v} \rightarrow \Re^{m_c})$ are $m_c (< 6v)$ mutually independent hypersurfaces and differentiable functions with respect to $\mathbf{p}_e$ and time. Then, the corresponding velocity constraints can be written as

$$\mathbf{S}^T \mathbf{v}_e = \mathbf{S}^T \mathbf{J}_s \dot{\mathbf{q}}_s = \mathbf{0}_{m_c}, \tag{31}$$

where $\mathbf{S}^T = \dfrac{\partial \varphi_f(\mathbf{p}_e)}{\partial \mathbf{p}_e}$. Now, combining Eqs. (29) and (31) yields the total velocity constraints as

$$\mathbf{J}_{fl} \dot{\mathbf{q}}_s = \mathbf{0}, \tag{32}$$

where $\mathbf{J}_{fl} = \begin{bmatrix} \mathbf{S}^T \mathbf{J}_s \\ \mathbf{J}_f \mathbf{J}_{sL} \end{bmatrix} \in \Re^{l \times 6v}$, and $l (= m + m_c)$ is the number of total contact constraints, namely, the dimension of force-controlled subspaces. Thus, the constraint Jacobian matrix $\mathbf{J}_{fl}$ with a full rank projects the joint-space velocities into the normal directions of a set of hypersurfaces, $\varphi_f(\mathbf{p}_e) = \mathbf{0}$ and $\phi_f(\mathbf{p}_o) = \mathbf{0}$, respectively. Based on the above observations, the vector of the generalized contact forces (the internal grasping forces and the constraint forces) being required to control can be defined as

$$\mathbf{F}_{cl} = \begin{bmatrix} \mathbf{f}_{cl} \\ \lambda \end{bmatrix} \in \Re^l, \tag{33}$$

and the corresponding contact forces can be expressed in the joint-space as

$$\mathbf{T}_{cl} = \mathbf{J}_{fl}{}^T \mathbf{F}_{cl}. \tag{34}$$

Note that the number of degrees of freedom (DOF's) lost in motion due to the closed kinematic chains equals to the number of the contact forces (the internal forces and the constraint forces) exerted on the object, that is, m_c constraint conditions from the contacts

between v robots and object, and m constraints from the contact between the object and the external surfaces.

Now, the kinematic and the dynamic constraints are combined with the extended manipulator dynamics through the common object to form the entire mathematical model of the system. To do this, introducing (25) through (27) into (28) and substituting the resulting equation into (24) yields

$$\mathbf{M}_s\ddot{\mathbf{q}}_s + \mathbf{C}_s\dot{\mathbf{q}}_s + \mathbf{G}_s + \mathbf{J}_s^T\{(\mathbf{Q}_s)^+[\mathbf{M}_o\dot{\mathbf{v}}_o + \mathbf{C}_o\mathbf{v}_o + \mathbf{G}_o + \mathbf{J}_f^T\lambda] + \mathbf{Sf}_{cl}\} + \mathbf{T}_{us} = \mathbf{T}_s.$$

After some algebraic manipulations using $\mathbf{J}_s^T(\mathbf{Q}_s)^+ = \mathbf{J}_{sL}^T$, one obtains

$$(\mathbf{M}_s + \mathbf{J}_{sL}^T\mathbf{M}_o\mathbf{J}_{sL})\ddot{\mathbf{q}}_s + \{\mathbf{C}_s + \mathbf{J}_{sL}^T\mathbf{M}_o\dot{\mathbf{J}}_{sL} + \mathbf{J}_{sL}^T\mathbf{C}_o\mathbf{J}_{sL}\}\dot{\mathbf{q}}_s + \mathbf{G}_s + \mathbf{J}_{sL}^T\mathbf{G}_o + \mathbf{J}_{sL}^T\mathbf{J}_f^T\lambda + \mathbf{J}_s^T\mathbf{Sf}_{cl} + \mathbf{T}_{us} = \mathbf{T}_s$$

which, by using (32) and (33), can be abbreviated in a concise form as

$$\mathbf{M}_u\ddot{\mathbf{q}}_s + \mathbf{C}_u\dot{\mathbf{q}}_s + \mathbf{G}_u + \mathbf{T}_{us} = \mathbf{T}_s - \mathbf{J}_{fl}^T\mathbf{F}_{cl}, \tag{35}$$

where the effective quantities in the extended joint-space are given as

$$\mathbf{M}_u = \mathbf{M}_s + \mathbf{J}_{sL}^T\mathbf{M}_o\mathbf{J}_{sL}, \quad \mathbf{M}_u \in \Re^{6v\times 6v}$$

$$\mathbf{C}_u = \mathbf{C}_s + \mathbf{J}_{sL}^T\mathbf{M}_o\dot{\mathbf{J}}_{sL} + \mathbf{J}_{sL}^T\mathbf{C}_o\mathbf{J}_{sL}, \quad \mathbf{C}_u \in \Re^{6v\times 6v}$$

$$\mathbf{G}_u = \mathbf{G}_s + \mathbf{J}_{sL}^T\mathbf{G}_o, \quad \mathbf{G}_u \in \Re^{6v}$$

Consequently, the equation (35) represents the complete dynamic model of multiple robot systems coupled with the object dynamics and the contact constraints, which is a similar form to a single robot system (23). All fundamental properties stated in Eq. (23) are also preserved by this transformation. Note particularly that $\dot{\mathbf{M}}_u - 2\mathbf{C}_u$ is a skew-symmetric matrix, as shown in the following.

Property 3: $\dot{\mathbf{M}}_u - 2\mathbf{C}_u$ is a skew-symmetric matrix, that is, $\mathbf{x}^T(\dot{\mathbf{M}}_u - 2\mathbf{C}_u)\mathbf{x} = \mathbf{0}$, $\forall \mathbf{x} \in \Re^{6v}$.

Proof: Let $\mathbf{N}_u = \dfrac{d}{dt}(\mathbf{M}_u) - 2\mathbf{C}_u$, then

$$\mathbf{x}^T\mathbf{N}_u\mathbf{x} = \mathbf{x}^T\{\dot{\mathbf{M}}_s + 2\mathbf{J}_{sL}^T\mathbf{M}_o\dot{\mathbf{J}}_{sL} + \mathbf{J}_{sL}^T\dot{\mathbf{M}}_o\mathbf{J}_{sL} - 2(\mathbf{C}_s + \mathbf{J}_{sL}^T\mathbf{M}_o\dot{\mathbf{J}}_{sL} + \mathbf{J}_{sL}^T\mathbf{C}_o\mathbf{J}_{sL})\}\mathbf{x}$$

$$= \mathbf{x}^T(\dot{\mathbf{M}}_s - 2\mathbf{C}_s)\mathbf{x} + \mathbf{y}^T(\dot{\mathbf{M}}_o - 2\mathbf{C}_o)\mathbf{y}, \ \forall \ \mathbf{x} \text{ and } \mathbf{y} = \mathbf{J}_{sL}\mathbf{x}$$

where $(\dot{\mathbf{M}}_s - 2\mathbf{C}_s)$ and $(\dot{\mathbf{M}}_o - 2\mathbf{C}_o)$ are both skew-symmetric matrices, hence, $(\dot{\mathbf{M}}_u - 2\mathbf{C}_u)$ is also skew-symmetric matrix. $\nabla\nabla$

Unfortunately, there exist the coupled relationships among the position variables and the contact force variables in Eq. (35), furthermore, some variables are no longer independent due to internal and external constraints imposed on the system. Due to the above observations, the dynamic model (35) (DAEs) may not be a suitable form for dynamic analysis and hybrid controller design purposes. In what follows, we will derive an appropriate form of the overall system dynamics in which the position- and force-controlled subsystems can be easily decoupled. Based on this consideration, we introduce a new generalized coordinate system (Σ_c) such that

$$\mathbf{x}_c = [\mathbf{x}_f{}^T, \ \mathbf{x}_t{}^T]^T \in \Re^{6v} \tag{36}$$

which is completely parameterized by the position variables, $\mathbf{x}_f = [\varphi_f(\mathbf{p}_e)^T, \phi_f(\mathbf{p}_o)^T]^T$ and $\mathbf{x}_t = \phi_t(\mathbf{p}_o)$. Here, $\mathbf{x}_f \in \Re^l$ and $\mathbf{x}_t \in \Re^{(6-m)}$ are the vectors of the position variables in the constrained and unconstrained directions, respectively [17]. Since the contact surfaces are infinitely rigid, then $\mathbf{x}_f = \mathbf{0}_l$ (algebraic holonomic constraints), or equivalently,

$$\varphi_f(\mathbf{p}_e) = \mathbf{0}_{m_c} \text{ and } \phi_f(\mathbf{p}_o) = \mathbf{0}_m.$$

Differentiating (36) with respect to time yields

$$\dot{\mathbf{x}}_c = [\dot{\mathbf{x}}_f{}^T, \ \dot{\mathbf{x}}_t{}^T]^T = [\mathbf{J}_{fl}{}^T, \ \mathbf{J}_{\phi p}{}^T]^T \dot{\mathbf{q}}_s = \mathbf{J}_c \dot{\mathbf{q}}_s, \ \mathbf{J}_c \in \Re^{6v \times 6v} \tag{37}$$

where

$$\dot{\mathbf{x}}_f = \begin{bmatrix} \mathbf{S}^T\mathbf{J}_s \\ \mathbf{J}_f\mathbf{J}_{sL} \end{bmatrix} \dot{\mathbf{q}}_s = \mathbf{J}_{fl}\dot{\mathbf{q}}_s, \ \mathbf{J}_{fl} \in \Re^{l \times 6v}$$

$$\dot{\mathbf{x}}_t = \mathbf{J}_t\mathbf{v}_o = \mathbf{J}_{\phi p}\dot{\mathbf{q}}_s, \ \mathbf{J}_{\phi p} = \mathbf{J}_t\mathbf{J}_{sL} \in \Re^{(6-m)\times 6v}.$$

In the above equations, the Jacobian matrices $\mathbf{J}_{fl}$ and $\mathbf{J}_{\phi p}$ represent the force-controlled directions (or the normal subspace) and position-controlled directions (or the tangential

subspace), respectively, and have full rank, i.e., $rk(\mathbf{J}_{fl}) = l$ and $rk(\mathbf{J}_{\phi p}) = 6 - m$. Thus the following relation holds:

$$\mathbf{J}_{\phi p} \bullet \mathbf{J}_{fl}{}^{T} = \mathbf{0} \text{ (or } \mathbf{J}_{fl} \bullet \mathbf{J}_{\phi p}{}^{T} = \mathbf{0}),$$

which implies that $\mathbf{J}_{fl}$ is an orthogonal complement to $\mathbf{J}_{\phi p}$ in the $6v$-dimensional space (meaning $RS(\mathbf{J}_{fl}{}^{T}) \subseteq NS(\mathbf{J}_{\phi p})$). Using the above relation, we also have the basic decomposition of $\Re^{6v}$ into two orthogonal subspaces in the sense that

$$\Re^{6v} = RS(\mathbf{J}_{fl}{}^{T}) \oplus RS(\mathbf{J}_{\phi p}{}^{T}), \text{ with } RS(\mathbf{J}_{fl}{}^{T}) \cap RS(\mathbf{J}_{\phi p}{}^{T}) = \{\mathbf{0}\},$$

from which a new basis is formed in the $6v$-dimensional space as shown previously. It has to be noticed that in case of constrained motions among the components of closed-chain mechanisms, some variables cannot be arbitrary in motions but satisfy the following constraint manifold

$$\overline{M}_f =: \{\mathbf{x}_f = \mathbf{0}_l,\ \dot{\mathbf{x}}_f = \mathbf{0}_l\}.$$

As we shall see, this condition leads to the dimension reduction of the system. Since there exist l contact constraints, then the overall system has total $(6-m)$ DOF of the motion. For the further development, we introduce a partitioned identity matrix as

$$\mathbf{E} = [\mathbf{E}_f \vdots \mathbf{E}_t] \in \Re^{6v \times 6v},$$

where $\mathbf{E}_f = [\mathbf{E}_l{}^{T},\ \mathbf{0}^{T}]^{T} \in \Re^{6v \times l}$ and $\mathbf{E}_t = [\mathbf{0}^{T},\ \mathbf{E}_{(6-m)}{}^{T}]^{T} \in \Re^{6v \times (6-m)}$. From (37), some joint-space variables are given below

$$\dot{\mathbf{q}}_s = \mathbf{J}_c{}^{-1}\dot{\mathbf{x}}_c, \tag{38a}$$

$$\ddot{\mathbf{q}}_s = \dot{\mathbf{J}}_c{}^{-1}\dot{\mathbf{x}}_c + \mathbf{J}_c{}^{-1}\ddot{\mathbf{x}}_c. \tag{38b}$$

Substituting (38a,b)) into (35) gives

$$\mathbf{M}_u(\dot{\mathbf{J}}_c{}^{-1}\dot{\mathbf{x}}_c + \mathbf{J}_c{}^{-1}\ddot{\mathbf{x}}_c) + \mathbf{C}_u\mathbf{J}_c{}^{-1}\dot{\mathbf{x}}_c + \mathbf{G}_u + \mathbf{T}_{us} = \mathbf{T}_s - \mathbf{J}_{fl}{}^{T}\mathbf{F}_{cl}.$$

By multiplying $\mathbf{J}_c{}^{-T}$ on the both sides of the above equation and using the following identity

$$\mathbf{J}_c{}^{-T}\mathbf{J}_{fl}{}^{T} = [\mathbf{J}_{fl}{}^{T}, \mathbf{J}_{\phi p}{}^{T}]^{-1}\mathbf{J}_{fl}{}^{T} = [\mathbf{E}_l{}^{T}, \mathbf{0}^{T}]^{T},$$

the complete dynamics of the constrained multiple robot system with closed chain mechanisms can be expressed as

$$\mathbf{M}_c(\mathbf{x}_c;\Theta)\ddot{\mathbf{x}}_c + \mathbf{C}_c(\mathbf{x}_c,\dot{\mathbf{x}}_c;\Theta)\dot{\mathbf{x}}_c + \mathbf{G}_c(\mathbf{x}_c;\Theta) + \mathbf{T}_{uc} = \mathbf{T}_{cs} - \mathbf{E}_f\mathbf{F}_{cl} \tag{39a}$$

$$\mathbf{x}_f = \mathbf{0}, \tag{39b}$$

where

$$\mathbf{x}_c = [\mathbf{0}^T, \mathbf{x}_t^T]^T$$
$$\mathbf{M}_c = \mathbf{J}_c^{-T}\mathbf{M}_u\mathbf{J}_c^{-1}$$
$$\mathbf{C}_c = \mathbf{J}_c^{-T}\mathbf{M}_u\dot{\mathbf{J}}_c^{-1} + \mathbf{J}_c^{-T}\mathbf{C}_u\mathbf{J}_c^{-1}$$
$$\mathbf{G}_c = \mathbf{J}_c^{-T}\mathbf{G}_u$$
$$\mathbf{T}_{uc} = \mathbf{J}_c^{-T}\mathbf{T}_{us}$$
$$\mathbf{T}_{cs} = \mathbf{J}_c^{-T}\mathbf{T}_s$$
$$\mathbf{E}_f = [\mathbf{E}_t^T, \mathbf{0}^T]^T$$

In this formulation, all terms have the corresponding meanings as in (23). Finally, we have derived the dynamic model for the entire system in terms of the generalized coordinate system ($\mathbf{x}_c$). Since $\mathbf{x}_f = \mathbf{0}$, in the transformed frame, the motion of entire system is actually governed by the independent variables $\mathbf{x}_t$. As noted earlier, the position- and force-controlled subspaces can be easily separated (or decoupled) in this formulation. That is, the dynamic model can be decomposed into two orthogonal subsystems:

$$\mathbf{E}_t^T\mathbf{T}_{cs} = \mathbf{E}_t^T\mathbf{M}_c\mathbf{E}_t\ddot{\mathbf{x}}_t + \mathbf{E}_t^T\mathbf{C}_c\mathbf{E}_t\dot{\mathbf{x}}_t + \mathbf{E}_t^T\mathbf{G}_c + \mathbf{E}_t^T\mathbf{T}_{uc}, \tag{40a}$$

$$\mathbf{E}_f^T\mathbf{T}_{cs} = \mathbf{E}_f^T\mathbf{M}_c\mathbf{E}_t\ddot{\mathbf{x}}_t + \mathbf{E}_f^T\mathbf{C}_c\mathbf{E}_t\dot{\mathbf{x}}_t + \mathbf{E}_f^T\mathbf{G}_c + \mathbf{E}_f^T\mathbf{T}_{uc} + \mathbf{F}_{cl}. \tag{40b}$$

Consequently, the first subsystem constitutes the reduced-order equations of motion which contain no generalized contact forces (i.e., purely kinetic differential equations), while the other subsystem is used to regulate the contact forces. In fact, this formulation is now a convenient form for the subsequent controller designs. Assuming that the robotic systems are equipped with joint position and velocity sensors as well as the contact force sensors at each end-effector (e.g., a wrist force sensor), the control synthesis is to provide a set of the joint torques such that the common object tracks the specified "desired" trajectory while

maintaining the desired contact forces (the internal and the constraint forces) among the components of the closed kinematic structures.

It is worth realizing that the dynamic model (39a,b) or equivalently (40a,b) satisfy the following fundamental properties, as listed in the joint space dynamics (23).

Property 1: $\mathbf{M}_c$ is symmetric and positive-definite inertia matrix, namely, $\mathbf{M}_c = \mathbf{M}_c^T > \mathbf{0}$, and furthermore, $\underline{\rho} \le \|\mathbf{M}_c\| \le \bar{\rho}, \quad \forall \mathbf{x}_c \in \Re^{6v}$, where $\underline{\rho}(>0)$ and $\bar{\rho}(<\infty)$ are some positive constants.

Property 2: If $\mathbf{C}_c$ is properly chosen, then $\dot{\mathbf{M}}_c - 2\mathbf{C}_c$ is a skew-symmetric matrix, which implies that $\mathbf{x}^T(\dot{\mathbf{M}}_c - 2\mathbf{C}_c)\mathbf{x} = 0, \ \mathbf{x} \in \Re^{6v}$.

Proof: It is straightforward to verify that $\dot{\mathbf{M}}_c - 2\mathbf{C}_c$ is skew-symmetric matrix. Let $\mathbf{N}_c = \frac{d}{dt}(\mathbf{M}_c) - 2\mathbf{C}_c$, then

$$
\begin{aligned}
&\mathbf{x}^T\mathbf{N}_c\mathbf{x} \\
&= \mathbf{x}^T[2\mathbf{J}_c^{-T}\mathbf{M}_u\dot{\mathbf{J}}_c^{-1} + \mathbf{J}_c^{-T}\dot{\mathbf{M}}_u\mathbf{J}_c^{-1} - 2(\mathbf{J}_c^{-T}\mathbf{M}_u\dot{\mathbf{J}}_c^{-1} + \mathbf{J}_c^{-T}\mathbf{C}_u\mathbf{J}_c^{-1})]\mathbf{x} \\
&= \mathbf{x}^T\mathbf{J}_c^{-T}(\dot{\mathbf{M}}_u - 2\mathbf{C}_u)\mathbf{J}_c^{-1}\mathbf{x} \\
&= \mathbf{y}^T(\dot{\mathbf{M}}_u - 2\mathbf{C}_u)\mathbf{y}, \ \forall \ \mathbf{y} = \mathbf{J}_c^{-1}\mathbf{x}.
\end{aligned}
$$

Since $(\dot{\mathbf{M}}_u - 2\mathbf{C}_u)$ is skew-symmetric, $(\dot{\mathbf{M}}_c - 2\mathbf{C}_c)$ is indeed skew-symmetric.

Property 3: A part of the dynamics (39a,b) is still linear in terms of suitably selected set of dynamic parameters, that is,

$$\mathbf{M}_c(\mathbf{x}_c;\Theta)\mathbf{z} + \mathbf{C}_c(\mathbf{x}_c, \dot{\mathbf{x}}_c;\Theta)\mathbf{y} + \mathbf{G}_c(\mathbf{x}_c;\Theta) = \mathbf{R}(\mathbf{x}_c, \dot{\mathbf{x}}_c, \mathbf{y}, \mathbf{z})\Theta,$$

where $\mathbf{y} \in \Re^{6v}$, $\mathbf{z} \in \Re^{6v}$, $\mathbf{R} \in \Re^{6v \times k}$, and $\Theta \in \Re^k$. $\nabla\nabla$

A class of hybrid controllers are proposed next.

3. DESIGN OF CONTROL ALGORITHMS

In this section, based on the dynamic model (39a,b), a class of hybrid controllers for multiple robot systems are designed. As mentioned earlier, the control objective is to provide a set of joint torques for each robot to manipulate the common object so that the grasped object traces the constrained surfaces with appropriate contact forces. Notice that the position control of the object should be done in the unconstrained directions (namely, the tangential subspace), while the force control should be maintained in the constrained directions (namely, the normal subspace). As will be shown in the following subsections, two types of hybrid position/force controllers will be introduced, i.e., a modified computed torque control and a robust adaptive controller. A class of controllers are given in $\mathbf{T}_{cs}$, then the joint torques can be calculated as $\mathbf{T}_s = \mathbf{J}_c^T \mathbf{T}_{cs}$.

3.1 A Modified Computed Torque Method

Following the inverse dynamics approach for a single manipulator, a modified computed torque method is proposed for dynamic coordination control of multiple robot arms.

Before a controller design, a number of tracking errors are introduced as follows. The vector of motion tracking errors is given as

$$\mathbf{e}_c = \mathbf{x}_c - \mathbf{x}_{cd} = [\mathbf{0}^T,\ \mathbf{e}_t^T]^T, \text{ with } \mathbf{e}_t = \mathbf{x}_t - \mathbf{x}_{td},$$

where $\mathbf{x}_{cd} \in \Re^{6v}$ (or $\mathbf{x}_{td} \in \Re^{(6-m)}$) is the vector of desired position trajectories for the object to follow, while the contact force tracking errors are defined as

$$\mathbf{e}_f = \mathbf{F}_{cl} - \mathbf{F}_{cld},$$

$$\mathbf{e}_F = \int_0^t \mathbf{e}_f(\tau) d\tau,$$

where $\mathbf{F}_{cld} = [\mathbf{f}_{cld}{}^T, \lambda_d{}^T]^T \in \Re^l$ is the vector of the desired contact forces (the derived internal forces and constraint forces). Note that $\mathbf{f}_{cld}$ lies in the null space of $\mathbf{Q}_s$ at all times. With complete knowledge of the system dynamics along with $\mathbf{T}_{uc} = \mathbf{0}$ in Eq. (40), the following control law can be utilized:

$$\mathbf{T}_{cs} = \mathbf{M}_c(\ddot{\mathbf{x}}_{cd} - \mathbf{k}_v\dot{\mathbf{e}}_c - \mathbf{k}_p\mathbf{e}_c) + \mathbf{C}_c\dot{\mathbf{x}}_c + \mathbf{G}_c + \mathbf{E}_f(\mathbf{F}_{cld} - \mathbf{k}_f\mathbf{e}_F), \tag{41}$$

where $\mathbf{k}_v \in \Re^{6v\times 6v}$, $\mathbf{k}_p \in \Re^{6v\times 6v}$, and $\mathbf{k}_f \in \Re^{l\times l}$ are all positive-definite feedback gain matrices. Note that the integral force feedback is used in this algorithm. Now, the tracking properties of the corresponding closed-loop system are given in the following theorem.

Theorem 1: Consider the system dynamics (39a,b) without system uncertainties (i.e., with full knowledge of the robot dynamic parameters and $\mathbf{T}_{uc} = \mathbf{0}$). Then the closed-loop system with control law (41) is globally asymptotically stable, that is,

$$\mathbf{x}_t \to \mathbf{x}_{td},\ \lambda \to \lambda_d, \text{ and } \mathbf{f}_{cl} \to \mathbf{f}_{cld} \text{ as } t \to \infty.$$

Proof: With control law (41), the closed-loop error dynamics can be expressed as

$$\mathbf{M}_c(\ddot{\mathbf{e}}_c + \mathbf{k}_v\dot{\mathbf{e}}_c + \mathbf{k}_p\mathbf{e}_c) = -\mathbf{E}_f(\mathbf{e}_f + \mathbf{k}_f\mathbf{e}_F). \tag{42}$$

To eliminate the contact force tracking terms, multiplying by $\mathbf{E}_t{}^T$ on both sides of equation (42) yields a pure position error subsystem as

$$\mathbf{E}_t{}^T\mathbf{M}_c(\ddot{\mathbf{e}}_c + \mathbf{k}_v\dot{\mathbf{e}}_c + \mathbf{k}_p\mathbf{e}_c) = \mathbf{0}.$$

It follows that

$$\mathbf{E}_t{}^T\mathbf{M}_c\mathbf{E}_t(\ddot{\mathbf{e}}_t + \bar{\mathbf{k}}_v\dot{\mathbf{e}}_t + \bar{\mathbf{k}}_p\mathbf{e}_t) = \mathbf{0},$$

where the feedback gain matrices are defined as

$$\mathbf{k}_v = \mathbf{E}_t\bar{\mathbf{k}}_v\mathbf{E}_t{}^T, \quad \bar{\mathbf{k}}_v \in \Re^{(6-m)\times(6-m)}$$

$$\mathbf{k}_p = \mathbf{E}_t\bar{\mathbf{k}}_p\mathbf{E}_t{}^T, \quad \bar{\mathbf{k}}_p \in \Re^{(6-m)\times(6-m)}$$

Since $\mathbf{E}_t{}^T\mathbf{M}_c\mathbf{E}_t$ is a positive-definite matrix, the linearized position error dynamics is expressed as

$$\ddot{\mathbf{e}}_t + \bar{\mathbf{k}}_v\dot{\mathbf{e}}_t + \bar{\mathbf{k}}_p\mathbf{e}_t = \mathbf{0}, \tag{43}$$

which is a Hurwitz. Hence, with proper choice of feedback gain matrices $\bar{\mathbf{k}}_v$ and $\bar{\mathbf{k}}_p$ (i.e., positive-definite matrices), the position tracking errors converge to zero, that is,

$$\mathbf{e}_t \text{ (or } \mathbf{e}_c) \rightarrow \mathbf{0} \text{ as } t \rightarrow \infty.$$

From (42) and (43), we can also obtain the force error subsystem as

$$\mathbf{E}_f(\mathbf{e}_f + \mathbf{k}_f \mathbf{e}_F) = \mathbf{0}.$$

Premultiply the above equation by $\mathbf{E}_f^T$ to obtain

$$\mathbf{e}_f + \mathbf{k}_f \mathbf{e}_F = \mathbf{0}. \tag{44}$$

By choosing a gain matrix $\mathbf{k}_f$ appropriately, the contact force errors also converge to zero, that is,

$$\mathbf{e}_f \rightarrow \mathbf{0} \text{ as } t \rightarrow \infty.$$

Since the rates of convergence of all tracking errors are determined by the choices of the control gain matrices, the gains can be chosen such that they satisfy some design criteria (or performance requirements).

As consequence, the global asymptotic trackings of both the object positions and the contact forces are achieved simultaneously by the proposed control law.

3.2 A Robust Hybrid Adaptive Control

In general, the system dynamics is considered to have some parametric uncertainties and external disturbances, thus it is necessary to design a robust control algorithm in order to compensate for their effects.

To formulate the adaptive control law, some tracking variables are introduced as follows. The "reference" tracking errors, $\dot{\mathbf{x}}_{cr}$, are defined as

$$\dot{\mathbf{x}}_{cr} = [\dot{\mathbf{x}}_{fr}^T, \ \dot{\mathbf{x}}_{tr}^T],$$

with $\dot{\mathbf{x}}_{fr} = \mathbf{0}$ and $\dot{\mathbf{x}}_{tr} = \dot{\mathbf{x}}_{td} - \mathbf{k}_a \mathbf{e}_t$, where $\mathbf{k}_a \in \Re^{(6-m)\times(6-m)}$ is selected as a positive-definite and diagonal matrix. The sliding variable vector, $\mathbf{x}_{cs}$, is defined as

$$\mathbf{x}_{cs} = \dot{\mathbf{x}}_c - \dot{\mathbf{x}}_{cr} = [\mathbf{x}_{fs}^T,\ \mathbf{x}_{ts}^T]^T,$$

with $\mathbf{x}_{fs} = \mathbf{0}$ and $\mathbf{x}_{ts} = \dot{\mathbf{e}}_t + \mathbf{k}_a \mathbf{e}_t$. Let $\tilde{\Theta}(t) = \hat{\Theta}(t) - \Theta$ be the error vector of the system parameter estimates, where $\hat{\Theta}(t)$ denotes the current estimated values of the parameter vector Θ. In this study, the circumflex $(\hat{\bullet})$ represents the estimated value of $(\bullet)$ provided by the adaptation law, and the notation $(\tilde{\bullet})$ refers to $(\tilde{\bullet}) = (\hat{\bullet}) - (\bullet)$. By recalling Property 3 (i.e., linear parametrization) in equation (39a,b), the following functions can be defined

$$\mathbf{M}_c(\mathbf{x}_c;\Theta)\ddot{\mathbf{x}}_{cr} + \mathbf{C}_c(\mathbf{x}_c,\dot{\mathbf{x}}_c;\Theta)\dot{\mathbf{x}}_{cr} + \mathbf{G}_c(\mathbf{x}_c;\Theta) = \mathbf{R}_r(\mathbf{x}_c,\dot{\mathbf{x}}_c,\dot{\mathbf{x}}_{cr},\ddot{\mathbf{x}}_{cr})\Theta, \tag{45a}$$

$$\hat{\mathbf{M}}_c(\mathbf{x}_c;\hat{\Theta})\ddot{\mathbf{x}}_{cr} + \hat{\mathbf{C}}_c(\mathbf{x}_c,\dot{\mathbf{x}}_c;\hat{\Theta})\dot{\mathbf{x}}_{cr} + \hat{\mathbf{G}}_c(\mathbf{x}_c;\hat{\Theta}) = \mathbf{R}_r(\mathbf{x}_c,\dot{\mathbf{x}}_c,\dot{\mathbf{x}}_{cr},\ddot{\mathbf{x}}_{cr})\hat{\Theta}, \tag{45b}$$

where $\mathbf{R}_r \in R^{6v\times k}$ is a known regressor matrix, and the vector of exact dynamic parameters, $\Theta \in R^k$, is assumed to be unknown but constant in this study. Note that the regressor matrix $\mathbf{R}_r$ is not a function of the acceleration $\ddot{\mathbf{x}}_t (or\ \ddot{\mathbf{x}}_c)$. For the purpose of stability analysis, it is assumed that the unstructured uncertainties (or the external disturbances in this study), $\mathbf{T}_{us}$ in Eq. (24), are bounded by

$$\|\mathbf{T}_{us}\| \le d_u, \tag{46}$$

where $d_u (< \infty)$ is a positive constant. Since $\mathbf{J}_c^{-1}$ is a nonsingular matrix and uniformly bounded by $\|\mathbf{J}_c^{-1}\| \le d_J\ (< \infty)$, for all possible values of its arguments, there also exists a positive constant d_m such that

$$\|\mathbf{T}_{uc}\| = \|\mathbf{J}_c^{-1}\mathbf{T}_{us}\| \le \|\mathbf{J}_c^{-1}\|\|\mathbf{T}_{us}\| \le d_m,$$

where $d_m = d_u d_J < \infty$.

To cope with the system uncertainties, a hybrid adaptive control law, which determines the position/force control inputs, is now given by

$$\mathbf{T}_{cs} = \mathbf{R}_r(\mathbf{x}_c,\dot{\mathbf{x}}_c,\dot{\mathbf{x}}_{cr},\ddot{\mathbf{x}}_{cr})\hat{\Theta} - \mathbf{k}\mathbf{x}_{cs} + \mathbf{E}_f(\mathbf{F}_{cld} - \mathbf{k}_f\mathbf{e}_F), \tag{47}$$

where $\mathbf{k}$ and $\mathbf{k}_f$ are positive-definite gain matrices with appropriate dimensions. In this algorithm, the position and contact force control loops can be mutually decoupled, and rewritten in two subsystems. The adaptation law to adjust the parameter vector Θ is then chosen as

$$\dot{\hat{\Theta}} = -\Gamma^{-1}(\mathbf{R}_r{}^T \mathbf{x}_{cs} + \sigma\hat{\Theta}), \tag{48}$$

where $\Gamma = \Gamma^T$ $(> \mathbf{0})$ is an adaptation gain matrix and $\sigma \geq 0$. In this algorithm, the term σ referred to as the "leakage", is introduced to achieve the robustness of adaptive law in the presence of uncertainties (see [19] for details) and given by

$$\sigma = \begin{cases} 0 & , \|\hat{\Theta}\| \leq \Theta_0 \\ \sigma_0[\dfrac{\|\hat{\Theta}\|}{\Theta_0} - 1] & , \Theta_0 \leq \|\hat{\Theta}\| \leq 2\Theta_0 \\ \sigma_0 & , \|\hat{\Theta}\| \geq 2\Theta_0 \end{cases} \tag{49}$$

where $\sigma_0 (> 0)$ and $\Theta_0 > \|\Theta\|$ are some design parameters.

After substituting the control law (47) with adaptation law (48) into Eq. (39a,b) and subtracting (45a) on the both sides of the resulting equation, the closed-loop error dynamics is obtained as

$$\mathbf{M}_c \dot{\mathbf{x}}_{cs} = -\mathbf{C}_c \mathbf{x}_{cs} + \mathbf{R}_r \tilde{\Theta} - \mathbf{k}\mathbf{x}_{cs} - \mathbf{E}_f(\mathbf{e}_f + \mathbf{k}_f \mathbf{e}_F) - \mathbf{T}_{uc} \tag{50}$$

Now, the stability and robustness issues of the closed-loop system are analyzed in the following.

Theorem 2: Consider the control law (47) with the adaptation law (48) for the constrained multiple robot systems (39a,b), provided that all desired trajectories $(\mathbf{x}_{td}, \dot{\mathbf{x}}_{td}, \ddot{\mathbf{x}}_{td}, \lambda_d)$ are continuous and bounded functions. Then the closed-loop system (50) is globally stable in the sense that the system state variables $(\mathbf{x}_t, \dot{\mathbf{x}}_t, \lambda, \Theta)$ are uniformly ultimately bounded after finite time, that is, the corresponding tracking errors converge to the following compact set

$$\Delta_f = \{ \mathbf{x}_{ts} \in \Re^{(6-m)} : \|\mathbf{x}_{ts}\| \le \frac{d_m}{\rho_{\max}(\mathbf{k})} \}$$

Proof: To establish the global boundedness and stability properties of the closed-loop system, consider a Lyapunov function candidate, $V(\bullet): \Re^+ \times \Re^{6v+k} \rightarrow \Re^+$, as

$$V = \frac{1}{2} \bar{\mathbf{z}}^T Q \bar{\mathbf{z}}, \tag{51}$$

where $\bar{\mathbf{z}}^T = [\mathbf{x}_{cs}^T, \tilde{\Theta}^T]$ and $Q = Block\ diag[\mathbf{M}_c, \Gamma]$. By using Rayleigh's principle, an upper and lower bound on V can be estimated as

$$\frac{1}{2}\rho_{\min}(Q)\|\bar{\mathbf{z}}\|^2 \le V \le \frac{1}{2}\rho_{\max}(Q)\|\bar{\mathbf{z}}\|^2.$$

Since $\rho_{\min}(Q) > 0$, the function V is positive-definite. Differentiation of V with respect to time along Eq. (50) leads to

$$\begin{aligned} \dot{V} &= \mathbf{x}_{cs}^T[-\mathbf{C}_c\mathbf{x}_{cs} + \mathbf{R}_r\tilde{\Theta} - \mathbf{k}\mathbf{x}_{cs} - \mathbf{E}_f(\mathbf{e}_f + \mathbf{k}_f\mathbf{e}_F) - \mathbf{T}_{uc}] \\ &\quad + \frac{1}{2}\mathbf{x}_{cs}^T\dot{\mathbf{M}}_c\mathbf{x}_{cs} + \tilde{\Theta}^T\Gamma\dot{\tilde{\Theta}} \end{aligned} \tag{52}$$

which, by recalling Property 2 of the Eq. (39a,b) and $\dot{\tilde{\Theta}} = \dot{\hat{\Theta}}$ (by assuming $\dot{\Theta} = \mathbf{0}$), can be rewritten in the form

$$\dot{V} = -\mathbf{x}_{cs}^T\mathbf{k}\mathbf{x}_{cs} - \mathbf{x}_{cs}^T\mathbf{E}_f(\mathbf{e}_f + \mathbf{k}_f\mathbf{e}_F) - \mathbf{x}_{cs}^T\mathbf{T}_{uc} - \sigma\tilde{\Theta}^T\hat{\Theta}. \tag{53}$$

It is easy to prove that $\sigma\tilde{\Theta}^T\hat{\Theta} \ge 0$ and more details concerning this proof are outlined in Part II of the dissertation. By noting the fact that $\mathbf{x}_{cs}^T\mathbf{E}_f = \mathbf{0}$ and $\sigma\tilde{\Theta}^T\hat{\Theta} \ge \mathbf{0}$, it follows that

$$\dot{V} \le -\mathbf{x}_{cs}^T\mathbf{k}\mathbf{x}_{cs} - \mathbf{x}_{cs}^T\mathbf{T}_{uc}. \tag{54}$$

Hence, $\dot{V}$ can be shown to be upper bounded as

$$\begin{aligned} \dot{V} &\le -\rho_{\min}(\mathbf{k})\|\mathbf{x}_{cs}\|^2 + \|\mathbf{x}_{cs}\|d_m \\ &\le -\frac{\rho_{\min}(\mathbf{k})}{2}\|\mathbf{x}_{cs}\|^2 - \frac{\rho_{\min}(\mathbf{k})}{2}[\|\mathbf{x}_{cs}\| - \frac{d_m}{\rho_{\min}(\mathbf{k})}]^2 + \frac{d_m^{\,2}}{2\rho_{\min}(\mathbf{k})} \\ &\le -\frac{\rho_{\min}(\mathbf{k})}{2}\|\mathbf{x}_{cs}\|^2 + \frac{d_m^{\,2}}{2\rho_{\min}(\mathbf{k})}. \end{aligned} \tag{55}$$

Therefore, $\dot{V}$ is negative definite, for all $(t, \mathbf{x}_{cs}) \in \Re^+ \times \Re^{6v}$, until $\|\mathbf{x}_{cs}\|$ enters the target ball Δ_f (i.e., $\dot{V} < 0$, $\forall \mathbf{x}_{cs} \in \Delta_f^{\,c}$), where $\Delta_f^{\,c}$ denotes the complement of Δ_f. By utilizing

equation (51) and inequality (55), we can show that $\mathbf{x}_{cs}$ and $\tilde{\Theta} \in L_\infty$, which in turn implies that $\mathbf{R}_r\tilde{\Theta} \in L_\infty$ and $\mathbf{e}_t \in L_\infty$ (or $\mathbf{x}_t \in L_\infty$). Moreover, premultiplying $\mathbf{E}_t^T$ on both sides of Eq. (50) and using $\mathbf{E}_t^T\mathbf{E}_f = \mathbf{0}$ yields

$$\mathbf{E}_t^T\mathbf{M}_c\mathbf{E}_t\dot{\mathbf{x}}_{ts} = -\mathbf{E}_t^T\mathbf{C}_c\mathbf{E}_t\mathbf{x}_{ts} + \mathbf{E}_t^T\mathbf{R}_r\tilde{\Theta} - \mathbf{E}_t^T\mathbf{E}_t\bar{\mathbf{k}}\mathbf{E}_t^T\mathbf{E}_t\mathbf{x}_{ts} - \mathbf{E}_t^T\mathbf{T}_{uc}. \tag{56}$$

In light of the above results, all terms in the right hand side of (56) are bounded, which implies that $\dot{\mathbf{x}}_{ts} \in L_\infty$ (or $\dot{\mathbf{x}}_{cs} \in L_\infty$). Now, to establish the global boundedness of the contact forces, once again from (50),

$$(\mathbf{e}_f + \mathbf{k}_f\mathbf{e}_F) = -\mathbf{E}_f^T\mathbf{M}_c\mathbf{E}_t\dot{\mathbf{x}}_{ts} - \mathbf{E}_f^T\mathbf{C}_c\mathbf{E}_t\mathbf{x}_{ts} + \mathbf{E}_f^T\mathbf{R}_r\tilde{\Theta} - \mathbf{E}_f^T\mathbf{T}_{uc}, \tag{57}$$

which implies that $(\mathbf{e}_f + \mathbf{k}_f\mathbf{e}_F) \in L_\infty$. Hence, it can be concluded that $\mathbf{e}_f \in L_\infty$. Consequently, the global uniform ultimate boundedness of all tracking errors follows immediately. Summarizing the above results, all signals of the closed-loop system (i.e., positions, contact forces, and estimated parameters) remain bounded with respect to the closed ball Δ_f. Furthermore, the tracking error bound (or the size of residual set) for global stability can be made arbitrary small by choosing larger control gains. Therefore, it is shown that the proposed adaptive control algorithm is robust with respect to parametric uncertainties and external disturbances.

4. CONCLUSIONS

This article have presented the effective dynamic modeling, analysis, and coordinated controls of constrained multiple robot systems which consist of the multiple robots, the manipulated object, and the constraint surfaces. The first part of this study was devoted to formulating the kinemaitic and dynamic constraints of the overall systems and to developing the effective mathematical model of the system with closed-chain mechanisms. Based on the reduced-order (or decoupled) dynamic model, a class of hybrid position/force controllers have been synthesized. When the physical parameters of robots are exactly known, the modified computed torque controller has been employed to achieve asymptotic stability of the closed-loop systems. To cope with system uncertainties, we proposed the robust adaptive hybrid controller in which a rigorous stability analysis of the corresponding closed-loop systems have been given by a Lyapunov stability method. Thus, it has been shown that the proposed control algorithms guarantee the global boundedness of the object positions as well as the contact forces (the internal forces and the constraint forces). The methods presented in this study can be easily extended to cover many other applications of the constrained multiple robot systems with minor modifications.

REFERENCES

[1] A.J. Koivo and M.A. Unseren, "Modeling closed chain motion of two manipulators holding a rigid object," *Mech. Mach. Theory*, vol. 25, no. 4, pp. 427-438, 1990.

[2] P. Chiacchio, S. Chiaverini, L. Sciavicco, and B. Siciliano, "Global task space manipulability ellipsoids for multiple-arm systems," *IEEE Trans. Robotics and Automation*, vol. (7), no. 5, pp. 678-685, 1991.

[3] Y. Nakamura, "Advanced robotics (redundancy and optimization)," Addison-Wesley Publishing Co., Reading, MA, 1991.

[4] S. Arimoto, F. Miyazaki, and S. Kawamura, "Cooperative motion control of multiple robot arms or fingers," *Proc. IEEE Int. Conf. on Robotics and automation*, pp. 1407-1412, 1987.

[5] J.Y.S. Luh and Y.F. Zheng, "Constrained relations between two coordinated industrial robots for motion control," *Int. J. Robotics Res.*, vol. 6, no. 3, pp. 60-70, 1988.

[6] M. Raibert and J.J. Craig, "Hybrid position/force control of manipulators," *ASME J. Dyn. Systems Meas. Control* 102, pp. 126-133, 1981.

[7] O. Khatib, "A unified approach for motion and force control of robot manipulators; the operational space formulation," *IEEE J. Robotics and Automation* 3(1), pp. 43-53, 1987.

[8] T. Yoshikawa, "Dynamic hybrid position/force control of robot manipulators-description of hand constraints and calculation of joint driving force," *IEEE J. Robotics Automation*, vol. RA-3 (5), pp. 386-392, 1987.

[9] N.H. McClamroch and D. Wang, "Feedback stabilization of constrained robots," *IEEE Trans. Autom. Control* 33 (5), pp. 419-426, 1988.

[10] Z. Li and S. Sastry, "A unified approach for the control of multifingered robot hands," *American Mathematical Society, Contemporary Mathematics*, vol. 97, pp. 217-239, 1989.

[11] T. Yoshikawa and X. Zheng, "Coordinated dynamic hybrid position/force control for multiple robot manipulators handling one constrained object," *In Proc. of IEEE Int. Conf. on Robotics and Automation*, pp. 1178-1183, 1990.

[12] X. Yun, "Modeling and control of two constrained manipulators," *J. Int. Robotics Syst.* 4, pp. 363-377, 1991.

[13] R. Carelli and R. Kelly, "Adaptive control of constrained robots modeled by singular systems," *In Proc. IEEE Conf. CDC*, pp. 2635-2640, 1989.

[14] Y. Hu and A.A. Goldenberg, "An adaptive approach to motion and force control of multiple coordinated robot arms," *in Proc. IEEE Conf. Robotics Automat.*, pp. 1091-1096, 1989.

[15] S. Ahmad and M. Zribi, "Lyapunov based control design for multiple robots handling a common object," *in Proc.U.S.C. Control Mechanics Workshop*, pp. 1-17, Los Angles, CA, 1991.

[16] Y.D. Song and J. D. Anderson, "Adaptive control of a colleague-like multi-robots system handling a common unknown object," *Proc. 30th CDC*, pp. 2787-2792, Brighton, England, 1991.

[17] B. Yao, W.B. Gao, and S.P. Chan, "Robust constrained motion control of multiarm robots holding a common robot arms," *in Proc. IEEE Int. Conf. IECON'90*, pp.232-237, 1990.

[18] R. Ortega and M.W. Spong, "Adaptive motion control of rigid robots: a tutorial," *Automatica*, vol. 25, no. 6, pp. 877-888, 1989.

[19] J.S. Reed and P. Ioannou, "Instability analysis and robust adaptive control of robotic manipulators," *IEEE J. Robotics and Automat.*, vol. RA-5, no., 3, pp. 381-386, 1986.

[20] Y.H. Chen, "Robust control system design: non-adaptive versus adaptive," *Int. J. Contrl.*, vol. 51, no. 6, pp. 1457-1477, 1990.

[21] R.L. Huston, "Multibody dynamics," Butterworth-Heinemann, Stoneham, MA, 1990.

GENERAL CONCLUSIONS

This dissertation deals with dynamics and controls for robot manipulators containing open and closed kinematic chain mechanisms.

The first part of this research (Part I) has presented dynamic compensation methodology for the robust trajectory tracking control of uncertain single robot model. The proposed control scheme consists of two major parts; a fully model-based feedforward control with PD compensation and robust nonlinear controllers. The robust control synthesis adopted is based on the deterministic approach. Furthermore, the presented controllers can be implemented in decentralized ways. Both theoretical and simulation analysis are performed to ascertain the effectiveness of the proposed control algorithms. Stability and robustness issues of control laws have been investigated extensively and rigorously by Lyapunov stability method. The outstanding contributions of the proposed control algorithms are summarized as follows: (1) The joint accelerations are not required in the control law; (2) The presented control laws do not require the exact information about the system parameters and dynamics; (3) Torque computations in the model-based portion can be calculated off-line if the desired trajectories and the nominal values of dynamic parameters are known in advance. This implies high promises for real-time control; (4) The robust control parts are designed to cope with the effect of higher-order uncertainties in the system; (5) Finally, it is shown that the proposed control laws can guarantee at least the UUB of all signals under significant uncertainties.

The second part of this dissertation (Part II) has presented systematic approaches to the hybrid position/force controls for the constrained single robotic manipulator over known contact surfaces. The compact mathematical model has been derived in terms of the constraint-surface variables. The constraint frame is set up as a direct sum of force-controlled subspace and (purely kinetic) position-controlled subspace in which position and

force DOF are specified on the tangential and normal directions of the external surfaces, respectively. For the dynamic behavior of external environments, both elastic and rigid surfaces are considered. Based on a new reduced dynamic model, a class of hybrid control algorithms are synthesized to address the control issues of constrained robot system, that is, the generalized positions and forces are simultaneously regulated in two orthogonal directions during the contact task. In the ideal case, the modified computed torque has been adopted. Without exact knowledge of the robot dynamics, the robust adaptive hybrid control are formulated. In case of elastic environment, the adaptive impedance control has been synthesized in the presence of parametric uncertainties. The global stability and convergence issues of the corresponding closed-loop systems have been widely discussed by the Lyapunov approach. Finally, it is shown that the proposed control laws guarantee global stability (boundedness and convergence) of the position (or motion) tracking as well as the contact-force tracking errors.

In Part III of this dissertation, we have presented the effective dynamic model, analysis, and coordinated controls of constrained multiple robot system which consists of the multiple robots, the manipulated object, and the constraint surfaces. The first part of this study was devoted to formulating the kinemaitic and dynamic constraints of the overall systems and to developing the effective mathematical model of the system with closed-chain mechanisms. Based on the reduced-order (or decoupled) dynamic model, a class of hybrid position/force controllers have been synthesized. When the physical parameters of robots are exactly known, the modified computed torque controller has been employed to achieve asymptotic stability of the closed-loop systems. To cope with system uncertainties, we proposed an robust adaptive hybrid control in which a rigorous stability analysis of the corresponding closed-loop systems have been given by a Lyapunov stability method. Thus, it has been shown that the proposed control algorithms guarantee the global

boundedness of the object positions as well as the contact forces (the internal forces and the constraint forces).

ACKNOWLEDGMENTS

First of all, I would like to express my sincere gratitude to my major professor, Dr. Jerry L. Hall, for his invaluable advice, guidance, inspiration, and encouragement throughout my Ph.D. program. He always allowed me the time and opportunity to pursue a variety of other research interests (such as robot vision, pattern recognition, image processing, H_2 and H_∞ control, optimal control, fuzzy logic theory, and artificial neural network). I also would like to thank my committee members, Dr. Richard K. Miller, Dr. Peter J. Sherman, Dr. Greg R. Luecke, Dr. Donald R. Flugrad, and Dr. Patrick Kavanagh, for their helpful discussions, suggestions, and assistance.

I would like to extend special thanks to my wife, Sookhyang Lee, and our two sons, Hwangrok (Reynold H) and Hwangjin (Dennis H). I am heartily indebted to their unselfish love, patience, and sacrifices throughout this endeavor. In addition, I greatly appreciate all my family members and relatives.

Finally, I would earnestly like to dedicate this dissertation to my mother and to the memory of my departed father who inspired me to set lofty goals.